The University Of Sheffield.

Targeting SNARE proteins and the trafficking of sodium channels in inflammatory pain

Marta Luísa Alves Simões

A thesis submitted in partial fulfilment of the requirements for the degree of Doctor of Philosophy

The University of Sheffield
Faculty of Science
Department of Biomedical Sciences

September 2017

Abstract

Dorsal root ganglion (DRG) neurones perceive and discriminate diverse types of sensations. Nociceptors are a subgroup of DRG neurones specialised in translating noxious pain stimuli to the spinal cord and higher brain centres. Following a noxious insult, nociceptors are known to have enhanced excitability and peptide secretion both of which, are likely to be a consequence of increased membrane trafficking and vesicle fusion with the plasma membrane. Vesicle-associated membrane proteins (VAMPs) are vesicular SNARE proteins (v-SNAREs) which complex together with cognate target SNARE proteins (t-SNAREs) found on 'acceptor' compartments. Together they regulate membrane trafficking and vesicle fusion; while much is known about the v- and t-SNAREs involved in the fusion of neurotransmitter and neuropeptide-containing vesicles with the plasma membrane, to date the identity of SNAREs involved in ion channel trafficking or secretion in nociceptors is limited.

To explore the role of SNAREs on DRG neurones' secretion and excitability, an *in vitro* inflammation model was established. An inflammatory soup containing ATP, bradykinin, prostaglandin E2, histamine, noradrenaline, nerve growth factor, and serotonin was added for 22 h. This incubation induced hyperexcitability. In voltage-clamp, sodium currents resistant to tetrodotoxin, Nav1.9 and Nav1.8 currents, were increased. However, a decrease in the expression of Nav1.7 (TTX-sensitive) and Nav1.9 (TTX-resistant) at the plasma membrane was observed, which likely reflects changes in subcellular location of these channels induced by the inflammatory model. This study also identified the expression of seven vesicle membrane-associated proteins in DRG neurones (VAMP1-5, 7 and 8). This expression was found across all soma diameters. VAMP1/2/7 were observed in the neurites. The potential of the botulinum chimaeras, tetbot A and tetbot B, in reducing CGRP (calcitonin gene-related peptide) release and preventing excitability induced by an inflammatory soup was also explored. These chimaeras are designed to target isolectin B4-negative DRG neurones and cleave SNAP25 (t-SNARE) and

VAMP1/2/3 (v-SNAREs). Tetbot A cleaved SNAP25 and significantly reduced CGRP release elicited by 60 mM KCl. The interpretation of the electrophysiology results is problematic as the detergent used in the chimaera preparations altered baseline properties of the DRG neurones.

Author’s declaration

I declare that the work in this dissertation was carried out in accordance with the requirements of the University's Regulations and Code of Practice for Research Degree Programmes and that it has not been submitted for any other academic award. Except where indicated by specific reference in the text, the work is the candidate's own work. Work done in collaboration with, or with the assistance of, others, is indicated as such. Any views expressed in the dissertation are those of the author.

SIGNED: DATE:

Acknowledgments

First, I would like to thank Liz, my primary supervisor, for the opportunity to do this project and guidance. I wanted to study pain, and it was painful! I would also like to thank Mohammed Nassar, my secondary supervisor, for his guidance and advice throughout.

I felt part of a big family in Sheffield, and I am grateful for all your help during the past four years. Thank you: Rania Magadmi, Zainab Mohammed, Asma Almuhammadi, Nipa Konthapakdee, Hannah Wajdner, Jasmine Farrington, Deepa Bliss, Claudia Bauer, Donna Daly, Ciara Doran, Rebecca Bresnahan, Judit Mészáros, Friederike Uhlig, Agnieszka Skowronek and Charlotte Leese.

I will forever miss our coffee club and Thai food dinners. Those are great memories.

This thesis would not have been possible without the help of Bob and Matt from the electronics workshop. Thank you for helping me when things decided to fail! Likewise, I thank Michelle Bird for helping me manage the mouse colony and support throughout, and Lydia Taylor, my thesis writing mentor, for helping get through the final days of writing my thesis.

Tenho também que agradecer à minha família por todo o apoio que me deram ao longo destes anos. Já está, acabei a “escola toda”! Agora vou começar a ter férias com vocês a sério (sem coisas para estudar!). Obrigada pelo vosso apoio! E um especial obrigado à minha mãe que ouviu grandes misérias e dramas de uma estudante de doutoramento. Ajudou muito!

Schatje, I’m glad I was in your seat. Thank you for the energy, the listening, the advice and the motivation. Thank you for being there, for coming to the lab and cooking for me when I was working. It really made a difference!
P.S.: I’m ready to go to Vienna & Ik hou heel veel van jou.

Table of contents

List of abbreviations

4-HNE	4-Hydroxynonenal
5-HT	Serotonin
5,6-EET	Epoxyeicosatrienoic acid
AHP	Afterhyperpolarisation phase
Amp	Amplifier
AMPA	α-amino-3-hydroxy-5-methyl-4-isoxazolepropionic acid
ANOVA	Analysis of variance
APS	Ammonium persulfate
ASIC1	Acid-sensing ion channel 1
ATP	Adenosine triphosphate
BDNF	Brain-derived neurotrophic factor
BoNT	Botunlinum neurotoxin
BOTOX	Commercial name for BoNT/A
C-LTMR	C-fiber low-threshold mechanoreceptors
CACNA1H	Calcium Voltage-gated channel subunit alpha1 H
CALB1	Calbindin 1
CaMK	Ca^{2+}/calmodulin-dependent protein kinase
cAMP	Cyclic adenosine monophosphate
CCL2	CC-chemokine ligand 2
CFA	Complete Freud's adjuvant
CGRP	Calcitonin gene-related peptide
CNS	Central nervous system
CNTNAP2	Contactin-associated protein-like 2
CXCL	CXC-chemokine ligand
DAPI	4',6-diamidino-2-phenylindole
DRG	Dorsal root ganglion
EDTA	Ethylenediaminetetraacetic acid
EEA1	Early endosome antigen 1
EGTA	Ethylene glycol-bis(β-aminoethyl ether)-N,N,N',N'-tetraacetic acid
ELISA	Enzyme-linked immunosorbent assay
ER	Endoplasmic reticulum
ERK	Extracellular signalling-regulated kinase
FAM19A1	family with sequence similarity 19 member A1, C-C motif chemokine like
Fisher's LSD	Fishers Least Significant Difference
FITC	Fluorescein isothiocyanate
FP	N-foymylated peptides
FRAP	Fluoride-resistant acid phosphatase activity
FRP1	Frizzled-related protein

GAPDH	Glyceraldehyde 3-phosphate dehydrogenase
GCaMP	Genetically encoded calcium indicator of green fluorescent protein
GDNF	Glial-derived neurotrophic factor
GFRA2	GDNF family receptor alpha-2
GPCR	G-protein coupled receptors
GPI	Glycosylphosphatidylinositol
GTO	Golgi tendon organs
GTP	Guanosine triphosphate
HCN	Hyperpolarisation-activated cyclic nucleotide-gated ion channel
HEPES	4-(2-hydroxyethyl)-1-piperazineethanesulfonic acid
HETE	Hydroxyeicosatetraenoic acid
HMGB1	High mobility group protein B1
IB4	Isolectind B4
IFM	Hydrophobic triplet motif
IS	Inflammatory soup
JACoP	Just another colocalisaton software
KIT	Mast/stem cell growth factor receptor
KO	Knockout
LDHB	Lactate Dehydrogenase B
LTMR	Low-threshold mechanoreceptors
MAC	Magnetic cell sorting
MIA	mechanically insensitive afferents
MRGPRA3	Mas-related G-protein coupled receptor member A3
MRGPRD	MAS Related GPR Family Member D
MSA	mechanically sensitive afferents
NAV	Sodium channel
NECAB2	N-terminal EF-hand calcium-binding protein 2
NEFH	Neurofilament heavy
NF	Neurofilament
NF186	Neurofascin-186
NGF	Nerve growth factor
NMDA	N-methyl-D-aspartate
NP	Non-peptidergic
NrCAM	Neuronal cell adhesion molecule
NSF	N-ethylmaleimide-sensitive factor
OG	Octylglucoside detergent
P2X	Purinergic receptor
P2x3	Purinergic receptor 3
PBS	Phosphate-buffered saline
PBST	PBS with 0.1% tween
PC12 cells	Pheochromocytoma-derived cell line

PEP	Peptidergic
PGE	Prostaglandin E_2
PI3K	phosphatidylinositol-3-kinase
PKA	protein kinase A
PKC	protein kinase C
PLC	Phospholipase C
PLXNC1	Plexin C1
PM	Plasma membrane
PPLR	Probability of positive log-ratio
PV	Parvalbumin
PVDF	Polyvinylidene fluoride
RBDT	Tetanus receptor binding domain
RIPA	Radioimmunoprecipitation assay buffer
R_m	Membrane resistance
RNA	Ribonucleic acid
ROUT	Robust regression and outlier removal
R_p	Pipette resistance
R_s	Series resistance
RT	Room temperature
RTK	Receptor tyrosine kinase
RUNX3	Runt-related transcription factor 3
SDS	Sodium dodecyl sulphate
SEM	Standard error of the mean
SM protein	Sm core protein
SNAP25	soluble N-ethylmaleimide-sensitive attachment protein 25.
SNARE	N-ethylmaleimide-sensitive factor attachment protein receptors
SPP1	SecretedpPhosphoprotein 1
SST	Somatostatin
STORM	Stochastic optical reconrtruction microscopy
t-SNARE	target-SNARE
TAC1	Preprotachykinin-1
TBST	Tris-buffered saline with 0.1% tween
TEMED	Tetramethylethylenediamine
TeNT	Tetanus neurotoxin
TGN	Trans-Golgi network
TH	Tyrosine hydroxylase
Ti-VAMP	Tetanus insensitive VAMP
TLR	Toll-like receptors
TM	Transmembrane
TNF-α	Tumour necrosis factor alpha

TrkA	Tropomyosin receptor kinase A
TrkB	Tropomyosin receptor kinase B
TrkC	Tropomyosin receptor kinase C
TRPA1	Transient receptor potential ankyrin 1
TRPC3	Transient receptor protein 3
TRPV1	vanilloid receptor 1
TTX	Tetrodotoxin
TTX-R	Tetrodotoxin resistant
TTX-S	Tetrodotoxin sensitive
v-SNARE	Vesicle-SNARE
VAMP	Vesicle-associated membrane protein
VGCC	Voltage-gated calcium channel
VGLUT3	Vesicular glutamate transporter 3
VGSC	Voltage-gated sodium channel
WT	Wild type
α-HL	α-haemolysin

1 - General introduction

1.1 Why study pain?

The ability to translate the world that surrounds us into electrochemical information gives us the opportunity to react to environmental changes crucial to our survival. Pain signalling is one of such survival mechanisms built to alert us and to aid in tissue recovery. Dorsal root ganglion (DRG) neurones are part of this mechanism in the peripheral nervous system. They innervate our skin and viscera detecting and transducing signals such as heat, cold, pressure, and noxious stimuli to the spinal cord. Nociceptors are a subgroup of DRG neurones, specialised in pain signalling and the detectors of noxious stimuli. Hence, noxious stimuli such as extreme heat elicit pain signals via nociceptors that ultimately generate the complex sensation of feeling pain.

By definition, (acute) pain is the transitory sensory and emotional experience with actual or potential tissue damage. Pain signals may persist for weeks, months or years (chronic pain) without an identifiable cause (Costigan, Scholz and Woolf 2009). Chronic pain affects 43.5% of the adult British population, and it represents a severe emotional and physical burden for the individual but also for society (Fayaz et al. 2016). Current drug therapies are often ineffective, common analgesics are short-acting and cause adverse side effects which raise severe problems for repeated usage (Dolly and O'Connell 2012). For instance, the recent increase in opioid prescriptions has caused an opioid overdose crisis in the USA (Volkow and Collins 2017). Hence, an improvement of the current understanding of the pathophysiology of pain is essential not only to improve diagnosis but for the development of specific drug therapy that matches this unmet clinical need.

1.2 Nociceptor overview

First descriptions of specialised noxious stimulus detectors, nociceptors, were made by Charles Sherrington, “there is considerable evidence that the skin is

provided with a set of nerve-endings whose specific office it is to be amenable to stimuli that do the skin injury […] preferably termed nocicepient […].” (Sherrington 1903). Nociceptors are characterised by having a high threshold and by responding to multiple energy forms (thermal, mechanical and chemical). Different groups have shown that nociceptors may be subdivided according to distinct response characteristics, molecular markers, modalities of stimulation and soma diameter (Lawson and Waddell 1991, Stucky and Lewin 1999, Slugg, Meyer and Campbell 2000).

1.2.1 Fibre groups

There are four afferent fibre groups - Aα, Aβ, Aδ and C - and nociceptors are considered to be either Aδ- or C-fibres. Together they are thought to innervate skin and viscera, and mediate proprioception, mechanoception, nociception, thermoception and pruriception. In addition to having different sensor transducers they also end at different lamina in the spinal cord (Figure 1.1).

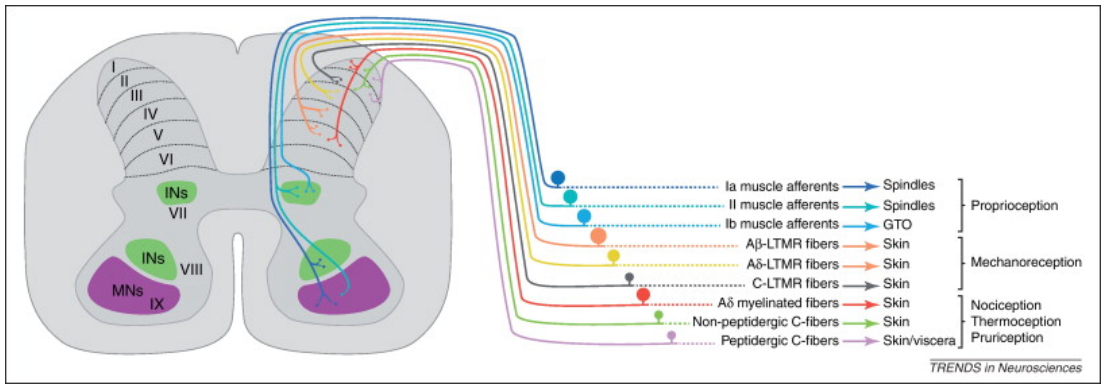

Figure 1.1 The Aα, Aβ, Aδ and C fibres terminate at different lamina.
DRG neurones innervating muscle spindles (spindles), golgi tendon organs (GTO), skin and viscera terminate at different lamina (I to V, and VII to IX). These relay proprioception, mechanoception, nociception, thermoception or pruriception information from the peripheral terminals. (Taken from Lallemend and Ernfors 2012)

1.2.2 Response characteristics

The response of Aδ- or C-nociceptors diverge in impulse propagation speed and this is due to myelination of the afferents. Myelination saves energy by restricting the action potentials to the nodes of Ranvier and enabling fast

saltatory impulse propagation. It has been shown that nociceptor Aδ-fibers are myelinated whereas nociceptor C-fibers are not. Hence, Aδ-fibers have faster impulse propagation when compared to C-fibers (Harper and Lawson 1985a, Harper and Lawson 1985b). Other studies have further characterised nociceptors according to their action potential configuration. The presence or absence of a inflection on repolarisation phase is an indicator of myelinated fibers (Fulton 1987). This inflection is the consequence of inward current carried out by Na^+ and Ca^{2+} while in the absence of the inflection is Na^+ (Gallego and Eyzaguirre 1978, Scott and Edwards 1980, Yoshida, Matsuda and Samejima 1978). Nociceptors are unique in their set of voltage-gated sodium channels (VGSCs) and their expression directly affects many of their electrophysiological properties and underlying excitability (Elliott and Elliott 1993).

1.2.3 Molecular markers

By responding to multiple energy forms nociceptors are equipped with a wide arrange of receptors and ion channels but they can be divided in two major neurochemical subtypes, peptidergic and non-peptidergic.

- Peptidergic neurones contain calcitonin-gene related neuropeptide (CGRP), substance P, and somatostatin.
- Non-peptidergic lack neuropeptides but contain fluoride-resistant acid phosphatase activity (FRAP) and bind plant lectin isolectin B4 (IB4) (Nagy and Hunt 1982, Silverman and Kruger 1988a, Silverman and Kruger 1988b).

IB4 belongs to a group of plant proteins, lectins, that bind to the carbohydrate portion of glycoproteins and glycolipids (Barondes 1988). IB4 binding has been used for further characterisation of these two subpopulations and it has shown that these two subtypes have distinct electrophysiological properties (Stucky and Lewin 1999, Choi, Dib-Hajj and Waxman 2007), are regulated by different neurotrophic factors – IB4-positive by glial-derived neurotrophic factor (GDNF)

and IB4-negative by nerve growth factor (NGF) – (Bennett et al. 1998, Molliver et al. 1997), and terminate at different regions in the spinal cord (Coimbra, Sodrebor.Bp and Magalhaes 1974, Silverman and Kruger 1990).

The peptidergic subpopulation of DRG neurones may also be identified by peripherin (Goldstein, House and Gainer 1991). Peripherin is an intermediate filament protein named after it being found on 'periphery reaching' neurones (Greene 1989). Peripherin-positive DRG neurones have been found to have predominantly a small diameter and 87% express substance P and 43% express CGRP(Goldstein et al. 1991).

1.2.4 Modalities of stimulation

Earlier studies of primary afferents used microneurography to assess the different modalities of stimulation (Meyer and Campbell 1988, Davis, Meyer and Campbell 1993, Treede et al. 1995). This has led to the classification of primary afferents as mechanically sensitive afferents (MSA) or mechanically insensitive afferents (MIA)(Meyer et al. 1991). In addition, it was used to describe further properties such as heat sensitivity, fiber sensitization and importantly hyperalgesia (Meyer et al. 1991, Treede et al. 1992).

1.2.5 Soma diameter

Nociceptors have been demonstrated to have a small mean diameter compared to other primary afferent fibres (Lawson and Waddell 1991). Specifically, small (< 17 μm), intermediate (17-25 μm) and large (> 25 μm). Although it varies slightly between mice and rats. Yet, recent molecular biology approaches to DRG classification are challenging this reference.

1.2.6 other classifications

During the course of this project several molecular biology approaches reclassified DRG neurones (Chiu et al. 2014, Thakur et al. 2014, Usoskin et al. 2015, Rouwette et al. 2016a). Using single cell RNA-seq Usoskin et al

unbiasedly grouped DRG neurones according to its molecular expression profile, revealing three distinct low-threshold mechanoreceptive neurones, two proprioceptive, and six principal types of thermosensitive, itch sensitive, type C low-threshold mechanosensitive and nociceptive neurones (Usoskin et al. 2015) (Figure 1.2). Thakur et al have used a novel application of magnetic cell sorting (MAC) to isolate nociceptors and compared them to other DRG neuronal subtypes, and Chiu et al have used two mouse reporter lines to identify and purify a subset of DRG neurones in combination with IB4 surface labelling. Understanding the subgroups of DRG neurones is also being challenged by the differences in their *in vitro* and *in vivo* responses. In vivo GCaMP experiments suggest polymodality is an infrequent characteristic *in vivo* (Emery et al. 2016a). Discrepancies between conclusions of these methods may reflect the analysed sample (e.g. RNA vs protein), but also the impact of isolating DRG neurones from the surrounding tissues and mediators (e.g. pro-inflammatory, neurotrophic factors).

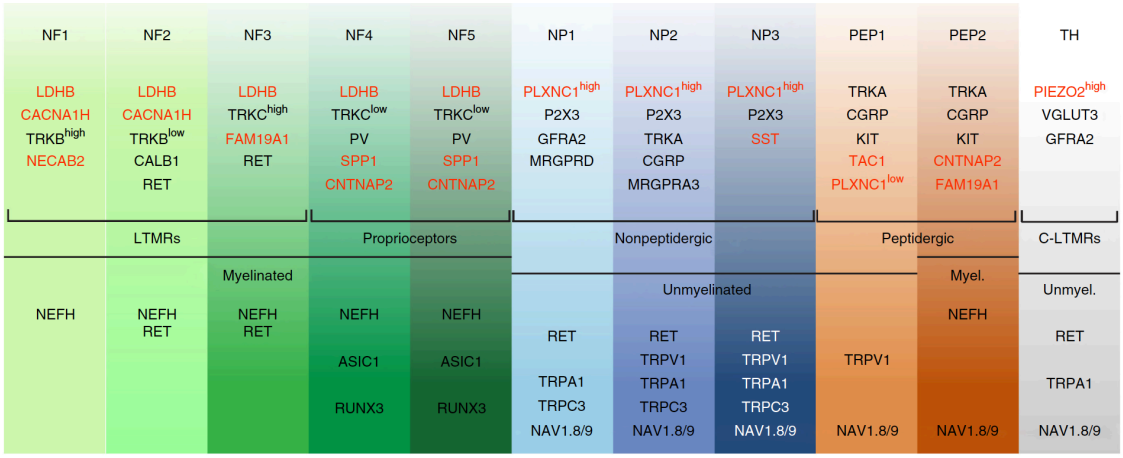

Figure 1.2 Novel DRG classification proposed by Usoskin et al. 2015.
This classification divides the DRG neurones into four main groups: neurofilament (NF), non-peptidergic (NP), peptidergic (PEP) and tyrosine hydroxylase (TH). This new classification proposes new markers (top half of the table) with new novel additions in red. The bottom of the table refers to common markers already used in the field. (see abbreviation list page 11 for further definitions)

1.3 Nociceptor transduction

The single unit of communication in the nervous system is an action potential. In contrast to the majority of central neurones, nociceptors do not normally

generate their action potentials at the axon of hillock but at peripheral nerve endings (Amir and Devor 1996, Amir and Devor 1997). Specific receptors at nociceptor's nerve endings trigger nociceptive action potentials (Melzack and Wall 1965). These specific receptors are sensory transducers. They convert the energy of the stimulus (chemotransducers, thermoceptors or mechanoceptors) to an electrical signal, action potential firing (Matzner and Devor 1992).

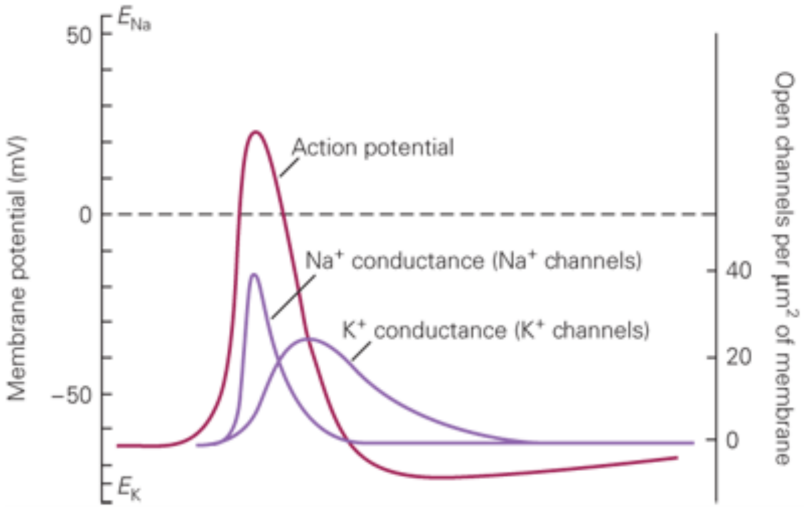

Figure 1.3 Voltage-gated Na^+ and K^+ conductances in action potentials.
During an action potential (red line) there is an initial flow of sodium ions through voltage-gated ion channels (Na^+ conductance) following by a repolarising conductance due to the flow of potassium ions (K^+ conductance) (purple lines). (Taken from Kandel et al 2000)

Action potentials are a result of flow of ions (conductance) through voltage-gated ion channels. These are voltage-dependent Na^+ currents, voltage-dependent Ca^{2+} currents, voltage-activated K^+ currents, calcium-activated K^+ currents and the hyperpolarisation-activated current (Bean 2007). Described by Hodgkin and Huxley in the 50's, these conductances occur in a defined sequence and shape an action potential (Figure 1.3) (Hodgkin and Huxley 1952). Depolarisation of the membrane induces fast opening of Na^+ channels (increase in Na^+ conductance), inducing an inward Na^+ current. This further discharges the neurone activating more Na^+ channels, leading to an additional increase in Na^+ conductance. This drives membrane potential up and causes the rising phase of the action potential. The rising phase is limited by the gradual inactivation of Na^+ channels, reducing the positive inward current, and

the delay opening of K^+ channels, creating an outward positive current that repolarises the membrane (repolarising phase, Figure 1.4). Other conductances such as Ca^{2+} also help to depolarise the neurone during the rising phase whereas Cl^- conductance and hyperpolarisation-activated cation currents contribute to membrane repolarisation (Kandel et al. 2013).

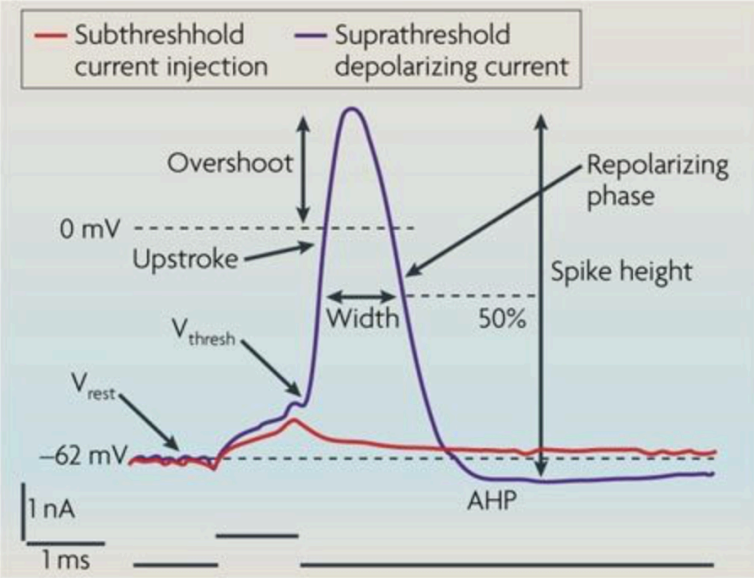

Figure 1.4 Different parameters of an elicited action potential.
Action potentials may vary in width, upstroke, overshoot height, repolarising phase, afterhypopolarisation phase (AHP), and spike height. The initial current injected in the neurone must be sufficient to change the cell's potential to reach the threshold (V_{thresh}) and produce a suprathreshold depolarising current (purple). Resting membrane potential (V_{rest}). (Adapted from Bean 2017)

Sensory transducers have to generate a change in membrane potential that reaches the threshold to elicit an action potential. Evidence suggests nociceptor neurites have a resting membrane potential (V_{rest}) of -40 mV and at the soma between -50 and -75 mV (Baccaglini and Hogan 1983, Gold et al. 1996). The threshold for action potentials of nociceptors *in vitro* is reported around -35 mV (V_{thresh}) (Gold et al. 1996). These are highly regulated events and in a disease state are known to be altered, resulting in abnormal firing and altered pain sensation (Matzner and Devor 1992).

1.4 Voltage-gated sodium channels in DRG neurones

Changes in membrane potential alter the conformation of the VGSCs to open configuration which allows Na^+ to flow. VGSCs are kinetically fast and have three basic conformations: open, closed and inactivated. The primary functional unit of VGSC is the α-subunit. It is the pore forming unit and it is sufficient for VGSC's functional expression. The α-subunit of VGSCs has four similar repeated domains (I-IV) (Figure 1.5). S5-S6 transmembrane regions form the pore and S4 is involved in voltage sensing. When the membrane is at resting potentials, the VGSC is closed. Once the membrane is depolarised, the VGSC changes to an open conformation. When the neurone repolarises, inactivation occurs. This may be due to occlusion of the pore by intracellular loop between domains III and IV (fast inactivation) or the deactivation of the channel via closure of the pore (closed state). Thus, generating transient Na^+ currents in DRG neurones (Cummins, Sheets and Waxman 2007).

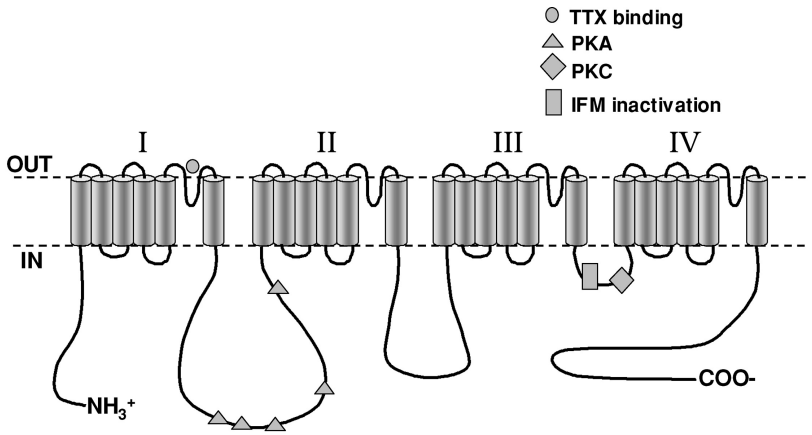

Subtype	Rat Orthologs	TTX Sensitivity (nM)	Activation Threshold	Inactivation Rate	Tissue Localization
$Na_V1.1$	Brain I	-	Low	Fast	CNS, also in DRG and motor neurons
$Na_V1.2$	Brain IIA	18	Low	Fast	CNS
$Na_V1.3$	Brain III	15	Low	Fast	Embryonic nervous system; adult CNS;
$Na_V1.4$	SkM1	5	Low	Fast	Skeletal muscle
$Na_V1.5$	H1	1,800	Low	Medium	Heart; embryonic DRG
$Na_V1.6$	SCP6, PN4	1	Low	Fast	DRG, motor neurons, also in CNS
$Na_V1.7$	PN1	2	Low	Fast	Mostly DRG, also in CNS
$Na_V1.8$	PN3, SNS	>100,000	High	Slow	DRG (80% small diameter; 20% large
$Na_V1.9$	PN5, NaN	39,000	Low	Medium	DRG (small diameter); also in CNS

Figure 1.5 and table 1.1 VGSC secondary structure and α-subunit characteristics.
Voltage-gated Sodium Channel (VGSCs) α-subunit has four repeated domains (I to IV), which are characterised by TTX, PKA, PKC interaction and the IFM inactivation. Different subtypes show different distribution within the nervous system and distinct TTX sensitivity. CNS, central

nervous system. DRG, dorsal root ganglion neurones. IFM, hydrophobic triplet motif. PKA, protein kinase A. PKC, protein kinase C. TTX, tetrodotoxin. (Taken from Lai et al. 2004)

There are 9 α-subunits (Nav1.1-Nav1.9, and a putative tenth Nax) and 4 β-subunits (Navβ_1-β_4). α-subunits have specific developmental and cellular expression and may be associated with β-subunits which may stabilise, aid in localization or change the kinetics of the channel. DRG neurones show large variations in VGSC expression (see table 1.1).They may be separated by their tetrodotoxin (TTX) sensitivity and unique biophysical properties (Elliott and Elliott 1993, Namadurai et al. 2015, Lai and Jan 2006).

1.4.1 TTX sensitivity

DRG neurones are unique in their set of VGSCs, they express both TTX resistant (TTX-R) and TTX sensitive (TTX-S) VGSCs (Elliott and Elliott 1993)(Table 1.1). TTX is a guanidinium compound more commonly known to be produced by bacteria in fish of the tetraodon genus such as the puffer fish (Moczydlowski 2013). It binds the pore of VGSCs and in a dose-dependent manner blocks the conductance of Na^+, thus VGSCs affected at lower concentration are referred as sensitive and those affected at a higher dose are referred as resistant (Nav1.5, Nav1.8 and Nav1.9)(Chen and Chung 2014).

1.4.2 Resurgent currents

Resurgent currents result from an unusual form of gating that lead to the reopening of VGSCs during the repolarisation phase. In Purkinje cells, where they were first identified, resurgent currents lead to bursting activity (Raman and Bean 1997). This mechanism is thought to arise from an interaction with Navβ4 and phosphorylation of the Nav1.6 channel. The cytoplasmic tail of Navβ4 obstructs the pore and stops Na^+ conductance (instead of the intracellular loop between domains III and IV of the α-subunit) and it blocks for a shorter time period than the normal inactivation (Grieco et al. 2005). In DRG neurones, resurgent currents are seen in 40% of the large diameter neurones (Cummins et al. 2005).

1.4.3 Persistent currents

Persistent currents were first identified in 1990 in hippocampal neurones (French et al. 1990). Persistent currents are Na^+ conductance seen at resting membrane potentials, they are sensitive to TTX and very resistant to inactivation by depolarisation of the membrane. Thus, they are likely to play a role in the repetitive firing of action potentials (French et al. 1990). This alternative open state could result from G protein modulation or protein kinase phosphorylation of the α-subunit. The amplitude of persistent sodium currents in voltage-clamp experiments can reach 10% of the peak transient current. Nav1.6 has been associated with persistent currents in spinal sensory neurones (Cummins et al. 2005) and ataxia in mice (Meisler et al. 2002). In DRG neurones, Nav1.9 underlies a persistent TTX-R current in smaller neurones (Dib-Hajj et al. 1998, Tate et al. 1998, Dib-Hajj et al. 2002). Furthermore, lidocaine has been shown to supress ectopic firing while maintaining normal action potential firing (Devor, Wall and Catalan 1992). This is believed to be due to persistent current suppression by lidocaine (Dong et al. 2008).

1.4.4 Action potential electrogenesis in DRG neurones

As previously mentioned, action potentials are generated by changes in membrane potential and VGSCs play a crucial role in their formation. Evidence suggests that different α-subunits contribute to different parts of the action potential. Nav1.8 is considerate to contribute to the action potential overshoot and repetitive firing, Nav1.7 to the subthreshold activity and Nav1.9 to the modulation of the resting membrane potential (Figure 1.4) (Rush, Cummins and Waxman 2007). Furthermore, Nav1.8 has been described to be mostly expressed in damage sensing, nociceptor, neurones (Akopian et al. 1999, Kobayashi, Ohta and Terada 1993). However, VGSC expressions are not fixed and have been shown to change with painful pathologies (Tanaka et al. 1998, Okuse et al. 1997, Coggeshall, Tate and Carlton 2004, Villarreal et al. 2005, Strickland et al. 2008), and experimental procedures such as axotomy (increased expression of Nav1.3) (Black et al. 1999). Nav1.3, Nav1.7, Nav1.8

and Nav1.9 are preferentially expressed in DRG neurones and are reviewed below.

1.4.5 Nav1.3

Nav1.3 is a TTX-S channel with fast kinetics and recovery from inactivation. These are similar characteristics to Nav1.7, yet, Nav1.3 expression in DRG neurones is much lower. It is predominant in developing neurones, but downregulated in mature neurones (Beckh et al. 1989). Its levels increase during inflammation and following nerve injury (Waxman, Kocsis and Black 1994, Kim et al. 2002, Black et al. 1999). Thus, there is a possible role in neuropathic pain. However, this role is controversial. Nav1.3 antisense administration intrathecally reduced chronic constriction injury's pain phenotype (Hains et al. 2004), but no changes were seen in a spinal nerve injury model (Lindia et al. 2005) or in Nav1.3-null mice pain behaviour (Nassar et al. 2006).

1.4.6 Nav1.7

Nav1.7 was first identified in humans in 1997 (Sangameswaran et al. 1997). Transient currents obtained by Nav1.7 are TTX-S, exhibit rapid activation and inactivation, and slow repriming (recovery from inactivation) (Klugbauer et al. 1995, Cummins, Howe and Waxman 1998). Thus, it is not considered to play a role in repetitive firing but in setting the threshold. Changes in the gating of Nav1.7 can induce painful pathologies such as inherited erythromelalgia and paroxysmal extreme pain disorder (Fertleman et al. 2006, McDonnell et al. 2016). In contrast, loss-of-function mutations, but also hypofuntional are associated with congenital insensitivity to pain (Cox et al. 2006, Goldberg et al. 2007, Emery et al. 2015). Furthermore, Nav1.7 is upregulated in models of inflammatory pain (details reviewed in section 1.5) (Tanaka et al. 1998, Black et al. 2004), which is supported by Nav1.7 knock out studies and shRNA (Nassar et al. 2004, Yeomans et al. 2005). Hence, Nav1.7 selective antagonists are an attractive idea but studies have been met with complex

signalling that interacts with endogenous opioids (Emery, Luiz and Wood 2016b, Isensee et al. 2017, Minett et al. 2015).

1.4.7 Nav1.8

Nav1.8 is resistant to TTX and contributes significantly to action potential electrogenesis in small DRG neurones (Renganathan, Cummins and Waxman 2001). Due to the depolarised voltage-dependence of activation of the Nav1.8, they are considered to contribute to the overshooting of action potentials and repetitive firing (Renganathan et al. 2001). Recordings from Nav1.9 null mice have shown that typical TTX recordings are mediated by Nav1.8 (Akopian et al. 1999). In the context of inflammatory pain, PKA, calmodulin and contactin have been implicated in its modulation and likely to contribute to increased excitability of DRG neurones (details reviewed in section 1.5) (Gold et al. 1996, Zhang, Vasko and Nicol 2002). Nav1.8 is also unique in maintaining excitability at low temperatures. Nav1.8 knock out mice do not respond to noxious cold and noxious mechanical stimuli (Abrahamsen et al. 2008).

1.4.8 Nav1.9

Nav1.9 is also TTX resistant and preferentially expressed in small DRG neurones. It was first identified as the remaining TTX-R current in Nav1.8 knock out mice (Cummins et al. 1999). It activates at potentials close to resting membrane potential (-60 mV to -70 mV), characterised by a steady-state inactivation curve, and also reported to produce persistent currents. Compared to other VGSCs α-subunits, Nav1.9 has very slow gating kinetics (Cummins et al. 1999). Multiple studies have demonstrated that Nav1.9 is heavily modulated (reviewed in section 1.5) (Baker et al. 2003, Coste et al. 2004, Rush and Waxman 2004). Since it is thought to contribute to threshold setting this can substantially impact firing thresholds.

1.4.9 Expression and trafficking

The expression profile of VGSCs in DRG neurones changes during development (Waxman et al. 1994, Benn et al. 2001). Once developed, small DRG neurones preferentially express three α-subunits: Nav1.7, Nav1.8 and Nav1.9 (Ho and O'Leary 2011). In the brain α-subunits are heavily glycosylated post-translation (Messner and Catterall 1985) and form an intracellular pool before joining the plasma membrane (Schmidt and Catterall 1986) in a process of regulated exocytosis mediated by SNARE (N-ethylmaleimide-sensitive factor attachment protein receptors) proteins (reviewed in section 1.6 and 1.7). In the process of regulated exocytosis, Nav1.7 has been shown to drive a positive feedback loop in Mat-LyLu prostate cancer cells via regulation of intracellular Na^+ concentration interaction with adenylyl cyclase, which upregulates Nav1.7 trafficking to the plasma membrane (Brackenbury and Djamgoz 2007). Additionally, other proteins regulate their membrane insertion. For instance, the binding of annexin II light chain (p11) and PKA phosphorylation have been shown to aid the translocation to the plasma membrane of Nav1.8 (Assisted export, Figure 1.6) (Okuse et al. 2002, Liu et al. 2010).

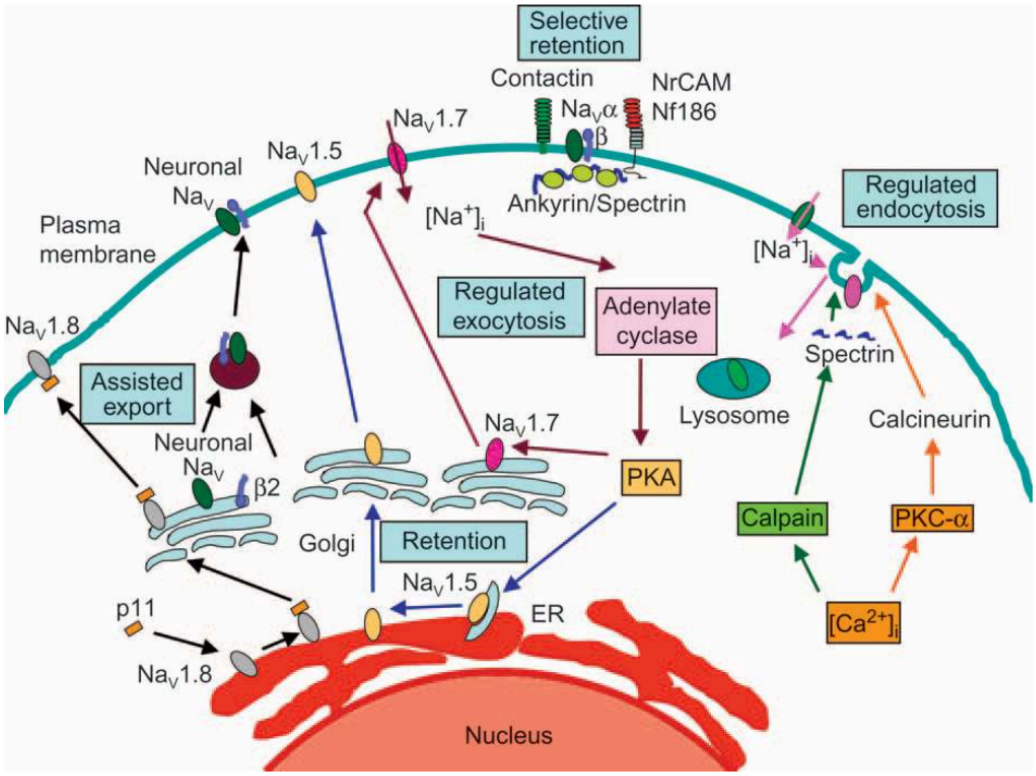

Figure 1.6 Multiple regulatory mechanisms for VGSCs expression.
Summary of voltage-gated sodium channels (VGSCs) regulatory mechanisms that may regulate surface expression, such as, ER retention, surface retention, regulated endocytosis, regulated exocytosis and assisted export. ER, endoplasmic reticulum. NrCAM, neuronal cell adhesion molecule. (Taken from Cusdin (2008)

Also regulating the expression at the plasma membrane are mechanisms for endocytosis and retention. In adrenal chromaffin cells, an increase in intracellular Ca2+ during sustained activation increases levels of PKCα and calcineurin (Yanagita et al. 2000, Yanagita et al. 1996). This pathway and changes in intracellular Na^+ concentration (Paillart et al. 1996) lead to endocytosis and subsequent lysosomal degradation (regulated endocytosis, Figure 1.6). Selective retention by specialised membrane proteins also interferes in VGSC regulation. For instance, contactin, a glycosyl-phosphatidylinositol-anchored CAM protein expressed by neurones, associates with VGSCs and increases its functional expression (Kazarinova-Noyes et al. 2001).

The balance of the VGSCs is tightly regulated and its imbalance alters the excitability and pain sensation. Changes in VGSCs leads to

electrophysiological changes that lead to spontaneous and altered frequency of action potential firing. Increased Na^+ conductance via increased VGSC expression at the plasma membrane may be sufficient to lower the threshold for action potential (Waxman et al. 1999). In inflammatory pain conditions, changes in pain sensation may be due changes in VGSCs expression induced by inflammatory mediators (Rush and Waxman 2004).

1.5 Inflammatory pain

Pain is a hallmark of inflammation. Tissue injury or infection lead to several inflammatory mediators to be released from damaged neurones, mast cells, t-cells, epithelial cells, macrophages and neutrophils (Figure 1.7). These powerful inflammatory mediators such as ATP, bradykinin, PGE_2, and serotonin are able to acutely change the excitability of DRG neurones (Ji and Strichartz 2004). Innocuous stimuli may be perceived as noxious (allodynia), responses to noxious stimuli may be exaggerated (hyperalgesia), and there is an increase in spontaneous firing leading to spontaneous pain (Meyer and Campbell 1981). These are a reflection of changes in ion channel and receptor's function and expression at the plasma membrane which directly influence many aspects of DRG excitability.

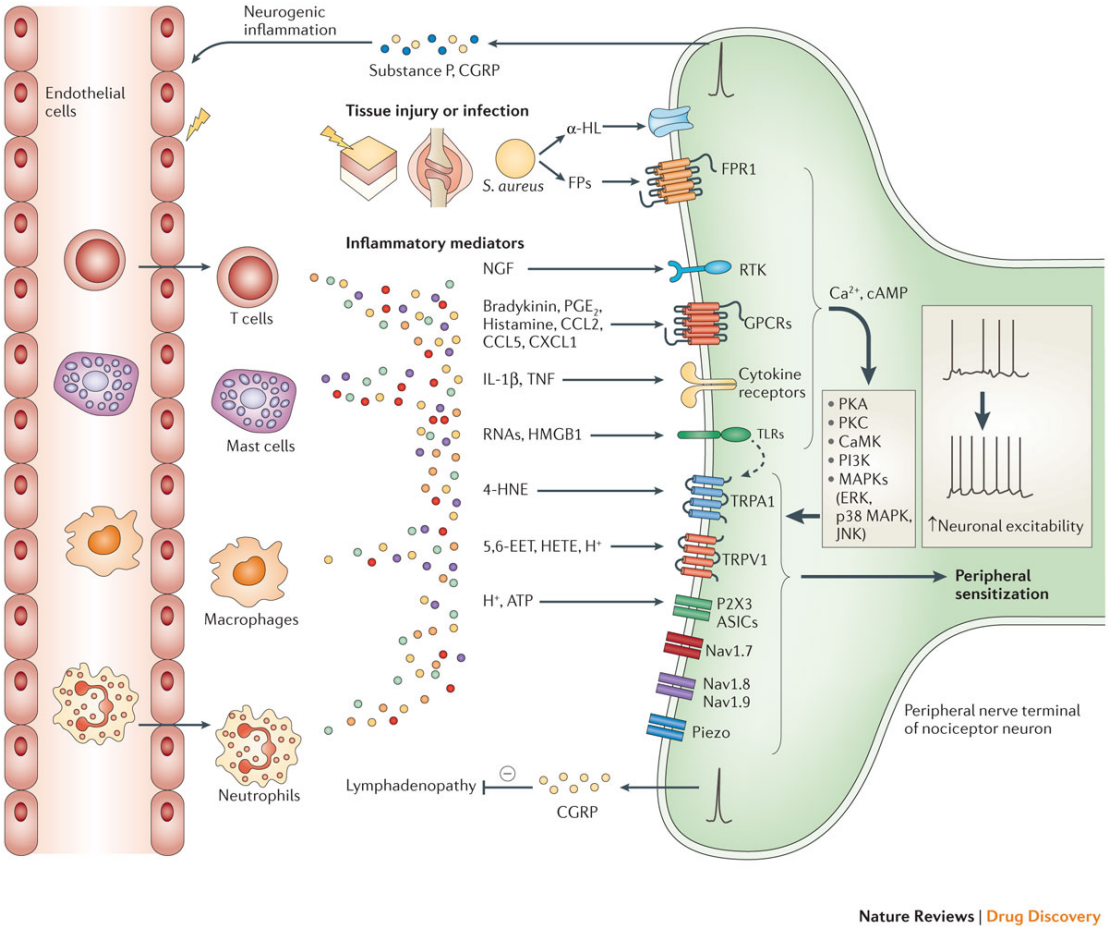

Nature Reviews | Drug Discovery

Figure 1.7 Inflammation elicits pain via inflammatory mediators and peripheral sensitization.

In the event of inflammation, several inflammatory mediators are released at the site of injury from damaged neurones, mast cells, Schwann cells, satellite glia cells, epithelial cells, and infiltrating leukocytes. Powerful inflammatory mediators such as ATP, bradykinin, PGE_2, and serotonin can acutely change the excitability of DRG neurones. (see abbreviation page 11 for further definitions) (Ji, Xu and Gao 2014)

Peripheral sensitization results in increased pain sensation. In subject responses, hyperalgesia is characterised by decreased pain threshold, increased pain in response to suprathreshold stimuli and spontaneous pain (Meyer and Campbell 1981). In *in vitro* models these are characterised by a decrease in the threshold for action potential firing, increased firing to suprathreshold stimuli and spontaneous activity (Cummins et al. 2009). Inflammatory mediators may increase the response given to a specific stimulus, by increasing the current activated, or alter the ease with which action potentials are generated. Focusing on 7 major inflammatory mediators' effects on DRG neurones – ATP, bradykinin, prostaglandin E2, histamine,

noradrenaline, NGF and serotonin – in the context of neuronal excitability are reviewed below.

1.5.1 ATP

ATP is known to alter DRG excitability (Cook and McCleskey 2002, Li et al. 1999). The concentration of ATP extracellularly is elevated following damage. Platelets and cell lysis are a rich source of extracellular ATP (Cook and McCleskey 2002). Injection of ATP in human skin induces pain that is dependent on capsaicin-sensitive neurones (Hamilton et al. 2000). The nociceptors responsible for this response are likely to express $P2X_3$ channels (Burnstock 2009). ATP directly activates nociceptors (Hamilton et al. 2000) and *in vitro* studies have demonstrated that cell damage directly activates inward currents in nearby nociceptors via ATP (Cook and McCleskey 2002). In addition, responses to ATP vary with soma size. Small diameter DRG neurones sensitive to capsaicin showed rapid-desensitizing ATP-activated currents whereas larger diameter insensitive to capsaicin had slower desensitizing ATP-activated currents (Li et al. 1999). In addition to P2X receptors, ATP may also activate P2Y receptors. These are G-protein coupled receptors (GPCRs) that are $G\alpha_{q11}$-linked. CFA increases the expression of $P2Y_2$ (Malin et al. 2008), a receptor that increases intracellular Ca^{2+} linked with increased DRG excitability (Malin and Molliver 2010, Yousuf et al. 2011).

1.5.2 Bradykinin

Bradykinin, a potent pain mediator, sensitizes nociceptors via B_1 and B_2, $G\alpha_q$-linked receptors (Steranka et al. 1988, Khan et al. 1992). B_2 receptors are constitutively expressed in a variety of cells, including DRG neurones. Antagonists to this receptor have shown analgesic and anti-hyperalgesic properties in inflammatory models (Valenti et al. 2010, Cunha et al. 2007). In contrast, B_1 receptors may be upregulated after tissue injury and potentiate currents elicited by TRPV1 activation (Vellani, Zachrisson and McNaughton 2004). Addition of bradykinin to DRG cultures has been shown to depolarise DRG neurones (Jeftinija 1994, Rang and Ritchie 1988). A body evidence

supports this depolarisation is via PKC-ε activation (Cesare et al. 1999). Excitatory effects of bradykinin are inhibited by PKC inhibitors and PKC activators depolarise DRG neurones by opening cation ion channels such as TRPV1 (Burgess et al. 1989, Premkumar and Ahern 2000, Vellani et al. 2001). However, TRPV1 knock out mice are susceptible to bradykinin effects (Katanosaka et al. 2008). Thus, bradykinin's sensitization of TRPV1 alone does not explain nociceptor's response. Furthermore, bradykinin has been shown to alter VGSC currents in DRG neurones. Bradykinin administration prolonged action potential length and inactivation is slowed, while activation was unaffected (Carratu and Mitolochieppa 1989). Possibly via PKA and PKC phosphorylation of the VGSCs. Bradykinin receptors are $G_q\alpha$-linked and may induce the activation of these kinases.

1.5.3 Prostaglandin E_2

Prostaglandin E_2 (PGE_2) is an eicosanoid. Although most eicosanoids do not act directly on nociceptors only enhance the sensation (Ballou et al. 2000), 10 μM PGE_2 has been found to up-regulate TTX-S sodium currents in capsaicin-insensitive type-4 DRG neurones via activation of adenylyl cyclase and PKA (Tripathi et al. 2011), and 1 μM PGE_2 to up-regulate TTX-R currents in neonatal DRG neurones via activation of adenylyl cyclase, PKA, and PKC (England, Bevan and Docherty 1996, Gold, Levine and Correa 1998). Furthermore, PGE_2 increases excitability by reducing the threshold for activation of Nav1.8 and by increasing a hyperpolarisation-activated cyclic nucleotide-gated ion channel (HCN) current (Momin and McNaughton 2009, Gold et al. 1998). Thus, decreasing the time interval between action potentials. PGE_2 administration has also been found to supress potassium outward currents, making the neurones more prone to action potential firing (Nicol, Vasko and Evans 1997). In addition to modulation of voltage-gated sodium channels, PGE_2 modulates the activity of other channels such as TRPV1(Moriyama et al. 2005). Hence, PGE_2 is a powerful modulator of DRG excitability.

1.5.4 Histamine

Histamine is a widely distributed neurotransmitter that has four different types of receptors (H1-4). It has a major role in inflammation, nociception and pruritogenesis. In the CNS, activation of H_1R (also $G\alpha_{q11}$) enhances neuronal excitability and induces strong membrane depolarisation (Brown, Stevens and Haas 2001). For instance, bath application of 10 μM histamine depolarises cholinergic septal neurones by increasing TTX-R conductance, suggesting VGSC modulation (Gorelova and Reiner 1996). Knock out studies (histidine decarboxylase) have shown that histamine modulates acute pain in a dose-response manner possibly due to an interaction with Nav1.8 (Yu et al. 2013). In DRG neurones, histamine potentiates the Bradykinin's effects on nociception (Mizumura et al. 1995) and PGE_2 sensitizes DRG neurones to histamine through cAMP-PKA pathway (Nicolson et al. 2007).

1.5.5 Noradrenaline

Noradrenaline is a key neurotransmitter and it is thought interact with DRG neurones via release from sympathetic nerve endings. It modulates pain through the binding of noradrenaline to α_{1A}, α_{1B}, α_{1D}, and α_{2A} adrenoceptors on DRG neurones (Maruo et al. 2006, Xie et al. 2001, Cheng et al. 2014). This excites DRG neurones and facilitates action potential firing (McLachlan et al. 1993, Devor, Janig and Michaelis 1994, Xie et al. 1995). Yet, activation of α_2 in the absence of nerve injury may have an inhibitory effect on nociception (Takeda et al. 2002, Chakraborty et al. 2017).

1.5.6 NGF

During development NGF is a survival factor but in mature DRG neurones maintains the phenotype by being required for the continued expression of genes (Snider and McMahon 1998). NGF is increased during inflammation and it activates TrkA receptors present in IB4-negative neurones. Binding of NGF to TrkA activates three major signalling pathways: ERK (extracellular signal-regulated kinase), PI3K (phosphatidylinositol-3-kinase) and phospholipase C gamma (PLC-γ) (Kaplan and Miller 2000) which induce the upregulation of various ion channels, including Ca^{2+}, K^{+}(Park et al. 2003), and Na^{+}. Both TTX-S and TTX-R sodium currents are increased by NGF (Fjell et al. 1999a, Leffler et al. 2002, Okuse et al. 1997, Kerr et al. 2001, Gold et al. 1996, Zhang et al. 2002). In NGF-induced hyperalgesia Nav1.8 is essential but not Nav1.9 (Kerr et al. 2001, Fjell et al. 1999b). Hence, increased TTX-R currents are likely due to Nav1.8 upregulation. In culture, NGF also increases TTX-R currents (Omri and Meiri 1990).

1.5.7 Serotonin

Serotonin (5-hydroxytryptamine, 5-HT) may be release by mast cells and platelets druing inflammation. DRG neurones have mRNA for 5-HT_{1B}, 5-HT_{1D}, 5-HT_{2A}, 5-HT_{2B}, 5-HT_{3B}, 5-HT_4 and 5-HT_7 receptors (Nicholson et al. 2003, Amaya-Castellanos et al. 2011). Receptor expression is distinct between DRG subpopulations. For example, 5-HT_3 agonists directly activate c-fiber nociceptors (Moalem, Grafe and Tracey 2005). Their expression is increased in inflammation and 5-HT_3 antagonists reduce pain induced by serotonin injection (Sufka, Schomburg and Giordano 1992). Serotonin has been shown to modulate hyperpolarisation-activated cation current in type-4 DRG neurones (capsaisin insensitive). It binds 5-HT_7 receptors which increase cAMP levels, shifting the voltage dependency of hyperpolarisation-activated cation currents and increasing excitability (Cardenas et al. 1999). In type-2 DRG neurones (capsaicin sensitive), serotonin reduced the threshold for action potential firing possibly via modulation of TTX-R sodium current (Cardenas, Cardenas and Scroggs 2001). Furthermore, it has been described

that the activation of 5-HT_{2C} increases neuronal excitability and mediates sensitisation of TRPV1 (Salzer et al. 2016).

1.4.8 VGSC trafficking in inflammatory pain

Taken together, the effects of the described inflammatory mediators highly modulate PKA, cAMP, and PKC which are known to regulate the expression of VGSCs (Figure 1.6 & 1.7). Single knock out studies for Nav1.7, Nav1.8, and Nav1.9 have shown the importance of these channels in inflammatory conditions (Nassar et al. 2004, Maingret et al. 2008, Amaya et al. 2006, Akopian et al. 1999, Abrahamsen et al. 2008) and changes in their expression are seen in different models of inflammatory pain. Tanaka and colleagues have reported in a carrageenan model of inflammation an increase in Nav1.8 mRNA and TTX-R current (Tanaka et al. 1998). The authors suggest a role for NGF as increased NGF levels have been detected following carrageenan injection (Woolf et al. 1994) and NGF upregulates Nav1.8 gene expression *in vitro* (DibHajj et al. 1996). However, Okuse and colleagues demonstrated in a carefully controlled RNAse experiments that Nav1.8 mRNA changes in a NGF-induced hyperalgesia model do not underlie protein expression changes. Instead these changes occur at the level of post-translation and post-transcription (Okuse et al. 1997). In other inflammation models such as CFA, the TTX-R Nav1.8 was also found to be upregulated (Coggeshall et al. 2004). Using a PGE_2-induced inflammatory model, the importance of Nav1.8 increased transcription was further supported in both acute and chronic inflammatory pain (Villarreal et al. 2005). In addition to TTX-R current increase, Nav1.7 expression and TTX-S current has also been demonstrated to increase in a carrageenan model (Black et al. 2004). Hence, although different inflammatory insults were used Nav1.7 and Nav1.8 seem to consistently upregulate in inflammation. To further understand, the mechanism behind the upregulation of Nav1.7 and Nav1.8, Gould and colleagues pre-treated the animals with ibuprofen (a cyclooxygenase 2 inhibitor and thus interferes PGE_2 synthesis) before injecting with CFA. The pre-incubation with ibuprofen prevented the Nav1.7 and Nav1.8 up-regulation and links the cyclooxygenase

pathway to the upregulation of these channels during inflammation (Gould et al. 2004).

1.7 SNARE proteins

Neurotransmitter release and ion channel upregulation during inflammation are a consequence of vesicular trafficking and membrane fusion (Black et al. 1999, Tanaka et al. 1998, Garry and Hargreaves 1992, Karanth et al. 1991, Kilo et al. 1997, Meng et al. 2016). Membrane fusion is a hallmark of eukaryotic cells. It provides the ability to segregate biochemical reactions within compartments, such as the endoplasmic reticulum, and to communicate between organelles through the exchange of vesicles (Figure 1.8). Organelles such as the endoplasmic reticulum contain proteins that define their functions but also transient proteins on the way to other parts of the cell (biosynthetic transport). A new vesicle is formed from a membrane-bound organelle, the donor, and the cargo loaded to be delivered to the acceptor organelle (Bock et al. 2001). SNARE proteins are the primary mediators of this process, and they regulate multiple trafficking pathways (Martens and McMahon 2008). Exocytosis is the best-studied event of membrane fusion. It is the fusion of a vesicle with the plasma membrane to release its contents such as neurotransmitters (Borisovska et al. 2005).

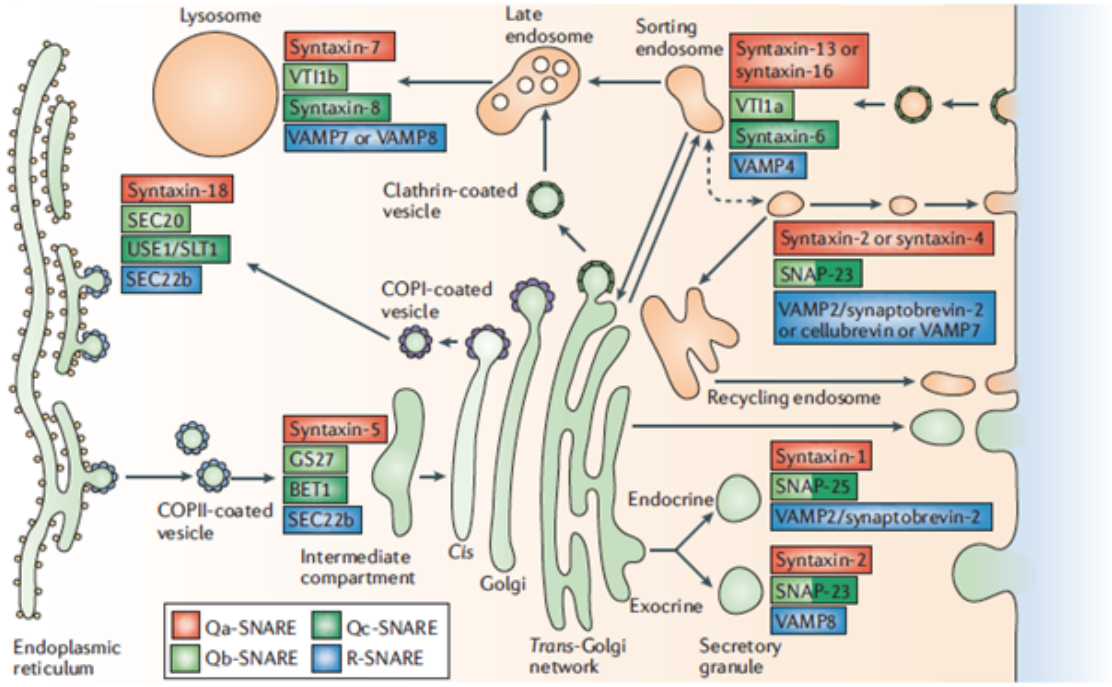

Figure 1.8 The assignment of SNAREs to intracellular membrane-trafficking pathways. VAMP isoforms, also R-SNAREs, are depicted in blue. Specific VAMP isoforms are thought to combine with other specific Q-SNAREs to perform fusion events within the biosynthetic transport pathway (Taken from Jahn and Scheller 2006).

The human SNARE superfamily has 36 members localised in different intracellular compartments (Figure 1.8), and members are characterised by the presence of one or two SNARE motifs (a unique 60 - 70 amino acid sequence). Originally, SNARE proteins were subdivided as t-SNAREs, those present at the ‘target’, the acceptor membrane, and v-SNARES, for ‘vesicular’, and present in vesicles. However, multiple SNAREs can be found in both the vesicles or the target. Hence, another classification subdivides them as Q-SNARES or R-SNARES and it is based on the presence of arginine and glutamine residues in the SNARE motif (Figure 1.8)(Fasshauer et al. 1998). Q-SNARES are further subdivided in Qa-, Qb-, Qc- and Qbc-SNAREs according to their similarity to syntaxin and SNAP25 (both members of the Q-SNARE subdivision) (Hong 2005, Bock et al. 2001).

The role of SNARE proteins in membrane fusion was first revealed from a crystal structure of a neuronal SNARE complex. The crystal exhibited four SNARE motifs: two SNARE motifs from SNAP25, one from syntaxin 1A and another from VAMP (Vesicle-associated membrane protein) (Sutton et al.

1998). One mechanistic model of vesicle fusion to the plasma membrane supports that 4 SNARE motifs are required to come together in a four-helix bundle (trans-SNARE complex, Figure 1.9). This trans-SNARE complex is composed of Qa-, Qb-, and Qc- SNAREs and R-SNAREs. Thus, one member of each class is necessary to form a SNARE complex (QabcR). These complexes are energetically favourable and drive docking and fusion of the vesicle with the membrane (Figure 1.9) (Jahn and Scheller 2006). Different combinations of Qa/Qb/Qc/R-SNAREs form at different steps intracellularly (Figure 1.8). However, some complexes, which do not contain one member of each class, such as Qaaaa or QbccR have been shown to fuse in artificial systems (Yang et al. 1999, Feldmann et al. 2009). It is possible that these non-viable complexes in biological systems are formed to inhibit the formation of other SNARE complexes (Feldmann et al. 2009).

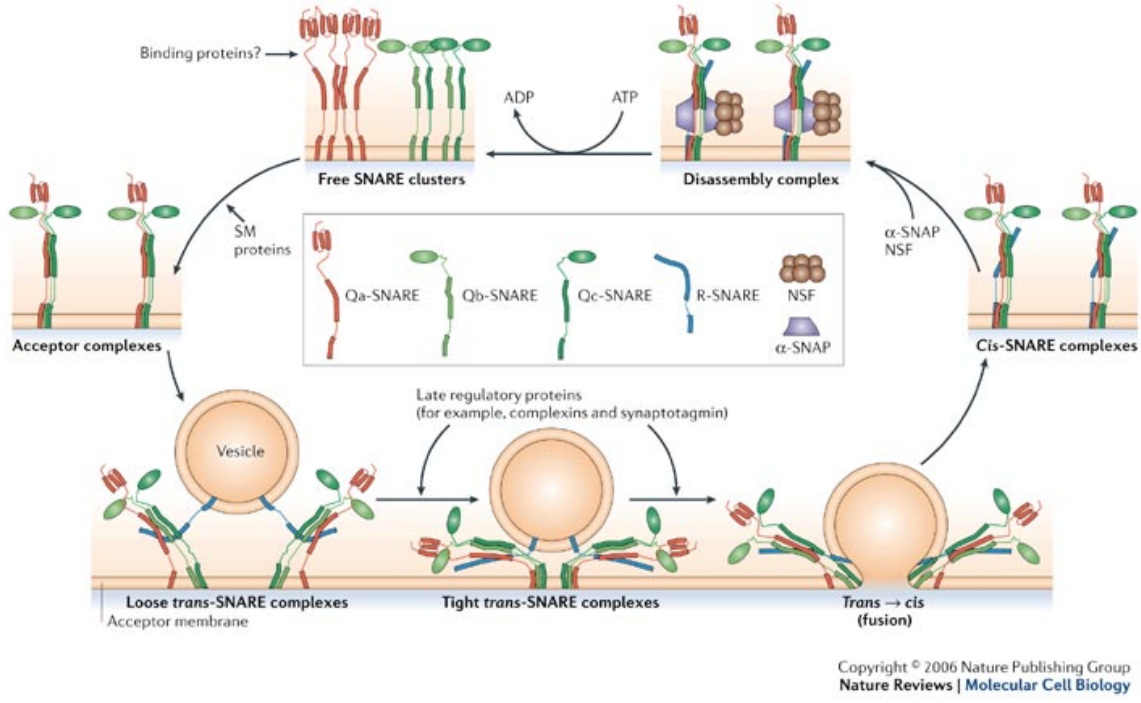

Figure 1.9 The SNARE conformational cycle during vesicle docking and fusion.
SNARE complexes assemble at the acceptor membrane first as “loose” complexes (bottom left). Regulatory proteins aid the in the fusion process, resulting in “cis”-SNARE complexes and complete membrane fusion (middle right). NSF and α-SNAP bind and form disassembly complexes which are then removed in an energy consuming reaction. SM proteins rearrange Trans-SNARE complexes spatially and temporally. NSF, N-ethylmaleimide-sensitive factor. SNARE, N-ethylmaleimide-sensitive factor attachment protein receptor. (Taken from Jahn and Scheller 2006)

Controlling the trans-SNARE complexes are complexins and SM proteins. Complexins associate with tight trans-SNARE complexes, acting as a clamp to fusion until the appropriate Ca^{2+} signal arises. Once the specific transient intracellular Ca^{2+} increase occurs, it triggers vesicle fusion by activating Ca^{2+} sensitive synaptotagmin which reverses the action of complexin and thus allowing fusion to be completed. SM proteins organise the trans-SNARE complex spatially and temporally. There are seven SM proteins: Munc18-1, Munc18-2, Munc18-3, VPS33A, VPS33B and SLY1 (Hong and Lev 2014). SM proteins may regulate the formation of acceptor t-SNARE dimers composed of syntaxin and SNAP-25 as well as contribute to the final fusion step through an as of yet undefined mechanism (Sudhof and Rothman 2009). Once membrane fusion has occurred the cis-SNARE complexes are unzippered and recycled by the N-ethylmaleimide-sensitive factor (NSF) and soluble NSF attachment proteins (SNAPs) (Jahn and Scheller 2006).

SNARE proteins may reside predominantly in one subcellular compartment and participate in specific intracellular fusion steps but this is not the case for all SNARES (Hong 2005). SNARE proteins cannot be the only determinants of specificity as they are present in both anterograde and retrograde vesicles. Additional specificity is provided by accessory and regulatory proteins such as Sec1p, Munc-18, synaptotagmins, Rab, GTPases and their effectors which vary across cell types and trafficking pathways (Bonifacino and Glick 2004).

1.7.1 VAMPs

VAMP proteins are a subgroup of the SNARE family composed of 7 isoforms: VAMP1 and 2 (also synaptobrevin 1 and 2), VAMP3 (cellubrevin), VAMP4, VAMP5 (myobrevin), VAMP7 (tetanus sensitive-VAMP, TI-VAMP) and VAMP8 (Jahn and Scheller 2006). VAMP proteins are anchored to the vesicular membrane through the C-terminal transmembrane domain (Baumert et al. 1989) (Figure 1.10). In contrast to VAMP1/2/3/5 and 8, VAMP4 and VAMP7 have additional N-terminus extensions. VAMP4 contains a di-leucine motif and acidic clusters corresponding to the recycling from the endosome to the trans-Golgi network (TGN) (Zeng et al. 2003) and VAMP7 has a longin domain

involved in both the endocytic and the secretory pathway (Schafer et al. 2012). This is reflected on their molecular size (Table 1.2). Each VAMP isoform has shown differences in tissue distribution and fusion events, which are described below.

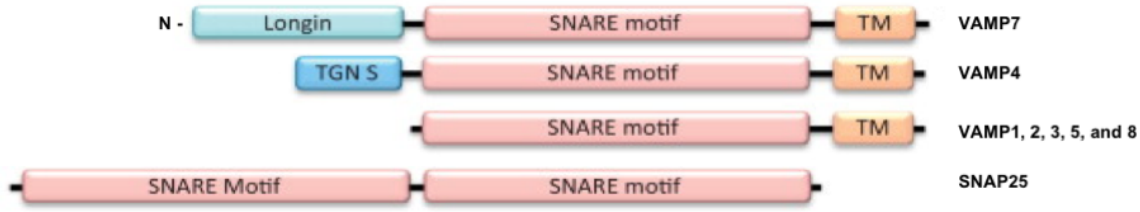

Figure 1.10 Domain organization of the SNAREs discussed in this thesis.
SNAP25, soluble N-ethylmaleimide-sensitive attachment protein 25. SNARE, N-ethylmaleimide-sensitive factor attachment protein receptors. TM, transmembrane. VAMP, vesicle-associated membrane protein. (Adapted from Hong and Lev, 2014)

VAMP isoform	Size (Da)
1	12,753-12,890
2	12,691
3	11,480
4	16,353
5	11,416
7	24,967
8	11,451

Table 1.2 The molecular size of the VAMP isoforms.
VAMP, vesicle-associated membrane protein. From "Emsembl Genome browser" for mouse C57BL6.

1.7.1.1 VAMP1

VAMP1 was the first VAMP isoform described. It was isolated from synaptic vesicles hence it is also known as synaptobrevin 1 (Trimble, Cowan and Scheller 1988, Baumert et al. 1989). VAMP1 knockout mice show severe neurologic defects and die by postnatal day 15 (Nystuen et al. 2007). In VAMP1-heterozygous mice there is loss of Ca^{2+} sensitivity at the

neuromuscular junction due to the absence of VAMP1. Thus, VAMP1 is essential and non-redundant in Ca^{2+} triggered exocytosis at the neuromuscular junction (Liu, Sugiura and Lin 2011). VAMP1 has been detected in CNS, pancreas, kidney, cardiac myocytes and in trigeminal ganglia (Rossetto et al. 1996, Ferlito et al. 2010, Meng et al. 2007). It is thought that VAMP1 also mediates regulated exocytosis in non-neuronal tissues. In mouse trigeminal ganglia neurones, VAMP1 mediates the CGRP release elicited by bradykinin and high K^+ (60 mM) *in vitro* (Meng et al. 2007).

1.7.1.2 VAMP2

VAMP2, or synaptobrevin 2, was also originally isolated from synaptic vesicles (Trimble et al. 1988, Baumert et al. 1989). It has an essential role in Ca^{2+} triggered neurotransmitter release. VAMP2-null mice have shown 100-fold decrease of evoked synaptic exocytosis and die at postnatal day zero (Schoch et al. 2001). In central synapses, VAMP2 is the predominant v-SNARE interacting with the plasma membrane SNAREs, SNAP25 and syntaxin 1, to promote exocytosis (Sudhof and Rothman 2009). VAMP2 has also been detected in non-neuronal tissues such as the kidney (Procino et al. 2008), lung (Wang et al. 2012), pancreas (Regazzi et al. 1995), stomach (Karvar et al. 2002), adipocytes (Martin et al. 1998) and skeletal muscle (Rose et al. 2009), where it also profiles in regulated exocytosis (Mendez et al. 2011, Wang et al. 2012, Regazzi et al. 1995), transport of aquaporin 2 (Procino et al. 2008), and glucose transporter 4 (Rose et al. 2009).

1.7.1.3 VAMP3

VAMP3, or cellubrevin, is ubiquitously expressed and it has been associated with sorting/early and recycling endosomes (McMahon et al. 1993). Yet, deletion of VAMP3 gene in mice exhibits little effects on development or physiological processes, suggesting functional redundancy (Pryor et al. 2004, Antonin et al. 2000a). For instance, VAMP2 and VAMP3 are capable of substituting each other to a varying degree in exocytosis in chromaffin cells (Sorensen et al. 2003, Borisovska et al. 2005).

1.7.1.4 VAMP4

VAMP4 is predominantly localised in the trans-golgi network and early/recycling endosomes (Peden, Park and Scheller 2001, Mallard et al. 2002). However, a recent study has placed VAMP4-enriched vesicles in the hippocampus as the key participants in asynchronous neurotransmitter release. So, in contrast to VAMP2, which is involved in rapid Ca^{2+}-dependent synchronous release, VAMP4 does not readily interact with complexins and synaptotagmin 1, which are required for the fast Ca^{2+}-dependent release (Raingo et al. 2012).

1.7.1.5 VAMP5

Originally cloned as muscle-specific isoform, VAMP5, or myobrevin, has been shown unable to drive vesicular fusion with the plasma membrane's t-SNAREs, syntaxin1/SNAP-25 and syntaxin5/SNAP25 (Hasan, Corbin and Hu 2010). It is not found in the CNS but it is expressed in skeletal and cardiac muscle cells where it is mainly associated with the plasma membrane and intracellular vesicles (Zeng et al. 2003).

1.7.1.6 VAMP7

VAMP7, or tetanus neurotoxin insensitive VAMP (TI-VAMP), was first identified in epithelial cells due to its insensitivity to tetanus neurotoxin (section 1.8) (Galli et al. 1998). Further studies have described VAMP7 in the vesicular transport between endosomes and lysosomes (Advani et al. 1999), trans-Golgi network (Chaineau, Danglot and Galli 2009), but it has also been correlated with synaptic vesicle fusion. Bal and colleagues (2013) have demonstrated that in presynaptic hippocampal neurones, the glycoprotein reelin, an endogeneous neuromodulator, selectively mobilizes vesicles containing VAMP7 (but not VAMP2, VAMP4 or vti1a) independent of electrical activity. In addition, VAMP7 is essential in vesicular mediated neurite outgrowth in staurosporine-differentiated PC12 cells (Martinez-Arca et al. 2000). In

neuronal cultures, VAMP7 has been associated with neurite outgrowth when cultures are coated with laminin (Gupton and Gertler 2010).

1.7.1.7 VAMP8

VAMP8, or endobrevin, is believed to mediate fusion of early and late endosomes. It is ubiquitously expressed and enriched in epithelial cells in the lung, pancreas, intestine and kidney (Wong et al. 1998). In pancreatic acinar cells, VAMP8 null mutations have shown that VAMP8 is the major v-SNARE of zymogen granules and thus enzymatic secretion (Wang et al. 2004).

1.8 Botulinum neurotoxins and chimaeras

Botulinum neurotoxins (BoNT) are extremely potent toxins produced by *clostridium* bacteria to cause muscle paralysis and death. They are subdivided in an enzymatic domain (light chain) and a binding domain (heavy chain) (Figure 1.11 A). All seven serotypes (A, B, C, D, E, F and G) interact with vesicle fusion machinery but all have different modes of action which reflect the duration of the paralysis they cause (Davletov, Bajohrs and Binz 2005). BoNT/A (commercial name BOTOX) cleaves the SNARE protein SNAP25 and is already used for a number of disorders arising from hyper activity of autonomic or motor neurones. Importantly, in a clinical trial with chronic migraine sufferers the administration of BOTOX significantly reduced the number of migraine attacks (Dolly and O'Connell 2012). Other serotypes such as BoNT/B, BoNT/D, BoNT/F and BoNT/G are known to cleave VAMP1, VAMP2 and VAMP3 (see Appendix 4 for cleave sites) (Foran et al. 2003, Schiavo et al. 1992, Yamasaki et al. 1994). Hence, BoNTs are powerful tool in understanding the function of SNARE proteins in cellular physiology.

Tetanus toxins (TeNT) have similar structural features to BoNTs. It also has an enzymatic and binding domain. However, TeNTs bind at the presynaptic membrane of the neuromuscular junction and it is transported to the spinal cord whereas BoNTs intoxicate the neuromuscular junction. The enzymatic domain of TeNTs cleave VAMP2 (Montecucco, Schiavo and Rossetto 1996).

1.8.1 Mechanism of action

Botulinum and tetanus neurotoxins bind gangliosides found at the plasma membrane (PM) to gain entry to the intracellular medium (Figure 1.11 B). Different BoNT serotypes and TeNT are thought to use different gangliosides: Synaptotagmin is used by BoNT/B and BoNT/G; synaptic vesicle protein 2 is used by BoNT/A/D/E/F; and glycosylphosphatidylinositol(GPI)-anchored proteins is used by TeNT (Blum et al. 2014). Once bound to the ganglioside the neurotoxin is endocytosed and the acidity of the endosome leads to the cleavage and reduction of the neurotoxin (Figure 1.11 B ii and A). Consequently, the separated enzymatic domain, the light chain, can then cleave the target SNARE as described above and impair neurotransmission (Davletov et al. 2005).

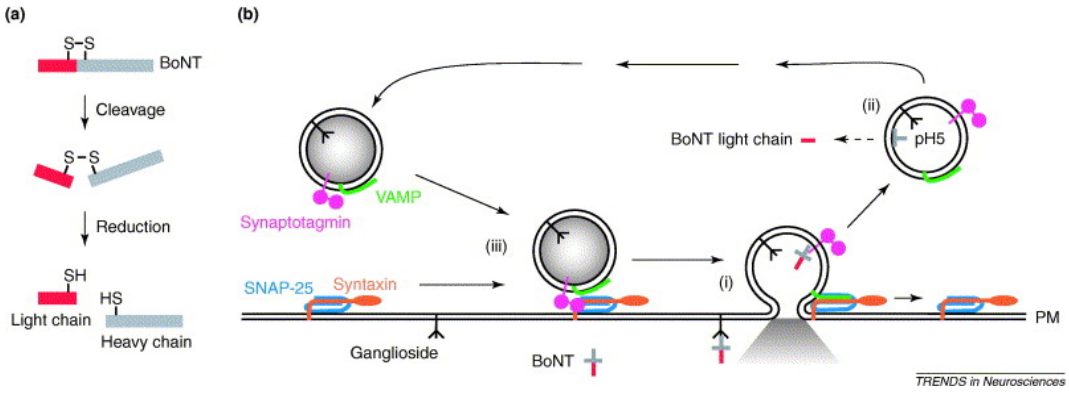

Figure 1.11 Mechanism of action of botulinum neurotoxins.
(A) Botulinum neurotoxins (BoNTs) have their disulphide bonds cleaved and reduced once they gain entry in the cell, and thus separating the enzymatic domain (light chain). (B) BoNTs gain entry intracellularly by binding gangliosides (via heavy chain) at the plasma membrane. During endocytosis (i) the BoNTs are taken in by the cells, low pH (ii) causes the separation of the light chain, which is then freed to cleave its target (iii). (Taken from Davletov 2005).

1.8.2 Tetbot A and tetbot B

Tetbot A and tetbot B are chimaeras of the botulinum and tetanus neurotoxins (Designed by the Davletov group, University of Sheffield). They both have the binding domain of TeNTs but differ in the enzymatic domain, tetbot A has BoNT/A, and tetbot B has BoNT/B. Hence, tetbot A cleaves SNAP25 (Ferrari et al. 2013) and tetbot B cleaves VAMP1/2/3. In rats, intrathecal pre-injection

of tetbot A has been shown to reduce the effects of CFA hindpaw injection by significantly reducing mechanical hypersensitivity (Ferrari et al. 2013).

1.8 Aim and objectives

During inflammatory pain, the release of inflammatory mediators alters the function of nociceptors (section 1.5). Nociceptors show increased neurotransmitter release, hyperexcitability and changes in the expression of ion channels. Although it is possible that other processes are involved in the regulation of ion channels' expression at the plasma membrane (section 1.4.9), this thesis aimed to explore the role of SNARE proteins in the excitability induced by inflammatory mediators.

Objectives:

- to establish an *in vitro* inflammation model
- to investigate the effects of combined inflammatory mediators on VGSC trafficking
- to identify the VAMP isoforms expressed in DRG neurones
- to explore the potential of the engineered toxins, tetbot A and tetbot B, to regulate peptide secretion and inhibit excitability changes induced by the inflammation model

2 – Materials and methods

2.1 Animals

C57/BL6 male mice were used in this project were from a house colony. The initial breeding pairs were purchased from Charles River (U.K.) and these were regularly replaced to avoid inbreeding. For immunocytochemistry and western blotting experiments mice were 8-14 weeks old whereas for patch clamp experiments mice were 6-8 weeks old. This difference is due optimisation of patch clamp recordings. More recordings were possible when younger animals were used. All animals were culled by cervical dislocation in accordance with the Animals (Scientific Procedures) Act 1986 Amendment Regulations 2012.

2.2 Plate and coverslip coating

2.2.1 Matrigel

Matrigel basement membrane matrix aliquots (BD, 356231) were defrosted at 4ºC for at least 2 h. Borosilicate glass coverslips (thickness 1.5, VWR) washed in 70% ethanol and autoclaved were added to 12 or 24 well plates and placed in the fridge to cool. Once the matrigel aliquot defrosted, it was diluted with sterile distilled water (25 µl/mL) and layered onto coverslips using ice-cold autoclaved pipette tips. The excess was removed by tipping the plate. The coated coverslips were then incubated for 20-30 min at 37ºC.

2.2.2 Poly-L-lysine

Borosilicate glass coverslips (thickness 1.5, VWR) were washed in 70% ethanol and autoclaved. Poly-L-lysine hydrobromide (Sigma-Aldrich) was prepared in sterile distilled water (100 µg/mL) and applied to the coverslips (or plate when generating lysates for western blot). The coverslips were subsequently incubated for 30min at room temperature and washed three times with phosphate-buffered saline (PBS, Sigma-Aldrich). The coverslips were left to dry in the hood until use.

2.2.3 Laminin

Laminin (Gibco) at 20µg/mL was added to poly-L-lysine coated coverslips and incubated for 1-2 h. The laminin excess was removed after incubation by washing the coverslips three times with sterile distilled water just before plating the cells.

2.3 DRG isolation and culturing

2.3.1 Cell preparation for Immunocytochemistry (Chapter 2)

Dorsal root ganglia neurones were removed from mice and put in ice-cold PBS. After removing the connective tissue the ganglia were put into an enzyme solution containing 0.588 mg/ml collagenase XI (2U/mg), 0.98 mg/mL Dispase II (0.84U/mg), 155 mM sodium cloride, 4.8 mM sodium hepes, 5.6 mM hepes, 1.5 mM dipotassium phosphate and 10 mM glucose (all Sigma-Aldrich) at pH7.3 37ºC 5% CO_2 for one hour. The neurones were then dissociated by triturating up and down with a 1000 µL pipette and spun down 134 g in a 15% Bovine albumin solution (Sigma-Aldrich). The pellet was resuspended in 5 mL culture medium [Dulbecco's modified Eagle's medium F12 with glutamax (Life technologies), 10% foetal bovine serum (Life technologies) and 1% penicillin/streptomycin (Gibco)] and spun down 134 g. The matrigel-coated coverslips were prepared and the isolated neurones (from the pellet) were added. After one hour, the wells were flooded with more culture medium (12 well plate 1 mL per well). Details about the duration of DRG culture (24h or 48h) are referred in the results section as it varies between experimental sets.

2.3.2 Cell preparation for immunocytochemistry (Chapter 1 and 3), patch clamp and western blot

Dorsal root ganglia neurones were removed and put in ice cold PBS. Once dissection was completed the supernatant was removed and the ganglia resuspended in medium [Dulbecco's modified Eagle's medium F12 with

glutamax (Life technologies), 10% foetal bovine serum (Life technologies), 1% penicillin/streptomycin (Gibco), 47 mM glucose (Sigma)] containing 500 μg/ml collagenase (Sigma). After incubating for 30 min at 37ºC the collagenase solution was removed and replaced with 0.25mg/ml trypsin-EDTA (Sigma) and incubated again for further 30min at 37ºC. Once the trypsin-EDTA digestion finished the neurones were washed by adding 9 mL of medium and centrifuged for 1 min 134 g twice. To isolate the neurones within the ganglia the pellet was resuspended in 2 mL and triturated with a 19G needle (5 times) and 23G needle (3 times). The isolated DRG neurones were then washed by adding 8 mL of medium and spun down for 3 min 134 g. The isolated neurones (pellet) were resuspended in medium and added to poly-L-lysine/laminin coated coverslips with cloning cylinders (Sigma-Aldrich).

2.3.3 *In vitro* inflammatory model

In this project I have used an inflammatory soup to produce an *in vitro* model of inflammation. This soup consisted of 2 μM ATP disodium salt hydrate (dissolved in dH_2O), 50 nM bradykinin acetate salt (dissolved in 0.1 M acetic acid), 500 nM prostaglandin E (dissolved in dH_2O), 1 μM histamine dihydrochloride (dissolved in dH_2O), 500 nM (-)-noradrenaline (dissolved in 0.5 M HCl), 50 ng/mL nerve growth factor β from rat (dissolved in 0.1% bovine serum albumin) and 1 μM serotonin hydrochloride (dissolved in dH_2O) all compounds from Sigma-Aldrich. This selection is based on previous published experiments by Maingret et al 2008. The appropriate solvent controls were performed side by side. All ingredients were mixed together in a master stock and frozen at -20ºC until use except for serotonin, which was made up fresh on each day to guarantee its full activity.

2.4 Immunocytochemistry

2.4.1 Immunocytochemistry

After 24-48h in culture medium the neurones were washed with PBS and fixed for 10 min at room temperature with 4% paraformaldehyde 4% sucrose in PBS.

Followed by permeabilization for 10 min with 0.1% Triton X100 (for intracellular epitopes), blocking for 2 h with 0.2% fish skin gelatin 0.02% Triton X100 (the latter for intracellular epitopes), and by exposure to the primary antibodies for 16 h. After the primary antibody incubation, the wells containing the coverslips were washed 3 times (each 15min incubation) with the blocking solution. The secondary antibodies were added afterwards and incubated for further 2 h at room temperature wrapped in foil. The unbound secondary antibodies were washed out with PBS with 3 incubations 15 min each. Just before mounting slides were cleaned with 70% ethanol solution and a drop of mounting media was added (southern biochem). Lastly, the coverslips were dipped in distilled water and carefully placed on top of each mounting media drop. The coverslips were then secured with nail varnish.

Antibody		Species	Source	Dilution Immunocytochemistry	Dilution Western blot
VAMP1	Polyclonal	Rabbit	Synaptic Systems	1:500	1:1000
VAMP2	Polyclonal	Rabbit	Synaptic Systems	1:500	1:2500
VAMP3	Polyclonal	Rabbit	Synaptic Systems	1:500	1:1000
VAMP4	Polyclonal	Rabbit	Andrew Peden's lab	1:500	1:1000
VAMP5	Polyclonal	Rabbit	Synaptic Systems	1:100	1:2000
VAMP7	Polyclonal	Rabbit	Andrew Peden's lab	1:100	1:500
VAMP8	Polyclonal	Rabbit	Andrew Peden's lab	1:100	1:1000
β -III tubulin	Monoclonal	Mouse	R&D systems	1:1000	1:1000
Nav1.7 (intracellular)	Monoclonal	Mouse	Neuromab	1:1000	N/A
Nav1.7 (extracellular)	Polyclonal	Rabbit	Alomone	1:1000	1:200
Nav1.8	Polyclonal	Rabbit	Alomone	1:500	1:200
Nav1.9	Polyclonal	Rabbit	Alomone	1:500	1:200
Navβ4	Polyclonal	Rabbit	Alomone	1:500	1:800
VR1	Polyclonal	Goat	Santa Cruz	1:100	N/A
SNAP25	Monoclonal	Mouse	Synaptic Systems	N/A	1:1000
Cleaved SNAP25	Polyclonal	Mouse	Bazbek Davletov's lab	1:1000	NA
Alexa Fluor 488	N/A	Goat	Life Technologies	1:1000	N/A
Alexa Fluor 594	N/A	Goat	Life Technologies	1:1000	N/A

Table 2.1 List of antibodies used.

2.4.2 Image deconvolution

High resolution deconvolved images were generated using a Deltavision RT system (Applied Precision, Issaquah, Washington). Images were collected using a 60x oil immersive objective 1.4 N.A., a Photometrics CoolSnap HQ2 CCD camera and the software SoftWorx. The landweber algorithm was used to deconvolve the images.

2.4.3 Confocal microscopy

Confocal line-scanning was performed using a Nikon A1 confocal system (Tokyo, Japan) with an oil immersive objective 60x 1.4 N.A.. Images were acquired with a resolution of 0.20 μm per pixel.

2.4.4 InCell analyser

The slides were imaged using an "InCell analyser 2200" (GE Healthcare, USA) and single cell analysis using "Developer's toolbox" (GE healthcare, USA). The average diameter of each soma was measured using the β-III tubulin staining when DAPI staining was present (Figure 2.1). DRG neurones were counted positive for the expression of VAMP proteins if the intensity of the staining was higher than 90% of the background intensity of no primary antibody control coverslips.

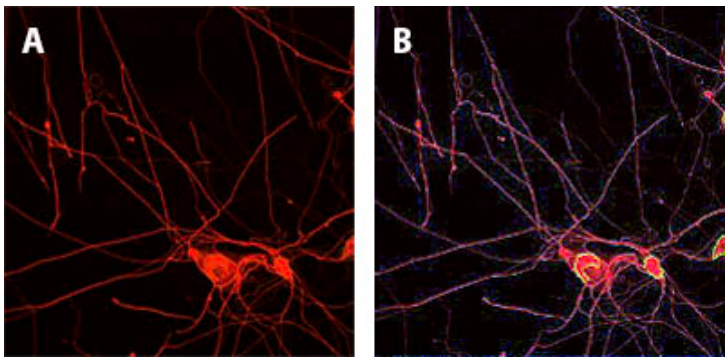

Figure 2.1 Single cell analysis.
(A) Raw image. (B) Image depicting a representative measurement of somata diameter. Using "InCell analyser 2200" software (GE Healthcare, USA) DRG neurones' average diameter was automatically measured (yellow line) according to β-III tubulin staining (red). This example depicts one DRG neurone (left) with a diameter of 10 μm and 5 μm (right).

2.5 Electrophysiology recordings

2.5.1 Patch clamp set up

DRG neurones platted on coverslips were placed on a perfusion chamber on the stage of an inverted microscope (Zeiss Axiovert 100). This chamber was fed by a perfusion system driven by gravity and balanced by an outflow generated by pump made vacuum. Electrophysiology recordings were acquired using an EPC10-USB amplifier (HEKA Elektronik, Germany) with PatchMaster software (HEKA software, version 2.65, Germany).

DRG neurones were chosen according to their binding properties to Isolectin B4 (IB4-FITC). Before each recording coverslips were incubated with 6μg/ml IB4-FITC (Sigma Aldrich) diluted in standard recording solution for 10 min at room temperature (20-22ºC). DRG neurones negative to IB4 were identified using a 488 nm wavelength generated by a monochromator (Polychrome IV unit TILL Photonics LPS-150) and imaged with a 512B CCD camera (Roper Scientific, Photometrics UK). Metamorph® (Meta Imaging) software was used to acquire transmitted and emitted light of each DRG neurone recorded (Figure 2.2).

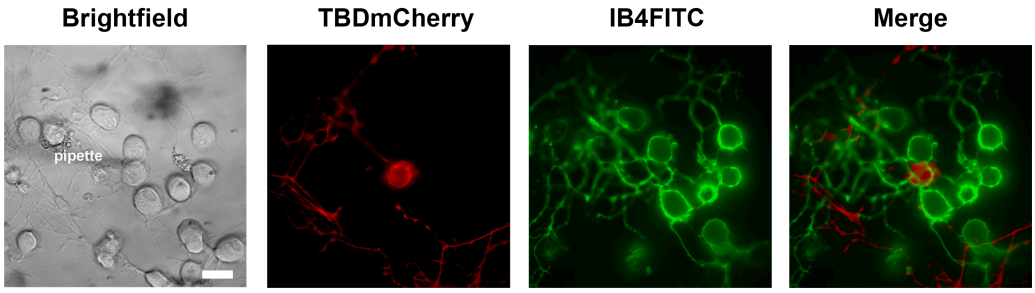

Figure 2.2 Patch-clamp set up, TBDmCherry and IB4-FITC.
(Brightfield) Brightfield representative image of dorsal root ganglia (DRG) neurone with a pipette tip on the left. (TBDmCherry) Tetanus binding domain conjugated with mCherry discriminate non-IB4 positive DRG neurones (Chapter 5, section 5.2.1). (IB4-FITC) FITC signal of the same field. The DRG neurone depicted in the image with the recording pipette position above is not IB4 positive. Scale bar 20μm.

2.5.2 Patch pipettes

Pipettes used for patch clamp recordings were filamented thin-wall galss capillaries (World precision instruments) pulled with a vertical gravity driven puller (Narishige model PC-10, Japan) to achieve a cone shape and resistance of 3.5 - 4.5 MΩ when filled with internal solution.

Patch pipettes were coated with Sylgard® (Dow corning) to reduce pipette capacitance transients during recordings. Sylgard® solution was prepared in advance by mixing 9 parts resin to with 1 part catalyst oil, mixing well and aliquoting in -20ºC until use. The Sylgard® solution was added to the shank of pulled pipettes and heat cured with a fine heating coil.

To increase the chances of a GΩ seal during recordings the sylgarded pipette tips were also fire-polished using a heat filament (Narishige microforge M-83, Japan).

2.5.3 Whole-cell configuration

Patch pipettes filled with internal solution were lowered into the bath while a 200 ms 5 mV voltage step at 5 Hz was applied to monitor pipette resistance. Positive pressure was applied to the patch pipettes to prevent any debri from blocking the tip. Once close to the soma, the positive pressure was released and gentle negative pressure was applied to form a GΩ seal between the pipette tip and the DRG neurone (cell-attached mode). A holding potential of -60 mV was set and pipette capacitance was compensated using the C-fast control. To achieve whole-cell mode, further suction was applied until the membrane at the tip of the pipette was removed and the DRG cell capacitance transients were observed. These were compensated using the C-slow control.

2.5.4 Recording solutions

Standard recording solution contained (in mM): 45 NaCl, 2 KCl, 5 $NaHCO_3$, 10 $C_8H_{18}N_2O_4S$ (HEPES), 10 $C_6H_{12}O_6$ (glucose), 2.5 $CaCl_2$ and 1 $MgCl_2$ adjusted

to pH 7.3 with NaOH and to 310 mOsm with $C_{12}H_{22}O_{11}$ (sucrose). For voltage clamp experiments the VGSC currents were isolated using (in mM): 45 NaCl, 3 KCl, 20 $(C_2H_5)_4N(Cl)$ (tretaethylammonium chloride), 75 $C_5H_{14}ClNO$ (choline chloride), 0.1 $CdCl_2$, 10 HEPES, 1 $MgCl_2$, 1 $CaCl_2$, 10 glucose adjusted to pH7.3 with NaOH and with 300 mOsm adjusted with sucrose. For zero sodium solutions used in voltage clamp 45 mM NaCl was replaced with 45 mM choline chloride.

The internal solution used for current clamp experiments contained (in mM): 130 KCl, 10 $[-CH_2OCH_2CH_2N(CH_2CO_2H)_2]_2$ (EGTA), 10 HEPES, 8 NaCl, 1 $CaCl_2$, 4 Mg_2ATP, adjusted to pH7.3 with NaOH and 300 mOSm with sucrose. The internal solution for voltage clamp experiments contained (in mM): 20 NaCl, 130 $CsMeSO_4$, 10 HEPES, 0.2 EGTA, 0.3 NaGTP, 4 Mg_2ATP adjusted to pH7.3 with CsOH and osmolarity 300-308 mOsm with sucrose. Internal solutions were filtered (pore size 0.2 μm) before added inside the pipettes.

2.5.5 Liquid junction potential

Liquid junction potentials in patch clamp recordings occur when the filled patch pipette enters the bath, this due to the different composition of the internal and the bath solutions. Thus, it is dependent on the diffusion coefficients of the solutions' components, which in turn are dependent on ionic charge and concentration. The liquid junction potential of each internal and recording solution combination can be measured experimentally (Neher 1992). Briefly, by setting the amplifier in current clamp mode with zero current injection and using a 3 M KCl filled pipette as ground electrode when both solutions are then put in contact (first same in the pipette and bath to zero) a voltage difference may be recorded. This is the liquid junction potential. For my experiments, the junction potential measured was 3 mV. Liquid junction potential is not present in whole-cell mode as the recordings were made after the pipette solution has diffused into the cell (Fenwick 1982).

2.5.6 Series resistance

The series resistance (R_s) is the sum of all resistances between the amplifier input and the cell membrane. The current flowing through the circuit goes through the resistance across the pipette (R_p) and the cell membrane (R_m) (Figure 2.3) and this can create two recording errors: voltage drop and reduction of the temporal resolution.

The voltage drop occurs when the series resistance decreases the amount of current flowing through the circuit and thus the voltage at which the cell is being clamped is not the one desired. If the series resistance is compensated the amplifier adjusts its input according to the calculated series resistance. Likewise, the series resistance affects the temporal resolution, as the access time constant is equal to C_m times R_s.

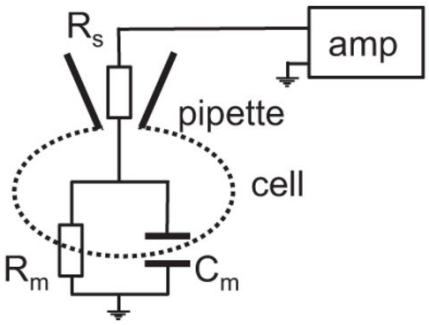

Figure 2.3 A simplified circuit schematic of the patch clamp amplifier.
(amp) amplifier, (R_s) series resistor, (R_m) cell membrane resistor, (C_m) cell membrane capacitance.

When series resistance could not be lowered physically (debris on the pipette tip) it was compensated electronically using R_s comp control. Ideally, the series resistance would be compensated 100% but due to a positive feedback circuitry this may lead to oscillation and cell death. In my experiments, series resistance was 6-15 MΩ compensated 60-70% at 5 μs.

2.5.7 Data analysis

Data analysis was performed using the built in online analysis of PatchMaster software (Heka Eletronik). Graphs were generated with IgorPro (version 6) and GraphPad Prism (version 6.0d).

2.5.7.1 Action potential analysis

Action potentials acquired in current clamp mode were analysed using the action potential analysis function built in from Fitmaster. The parameters are described in the figure below.

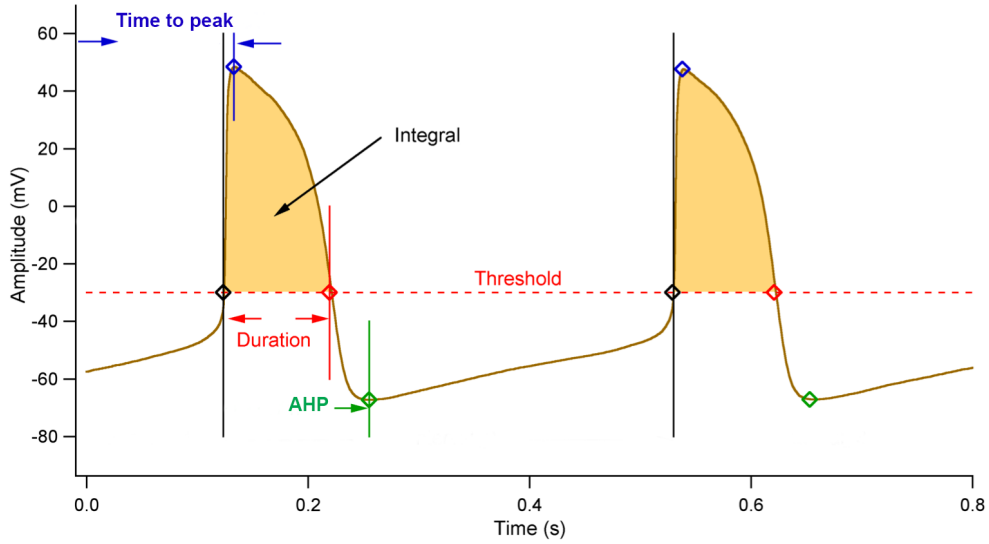

Figure 2.4 Parameters used in the analysis of action potentials.
Image adapted from Fitmaster manual reference 2.90 by Heka Elektronik. AHP, afterhyperpolarisation.

Other parameters not included in the figure:

- Amplitude – peak of the action potential (in blue) to trough of the action potential (in green)
- Overshoot – amplitude of the action potential between the peak (in blue) and 0 mV

2.6 Western blot

2.6.1 Lysate preparation

DRG lysates were prepared straight after dissection or after being cultured for 24-72h. When prepared after dissection, the DRG ganglia were washed in PBS and immersed in complete lysis buffer (RIPA, Sigma-Aldrich, with protease inhibitor II at 0.05%, Fisher Scientific). When collecting DRG from DRG culture, the neurones were washed twice with cold PBS before adding the complete lysis buffer, and scrapped off with a cell scrapper. This cell suspension was then homogenized using a motor pestle (VWR) for approximately 1min at 4ºC and placed on a horizontal rotator for 1 h at 4ºC. The lysed DRG neurones were then spun down for 15 min at 4ºC 15,279 g and the supernatant removed and aliquoted until needed -20ºC.

2.6.2 Protein content quantification

To determine the protein content of the DRG lysates, the DC protein assay kit II (Biorad) was used. The manufactor's instructions were followed. Briefly, a bovine albumin serum standard curve and triplicate sample dilutions were added to a 96 well plate, topped up with a protein detecting agent and incubated for 2 h at 37ºC. Absorbance was measured at 565 nm using a microplate reader, Expert Plus Microplate reader (Biochrom Ltd). The absorbance values generated were then used to determine the protein concentration of the samples.

2.6.3 Loading sample preparation

Loading samples were prepared using a 4X lamelli buffer (Bio-Rad laboratories) and made up at 1:1 ratio. These were boiled at 95ºC (VAMP proteins) or 55ºC (VGSC proteins) for 5 min and gently spun down to remove any precipitate. An equal amount of protein was loaded per lane and pre-stained ladder makers were loaded alongside to identify the size of the protein bands (Fisher scientific 26616 and 26619). To detect changes in protein

amount between samples, the loading concentrations used were below the saturating range of the imaging system (Figure 2.5).

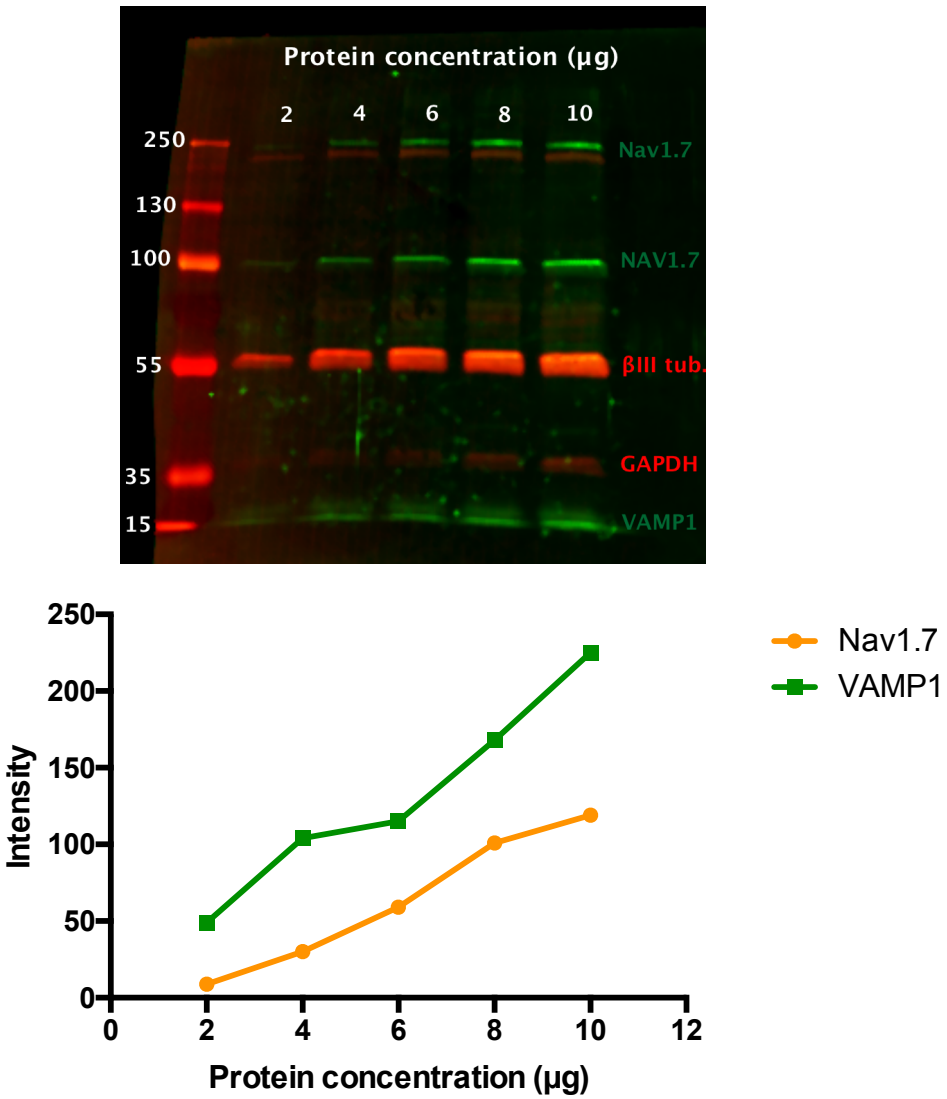

Figure 2.5 Determination of the maximum protein loading.
(Top) Fluorescent image of a western blot imaged with the LiCor system depicting increasing concentrations of DRG lysate. Leftmost lane is the protein size ladder in KDa. Rightmost lane lists the antibodies used. (Bottom) Signal intensity of each band according to the amount of protein loaded.

2.6.4 Protein electrophoresis

Handcast gels were prepared according to the size of the proteins of interest and included a running (7.5% or 15%) and stacking (4%) segment (Table 2.2). The handcast gels were placed in the mini-PROTEAN® electrophoresis system (Bio-Rad laboratories), submerged in running buffer (25 mM

trisaminomethane, 0.2 M glycine and 13.4 mM sodium dodecyl sulfate in dH_2O) and run at 100 mV until a desired protein separation was achieved.

	Stacking gel	Running gels	
	4%	7.5%	15%
Acrylamide 30%	13.5 %	23%	50%
1.5 M Tris-HCl pH8.8	23.5%	28.8%	25%
10% SDS	0.9%	1.15%	1%
dH_20	61.2%	69%	22.9%
10% APS	0.6%	0.3%	1%
TEMED	0.3 %	0.1%	0.1%

Table 2.2 Contents of the gels used for protein electrophoresis.
APS, ammonium persulfate. SDS, Sodium dodecyl sulfate. TEMED, Tetramethylethylenediamine.

2.6.5 Protein blotting

The protein-containing gels were transferred onto a wet transfer system, Mini Trans-Blot® cell (Bio-Rad laboratories), with either a nitrocellulose membrane (pore size 0.2 μm) [GE Healthcare, U.S.A.] or for detection of VAMP3 immune-Blot® PVDF membrane (Bio-Rad laboratories). The electrophoretic transfer was induced by a 100 mV for 1 h (VAMPs) or 20 mV overnight at 4ºC (VGSCs) while submerged in transfer buffer (25 mM trisaminomethane, 0.2 M glycine and 20% methanol in dH_2O).

2.6.6 Blocking and antibody incubations

All membranes were blocked against unspecific binding at room temperature (20-23ºC) for 1 h with 5% semi-skimmed milk – TBST (20 mM Tris, 137 mM NaCl and 0.1% TWEEN® 20 pH7.4 with HCl – all Sigma-Aldrich) except for experiments detecting VAMP3 where 5% semi-skimmed milk – PBST (PBS with 0.1% TWEEN® 20 pH7.4) was used instead.

Once the membranes were blocked for 1 h the primary antibodies were added (see Table 2.1 for details). GAPDH (1:2000 ThermoFisher, USA) and β-III tubulin (1:1000 R&D systems) were used as loading controls and to identify the neuronal content of the samples. All primary antibody incubations were done overnight at 4ºC on a roller and diluted in TBST (PBST for VAMP3).

To remove unbound primary antibodies the membranes were washed 3 times with TBST before the secondary antibodies were added (goat anti-mouse IgG (H+L) secondary antibody DyLight 680 conjugate and goat anti-rabbit IgG (H+L) secondary antibody DyLight 800 [Thermofisher Scientific] both at 1:5000) and incubated at room temperature for 1 h. Which was followed by 3 further washing steps to remove excess secondary antibody.

2.6.7 Membrane imaging and analysis

Once the membrane dried completely it was imaged, analysed and annotated using the Li-Cor odyssey CLx imaging system with Image Studio Lite software (Li-Cor Biosciences Ltd, U.K.). Protein bands were analysed by drawing a box of a set size to measure median intensity in all bands.

2.7 ELISA

DRG calcitonin-gene related peptide (CGRP) was measured using a commercial kit by Phoenix Pharmaceuticals, Inc (USA). This is a competitive enzyme immunoassay with 100% specificity for mouse CGRP within 0 – 100 ng/mL. Experiments were performed as per manufacturer's instructions and plate readings were taken with iMark ™ microplate absorbance reader at 450 nm. Data was plotted and analysed using Graphpad prism package (version 7).

2.8 Microarray

Mouse DRG cultures were cultured for 72 h using standard medium (experiments performed by Drs Seward, Bauer and Nassar). Total RNA was

extracted and processed in collaboration with Paul Heath (Sheffield Institute for Neuroscience). The microarray chip used was an Agilent SurePrint G3 Gene Expression 8X60K. Dr Marta Milo performed the statistical analysis. Probability of positive log-ratio (PPLR) was calculated due to the low n numbers used. This method uses a Baesian hierarchical model to calculate upregulated and/or downregulated genes rather than p values. In this thesis only the control group values are presented.

2.9 Other reagents used

Name	Source	Concentration
Tetbot A	Davletov lab	10 nM (dissolved in 0.4% n-octylglucoside)
Tebot B	Davletov lab	10 nM (dissolved in 0.4% n-octylglucoside)
BoNT/A	Thomas Binz, Hannover Medical School	10 nM
BoNT/D	Thomas Binz, Hannover Medical School	10 nM
Tetrodotoxin	Sigma-Aldrich	300 nM (dissolved in H_2O)

Table 2.3 List of other reagents used.

3 – The effects of an inflammatory soup on DRG excitability and VGSC trafficking

3.1 Introduction

In the event of inflammation, several inflammatory mediators are released at the site of injury from damaged neurones, mast cells, Schwann cells, satellite glia cells, epithelial cells, and infiltrating leukocytes. Powerful inflammatory mediators such as ATP, bradykinin, PGE_2, and serotonin can acutely change the excitability of DRG neurones (Ji and Strichartz 2004), causing innocuous stimuli to be perceived as noxious (allodynia), responses to noxious stimuli to be exaggerated (hyperalgesia), and an increase in spontaneous firing leading to spontaneous pain (Meyer and Campbell 1981). These are a reflection of changes in ion channel function and expression at the plasma membrane which directly influence many aspects of DRG excitability.

Voltage-gated sodium channels (VGSCs) are located in the plasma membrane and play a fundamental role in the generation of action potentials. Altered VGSC expression has a profound effect on the excitability of nociceptors (Lai et al. 2004). Numerous studies have shown increased expression of VGSCs in different models of inflammatory pain. For instance, there is evidence for Nav1.8's upregulation in a carrageenan (Tanaka et al. 1998), NGF (Okuse et al. 1997), CFA (Coggeshall et al. 2004), PGE_2 (Villarreal et al. 2005) inflammatory pain models, and in a model of chronic inflammatory joint pain (Strickland et al. 2008). Thus, VGSCs altered expression during inflammation poses a captivating target in the prevention of hypersensitivity and possibly the chronicity of pain. Here, I aim to further understand the effects of combined inflammatory mediators on VGSC trafficking by establishing an *in vitro* inflammation model and exploring its effects on sodium channel trafficking and activity.

3.2 Results

3.2.1 Inflammatory soup induces hyperexcitability in DRG neurones.

In order to establish an *in vitro* inflammation model, a selection of inflammatory mediators (2 μM ATP, 50 nM bradykinin, 500 nM prostaglandin E, 1 μM histamine, 500 nM noradrenaline, 50 ng/mL NGF and 1 μM serotonin) based on previous published experiments by Maingret et al 2008 were added to isolated DRG neurones 1-2 h after isolation (Figure 3.1) (more details on inflammatory soup see section 2.3.3). The DRG neurones were treated for 22h and before each recording, coverslips were incubated with IB4-FITC for 10 min at 6 μg/mL. As I am primarily interested in nociceptors, in this study, I chose to restrict investigations to only small (definition section 1.2.5) IB4-negative DRG neurones (mostly peptidergic). Furthermore, by only using IB4-negative neurones together with size as selection criteria, I hoped to avoid misinterpreting changes in ion channel function induced by inflammation with differences arising from different neuronal subpopulations. All recordings from DRG neurones included in the analysis had a stable (3 min) resting membrane potential more negative than – 45 mV before applying the protocol and action potential amplitude crossing the 0 mV threshold. All the recordings were paired: one mouse culture was used for the control (solvent control) and the treated group.

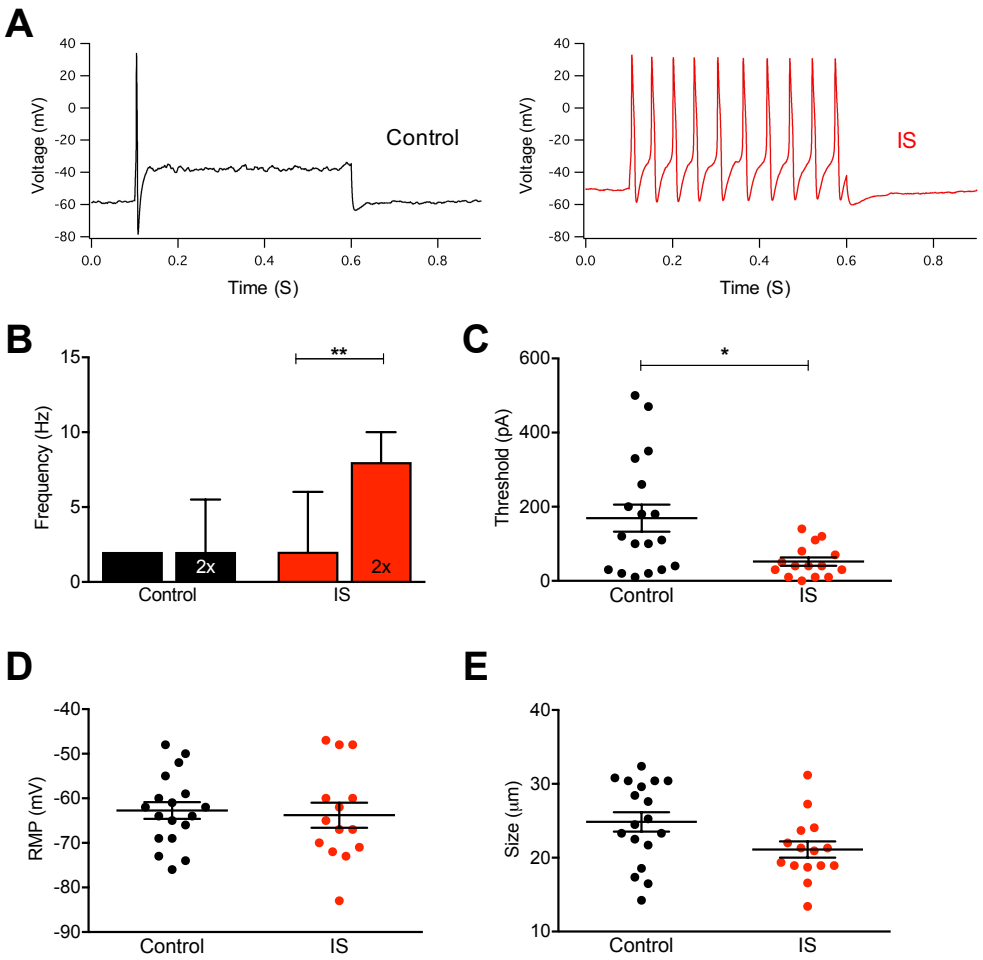

Figure 3.1 The inflammatory soup induces hyperexcitability in DRG neurones.
Isolated DRG neurones were incubated with the inflammatory soup (IS) for 22h, added to the medium 1h after flooding the culture. (A) Representative traces of current clamp recordings at twice rheobase of DRG neurones after 22 h incubation (right) and control (left). (B) Frequency of action potentials at rheobase and twice rheobase (2x, as indicated on the bar), (C) current threshold for action potential, (D) resting membrane potential, and (E) soma diameter. Error bars show SEM except (B) where median with interquartile range is plotted (non-parametric data set). Each data point corresponds to a DRG neuron. In total data from 7 mice are represented. **p<0.01 kruskal-wallis test *p=0.0214 Mann-Whitney test ($n_{Control}$=18, n_{IS}=15, N=7)

The hallmarks of hyperexcitability in neurones correspond to a decreased current threshold and increased firing frequency in response to suprathreshold stimulation (Cummins et al. 2009). Thus, to understand the effects of IS on DRG excitability a series of sequentially increasing current steps were applied to determine the action potential rheobase for each DRG neurone of matched treated and untreated cultures. The frequency of action potentials was quantified at rheobase and twice rheobase (suprathreshold stimuli). Under these conditions, the inflammatory soup induced a significant increase in

action potential frequency (Figure 3.1 B, Kruskal-Wallis test p=0.0003, multi comparisons p<0.01) and a significant reduction in threshold (Figure 3.1 C, Mann-Whitney test p=0.0214). The control DRG neurones had a median of 2 Hz frequency at both rheobase and twice rheobase in contrast to IS treated DRG neurones with a median of 2 Hz at rheobase and 8 Hz at twice rheobase. The threshold median for the untreated DRG neurones was 115 compared with 40 pA for treated neurones ($n_{Control}$=18, n_{IS}=15, N=7). These findings are not due to changes in the resting membrane potential of the neurones (Figure 3.1 D) or differences in size of the DRG neurones recorded (Figure 3.1 E). The resting membrane potential of control DRG neurones was -63 ± 8 mV and for the IS treated -64 ± 11 mV. The soma diameter of the DRG neurones selected for recording in each group was on average 25 ± 6 μm for the control group, and 21 ± 4 μm for the IS treated group. The results of Maingret et al. 2008 had shown increased excitability after 3 min incubation, and these results after 22 h of the addition of the inflammatory mediators further confirm the hyperexcitability in DRG neurones induced by IS incubation but are likely not due to the same mechanisms.

3.2.2 Inflammatory soup does not significantly alter action potential properties but alters timing of the first action potential at twice rheobase.

To further investigate the effects of IS on the action potential's electrophysiological properties, key measurements were taken from the first action potential of both treated and untreated group at rheobase and twice rheobase (Figure 3.2, $n_{Control}$=18, n_{IS}=15, N=7, detailed information on how the measurements were taken can be found in the methods' section 2.5.7.1). The threshold for action potential firing remained unchanged in all four groups of action potentials measured (Figure 3.2 A, control rheobase: -48 ± 7 mV, control twice rheobase: -40 ± 7 mV, IS rheobase: -46 ± 9 mV, IS twice rheobase: -41 ± 9 mV). The threshold is thought to be regulated by the activity of Nav1.7 and Nav1.9, and possibly Nav1.3 (Rush et al. 2007). Similarly, no significant changes were seen in amplitude where Nav1.8 activity is the major contributor

(Figure 3.2 B, control rheobase: 73 ± 28 mV, control twice rheobase: 69 ± 22 mV, IS rheobase: 76 ± 23 mV, IS twice rheobase: 77 ± 14 mV). The afterhyperpolarisation of neurones, mostly a combination of Na^+ channels' inactivation and K^+ conductance, also had no significant changes (Figure 3.2 C, control rheobase: 73 ± 11 mV, control twice rheobase: 70 ± 9 mV, IS rheobase: 66 ± 15 mV, IS twice rheobase: 70 ± 11 mV). The integral, which is an indication of net ionic current as function of voltage (Figure 3.2 D, control rheobase: 47 ± 36 μV, control twice rheobase: 34 ± 18 μV, IS rheobase: 43 ± 41 μV, IS twice rheobase: 33 ± 16 μV), and the action potential overshoot, contributed mainly by Nav1.8 (Figure 3.2 D, control rheobase: 36 ± 9 mV, control twice rheobase: 35 ± 12. mV, IS rheobase: 34 ± 9 mV, IS twice rheobase: 35 ± 8 mV) showed no significant differences with the pre-incubation of the IS. Furthermore, the duration of the action potential showed no differences between groups (Figure 3.2 F, control rheobase: 2± 0.6 ms, control twice rheobase: 2 ± 0.6 ms, IS rheobase: 2 ± 0.6 ms, IS twice rheobase: 2 ± 0.9 ms). Hence, these results suggest that neither the function nor the expression of these channels was altered in this *in vitro* model. Significant changes were only seen at the interval duration between the start of the stimulus and the peak of the action potential (Figure 3.2 G, control rheobase: 18 ± 15 ms, control twice rheobase: 4 ± 3 ms, IS rheobase: 33 ± 24 ms, IS twice rheobase: 8 ± 3 ms). This was significantly decreased with the IS incubation at twice rheobase compared to rheobase ($p=0.02$, one-way ANOVA with Brown-Forsythe post hoc test).

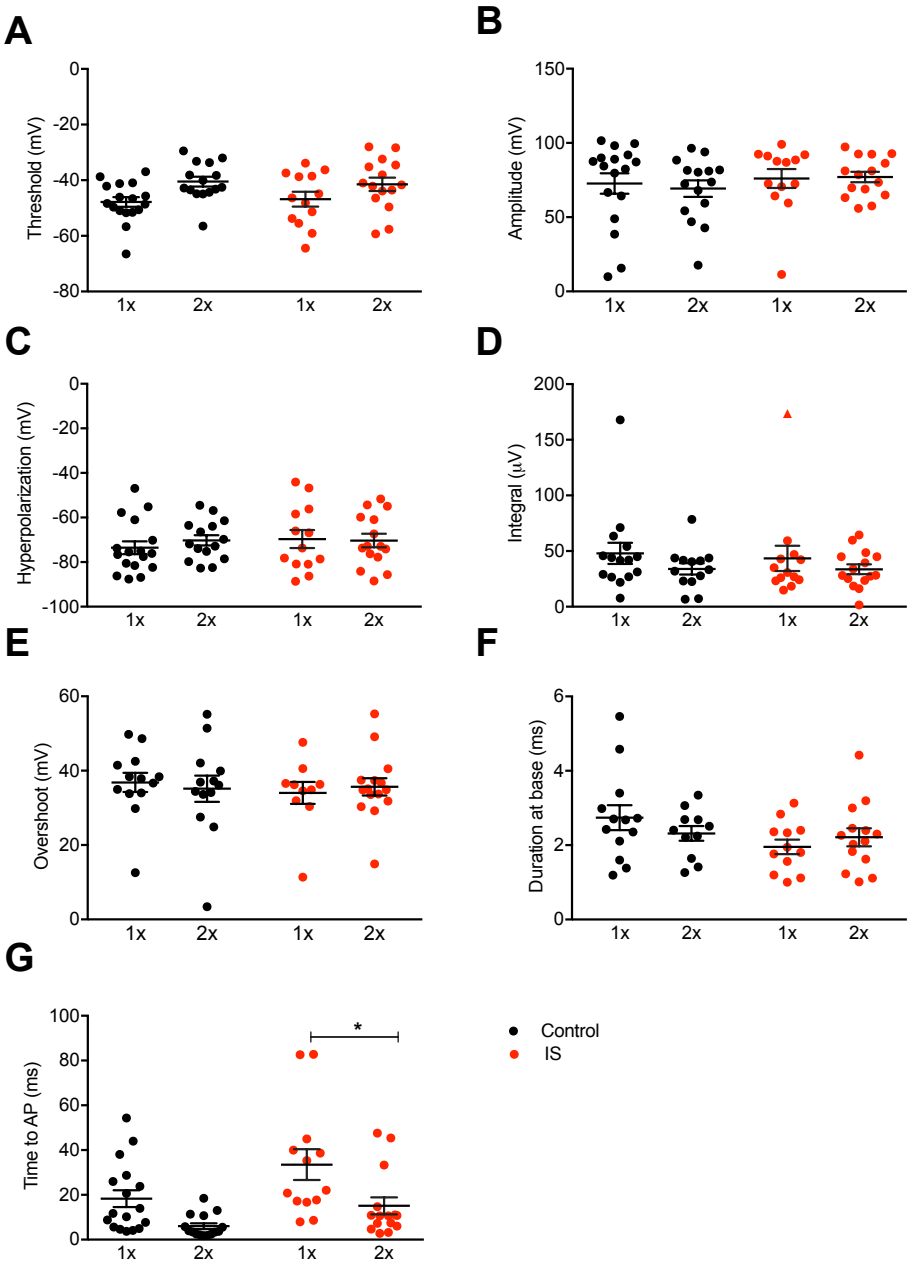

Figure 3.2 Inflammatory soup does not significantly alter action potential properties but alters timing of the first action potential at twice rheobase.
Isolated DRG neurones were incubated with the inflammatory soup (IS) for 22h. Only the first action potential of the rheobase (1x) or twice rheobase (2x) was analysed. (A) Threshold (ANOVA p=0.0304 but lost after post hoc analysis), (B) amplitude, (C) hyperpolarisation, and (D) integral of the action potential from the first to the second threshold crossing, relative to the threshold amplitude. (E) Overshoot and (F) duration of the action potential. (G) The time between protocol initiation and action potential amplitude maximum. Error bars show SEM. Each data point corresponds to a DRG neuron from seven mice. *p=0.02 one way ANOVA with Brown-Forsythe post hoc test ($n_{Control}$=18, n_{IS}=15, N=7)

3.2.3 Inflammatory soup induces hyperexcitability in DRG neurones after 6h incubation

Thus far, the IS soup was added to the DRG neurones' medium for 22h. This time point was chosen to further understand the impact of VGSC trafficking. To maximise the time between DRG culture and experiments, a time course of the effects of the IS incubation on DRG excitability was performed (Figure 3.3). The earliest the IS was added was one hour after plating, and for 22 h, 6 h and 2 h before patch clamp recordings were acquired (Figure 3.3 A). Hyperexcitability was seen only from 6 h (control rheobase: 2 ± 2 Hz, control twice rheobase: 2 ± 10 Hz; IS 6 h rheobase: 2 ± 5 Hz, IS 6 h twice rheobase: 16 ± 26 Hz $p<0.05$) and at 22 h (rheobase: 2 ± 6 Hz, twice rheobase: 8 ± 10 Hz, $p<0.05$ Kruskal-Wallis test, $n_{Control}=15$, $n_{2h}=5$, $n_{6h}=5$, $n_{22h}=12$, N=6). Similar to previous results (Figure 3.1 C), the threshold for action potential firing seems to decrease with the addition of IS. Data acquired in this set of experiments are not significantly different (Median for control: 100 pA, IS 2 h: 90 pA, IS 6 h: 50 pA and IS 22 h: 40 pA; Kruskal-Wallis test $p=0.1075$), revealing a degree of variability between the data sets. The resting membrane potential of the DRG neurones recorded was also not altered by the IS incubation at any of the time points measured (Figure 3.3. D; control: -62.93 ± 6.5 mV, IS 2 h: -65 ± 9.24 mV, IS 6 h: -61.2 ± 5.8 mV and IS 22 h -66.27 ± 8.84 mV).

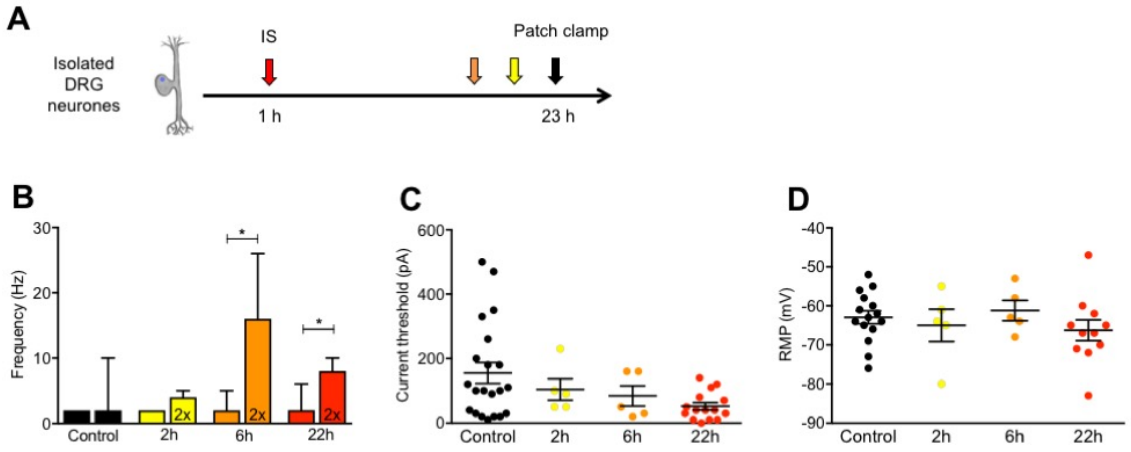

Figure 3.3 Inflammatory soup induces hyperexcitability after 6 h incubation.
(A) Isolated DRG neurones were incubated with the inflammatory soup (IS) for 2h, 6h and 22h. (B) Frequency of action potentials at rheobase and twice rheobase, (C) current threshold and (D) resting membrane potential. Error bars show SEM except (B) where median with interquartile range is plotted. Each data point corresponds to a DRG neuron from six mice. The control set is composed of DRG neurones recorded at 2, 6 and 22 hours, which were found not be significantly different (data not shown). *p<0.05 kruskal-wallis test ($n_{Control}$=15, n_{2h}=5, n_{6h}=5, n_{22h}=12, N=6).

3.2.4 Inflammatory soup (6 h) increases TTX-R sodium currents

Inflammatory mediators have been previously described to increase both TTX-resistant (TTX-R) and -sensitive (TTX-S) currents (Gold et al. 1996, Black et al. 2004, Maingret et al. 2008). After establishing that the IS affects DRG neurones' excitability at 6 h, I aimed to confirm if the observations of increased TTX-R and TTX-S sodium currents could be seen after a 6 h incubation with the IS. Voltage-clamp recordings were established, and the neurones were held at -70 mV. Increasing steps in voltage (-60 mV to 60 mV) were applied to record VGSC current flowing through voltage-gated sodium channels. To isolate VGSC currents, 20 mM tetraethylammonium chloride (blocks voltage-gated K^+ channels) and 0.1 mM cadmium chloride (blocks voltage-gated Ca^{2+} channels) were used in the extracellular solution. Three hundred nanomolar TTX was used to separate Nav1.1/Nav1.3/Nav1.7 (TTX-S) and Nav1.8 & Nav1.9 (TTX-R). No IS was perfused during the recordings.

Representative traces of voltage clamp recordings of DRG neurones of the similar cell capacitance depict an increase in TTX-R currents in DRG neurones treated with IS (Figure 3.4 A). I/V analysis of normalised current to cell body capacitance shows a significant increase in TTX-R current in IS treated DRG neurones (Figure 3.4 B). Average peak current increased from -40.21 pA/pF to -149.3 pA/pF. Total VGSC current also showed increased peak current in IS treated DRG neurones but did not reach significance (control: -117.4 pA/pF IS: -209 pA/pF). No significant changes were seen in TTX-S peak current (control: -105.6 pA/pF IS: -69.51 pA/pF; two-way ANOVA, $n_{vehicle}$=9, n_{IS}=8, N=6). Increased TTX-R peak current likely contributes to the increased excitability associated with IS (Figure 3.1 and Figure 3.3). Nav1.9, a TTX-R channel, is known to contribute to persistent sodium currents and the traces suggest a component of persistent current as the inactivation slope appears slower in treated cells (Figure 3.4 A).

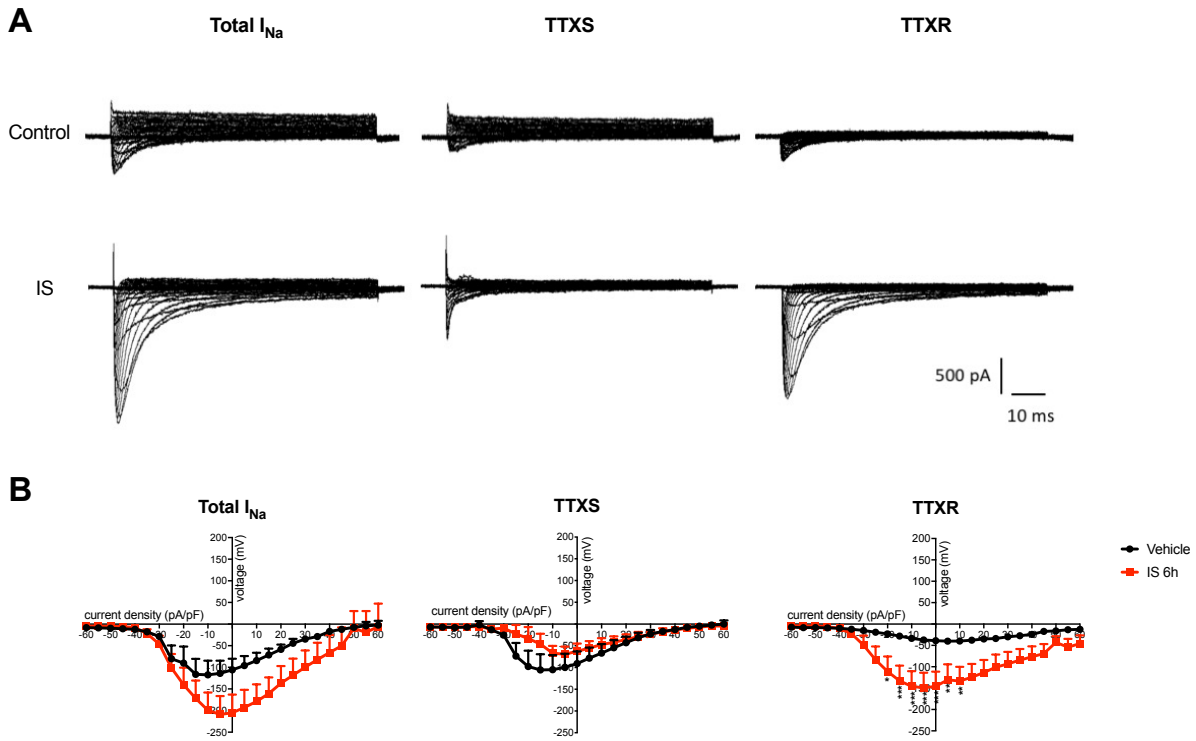

Figure 3.4 Inflammatory soup increases TTX-R sodium current in DRG neurones. Isolated DRG neurones were incubated with the inflammatory soup (IS) for 6h. (A) Representative traces of total VGSC current and the subtracted TTX sensitive and TTX resistant sodium current. (B) Respective I/V curves normalised to cell size (pA/pF). Error bars show SEM. TTXR sodium current is significantly different between control and IS. Two-way ANOVA *p<0.05, **p<0.01 and ***p<0.001($n_{vehicle}$=9, n_{IS}=8, N=6).

3.2.5 Does Inflammatory soup (6 h) induce trafficking of VGSC to the plasma membrane?

Evidence suggests that VGSCs are heavily regulated after an inflammatory insult through phosphorylation or changes in plasma membrane expression (Black et al. 1999, Tanaka et al. 1998, Devor et al. 1989, England et al. 1994, Khasar, Gold and Levine 1998). In this inflammation model, the inflammatory mediators induce hyperexcitability in DRG neurones after 6 h (Figure 3.3). It remains unknown the mechanism underlying these effects if it is due to trafficking of VGSCs, channel modulation and/or changes in other biophysical properties of the DRG neurones (e.g. voltage-gated calcium channels)(Zamponi et al. 2015). Hence, to explore the idea of changes in VGSC trafficking, isolated DRG neurones were fixed after being incubated for 6 h with IS. Antibodies against Nav1.7, Nav1.8, Nav1.9 and Navβ4 were incubated in combination with IB4 (all targeting extracellular epitopes except Nav1.9) (Figure 3.5). These antibodies were also tested in rat cortical neurones to assess specificity (see appendix 1).

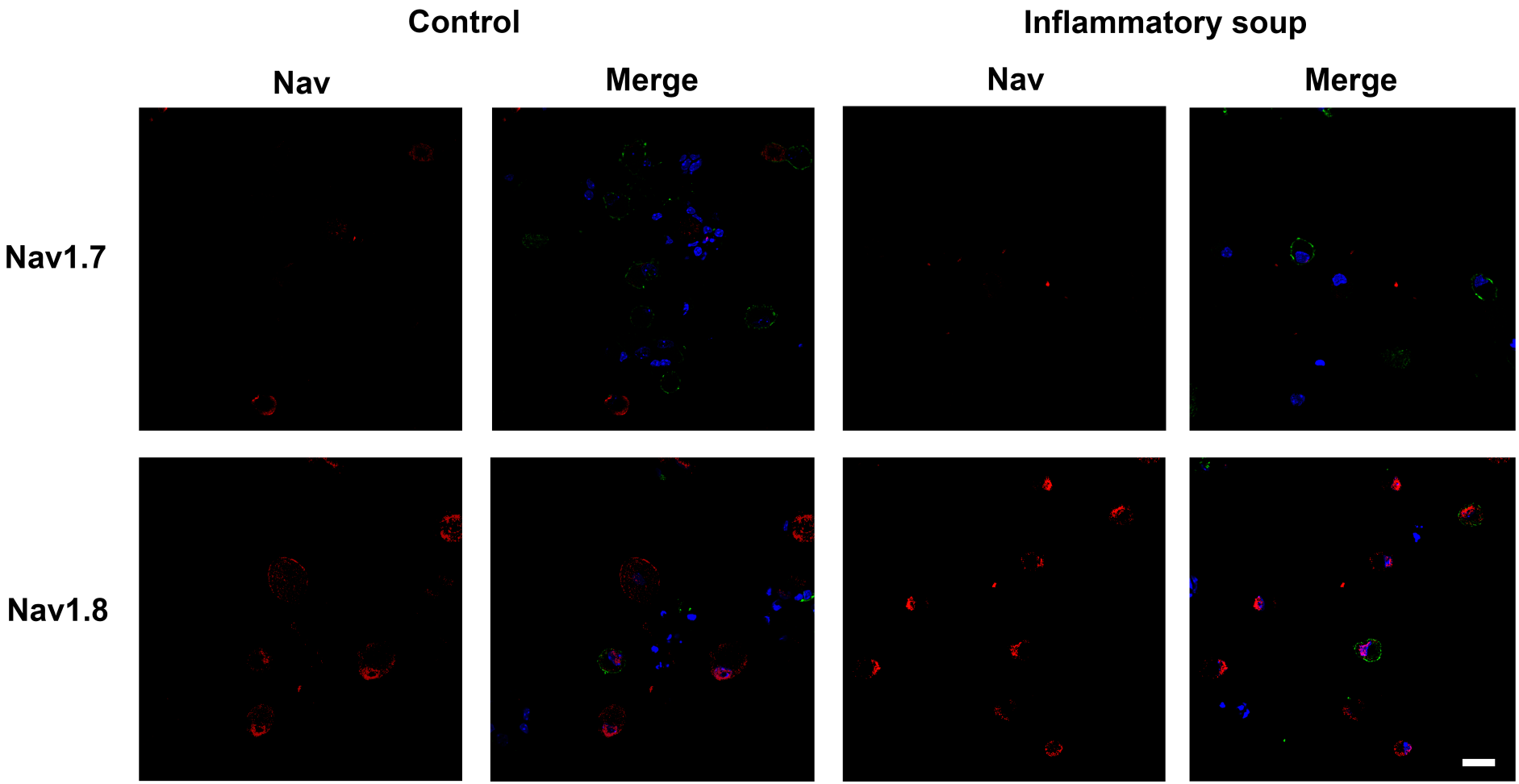
Control
Inflammatory soup
Nav
Merge
Nav
Merge
Nav1.7
Nav1.8

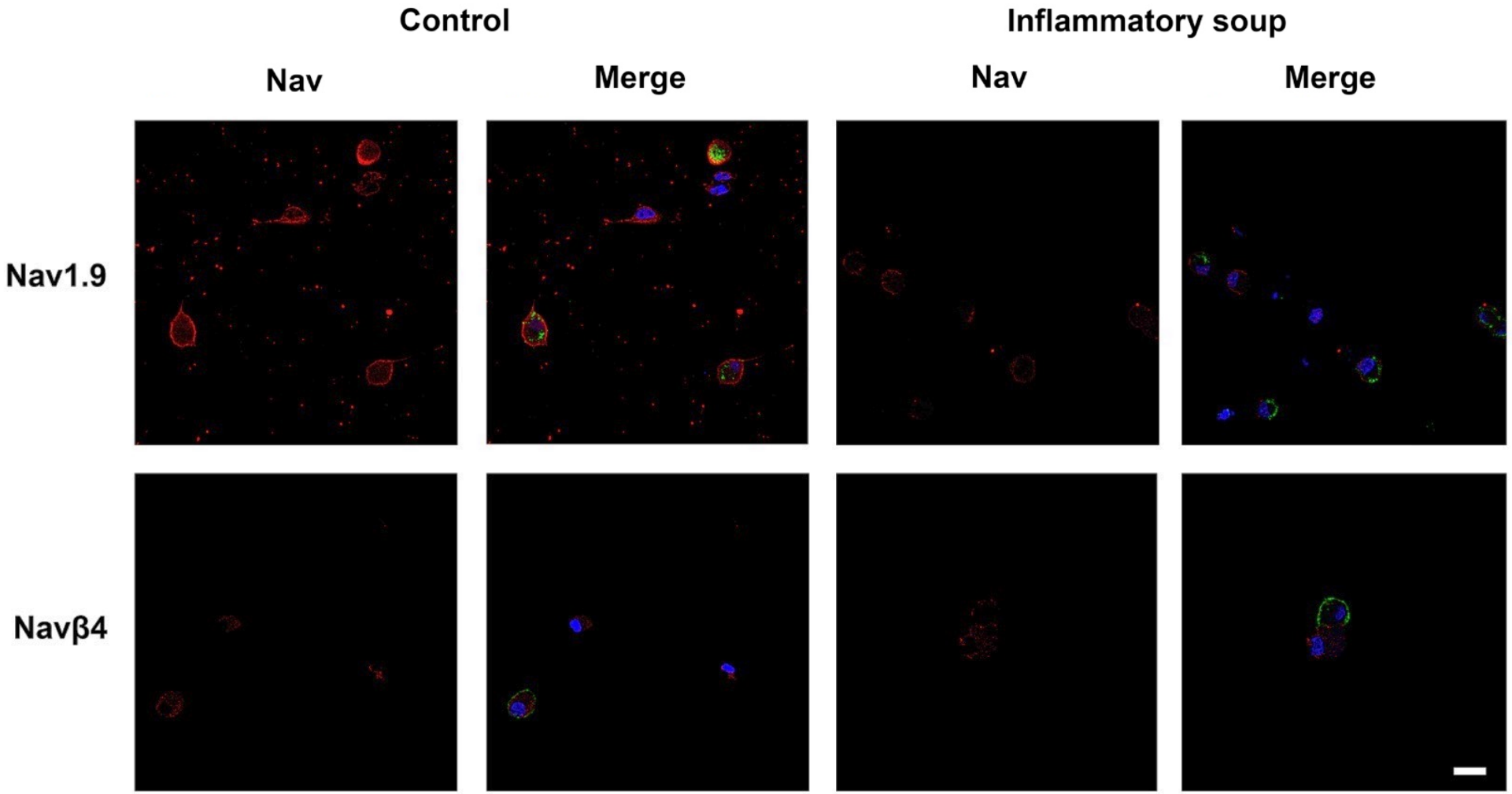
Control
Inflammatory soup
Nav
Merge
Nav
Merge
Nav1.9
Navβ4

Figure 3.5 Representative images of VGSC Nav1.7, Nav1.8, Nav1.9 and subunit Navβ4 expression at the plasma membrane of DRG neurones' soma.
Isolated DRG neurones were cultured for 24 h and incubated with and without inflammatory soup for 6 h before fixing with paraformaldehyde. Immunocytochemistry was performed to identify expression of VGSC Nav1.7, Nav1.8, Nav1.9 and subunit Navβ4 (in red) close to the plasma membrane of treated and untreated neurones. DRG neurones were also probed for IB4 (green) to identify the peptidergic population (IB4 negative) and DAPI (blue) to identify the nuclei. Images were acquired using a confocal microscope. Scale bar shows 20 μm.

VGSC Nav1.7, Nav1.8, Nav1.9 and the subunit Navβ4 were observed at the plasma membrane of both IB4 positive and negative DRG neurones (Figure 3.5). Representative images for each α-subunit and Navβ4 were taken with a confocal microscope at the level of the soma to assess changes in expression (to match electrophysiology recordings from the soma). Surprisingly and in contrast to what was indicated by the voltage clamp experiments (section 3.2.1 & 3.2.4), higher staining intensity was observed for Nav1.7 and Nav1.9 in control conditions than treated with IS. A total of 560 somas were analysed using ImageJ ($n_{Nav1.7}$=169 $N_{Nav1.7}$=3, $n_{Nav1.8}$=154 $N_{Nav1.8}$=4, $n_{Nav1.9}$=164 $N_{Nav1.9}$=3 and $n_{Navβ4}$=73 $N_{Navβ4}$=2). Each soma was analysed by hand drawing a band around the plasma membrane (delimited with the aid of the contrast function and IB4 staining) and measuring the integrated density of the signal. Surprisingly, it strongly suggests a decrease in expression of VGSC Nav1.7 and Nav1.9 at the plasma membrane of DRG neurones following 6 h incubation with IS (Figure 3.6 $p_{Nav1.7}$=0.0207 $p_{Nav1.9}$=0.0043).

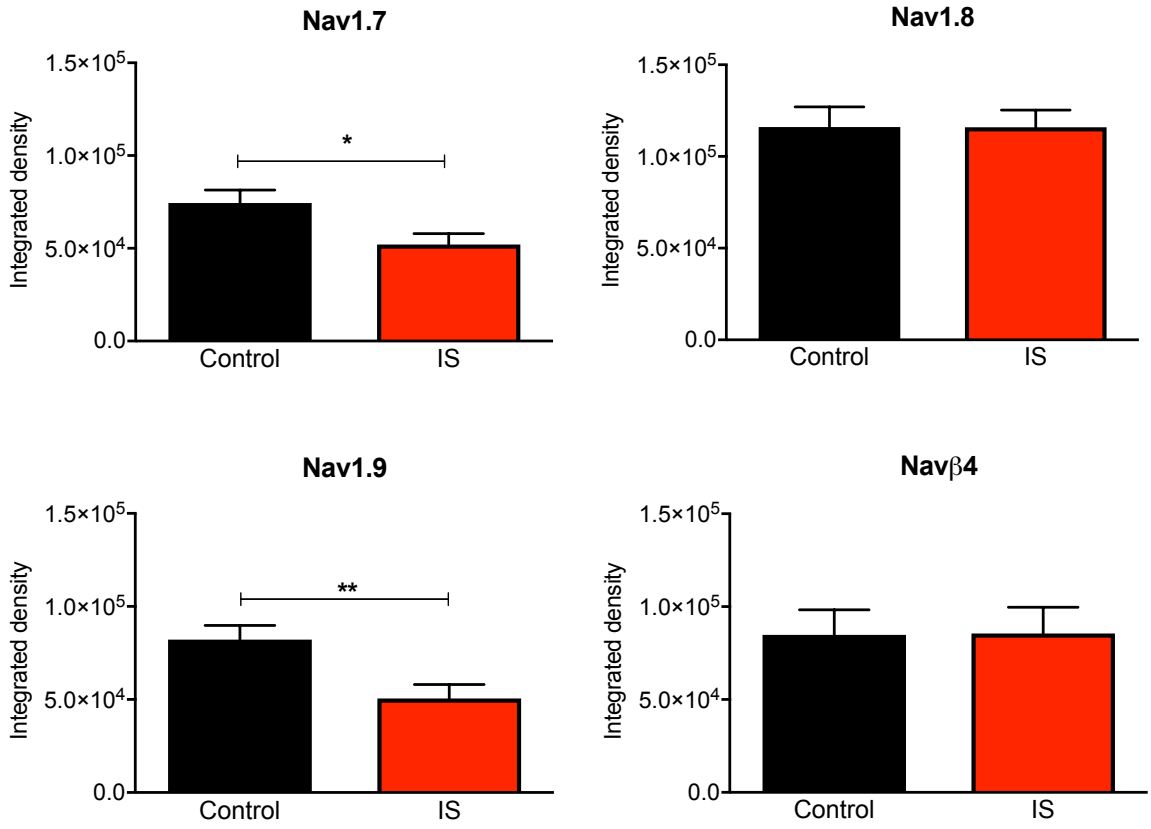

Figure 3.6 Quantification of VGSC Nav1.7, Nav1.8, Nav1.9 and subunit Navβ4 expression at the plasma membrane of DRG neurones' soma.
Isolated DRG neurones were cultured for 24 h and incubated with inflammatory soup for 6 h before fixing with paraformaldehyde. Immunocytochemistry was performed to identify expression of Nav1.7, Nav1.8, Nav1.9 and Navβ4 at the plasma membrane of treated and untreated neurones with inflammatory soup. Images were acquired using a confocal microscope. Integrated density was calculated using ImageJ and JaCOP plug in. Mean values are plotted and error bars show SEM ($n_{Nav1.7}$=169 $N_{Nav1.7}$=3, $n_{Nav1.8}$=154 $N_{Nav1.8}$=4, $n_{Nav1.9}$=164 $N_{Nav1.9}$=3 and $n_{Navβ4}$=73 $N_{Navβ4}$=2). *p=0.0207 **p=0.0043 unpaired t-test

Furthermore, VGSC expression was also quantified according to IB4 binding to non-peptidergic DRG neurones (Stucky and Lewin 1999) (Figure 3.7). Changes in expression of Nav1.8 and Navβ4 within IB4 negative and IB4 positive DRG neurones remained unchanged. In contrast, Nav1.7 expression decreased significantly in IB4 negative neurones only (p=0.0451 n=82 one-way ANOVA with Tukey's multiple comparison test) and Nav1.9 on both IB4 negative and positive (p<0.01 $n_{IB4positive}$=75 $n_{IB4negative}$=89 one-way ANOVA with Tukey's multiple comparison test). Measurements were selected after using robust regression and outlier removal (ROUT) method (Graph Pad Prism 2017) with Q at 1%.

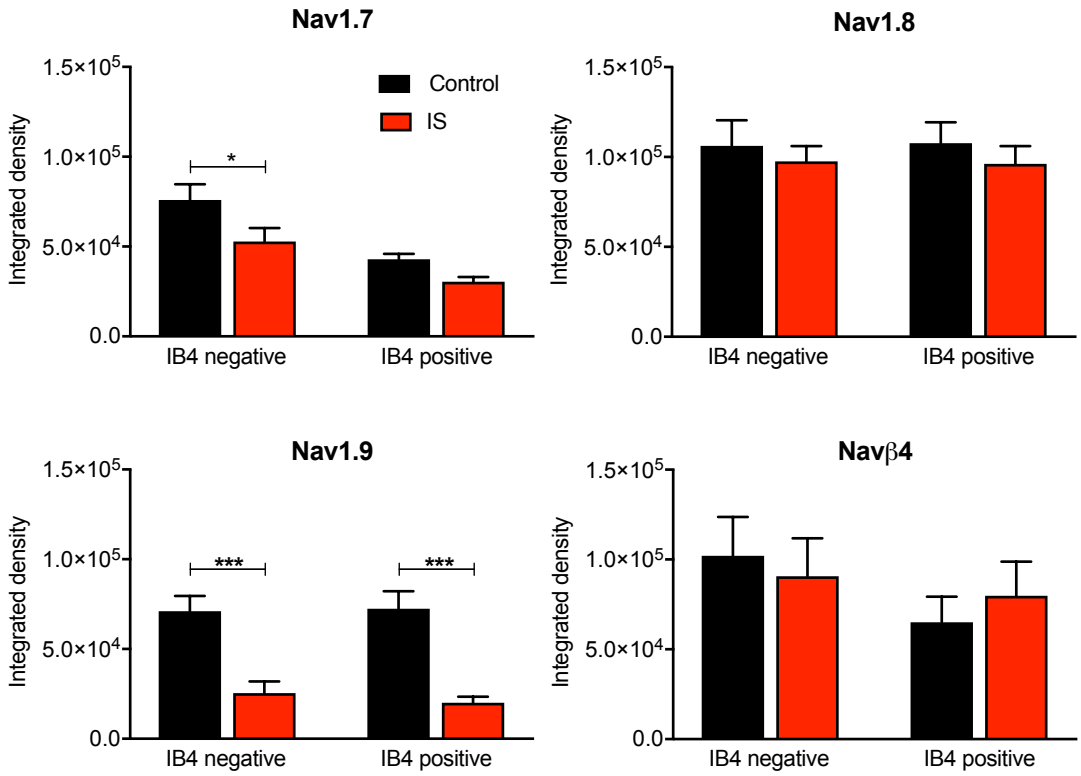

Figure 3.7 Quantification of VGSC Nav1.7, Nav1.8, Nav1.9 and subunit Navβ4 expression at the plasma membrane of IB4 positive and negative DRG neurones. Isolated DRG neurones were cultured for 24 h and incubated with inflammatory soup for 6 h before fixing with paraformaldehyde. Immunocytochemistry was performed to identify expression of Nav1.7, Nav1.8, Nav1.9 and Navβ4 at the plasma membrane of treated and untreated neurones with inflammatory soup. DRG neurones were also probed for IB4 to identify the peptidergic population (IB4 negative). Images were acquired using a confocal microscope. Integrated density was calculated using ImageJ and JaCOP plug in. Mean values are plotted and error bars show SEM (IB4 negative $n_{Nav1.7}$=82, $n_{Nav1.8}$=87, $n_{Nav1.9}$=89 and $n_{Navβ4}$=39, IB4 positive $n_{Nav1.7}$=87, $n_{Nav1.8}$=67, $n_{Nav1.9}$=73 and $n_{Navβ4}$=34). *p=0.0451 ***p<0.01 One-way ANOVA with Tukey's multiple comparison test.

Because these results were not in agreement with those in voltage clamp experiments, DRG neurones were also stained for TRPV1 (Figure 3.8 A). TRPV1 is a non-selective cation channel gated by noxious heat, protons and capsaicin previously reported to be upregulated in a CFA model of inflammation (Amaya et al. 2003). Intriguingly, the expression of TRPV1 close to the plasma membrane (intracellular epitope) was also significantly decreased in both IB4 negative and positive neurones (Figure 3.8 B) ($p<0.001$ $n_{IB4positive}$=54 $n_{IB4negative}$=66 one-way ANOVA). Previously reported increase in TRPV1 expression was observed in histochemical slices of intact dorsal root ganglion from CFA treated rats, suggesting that the effects of the IS do not

reproduce this effect *in vitro*. Hence, it raises the possibility that changes might be happening at the level of the neurites.

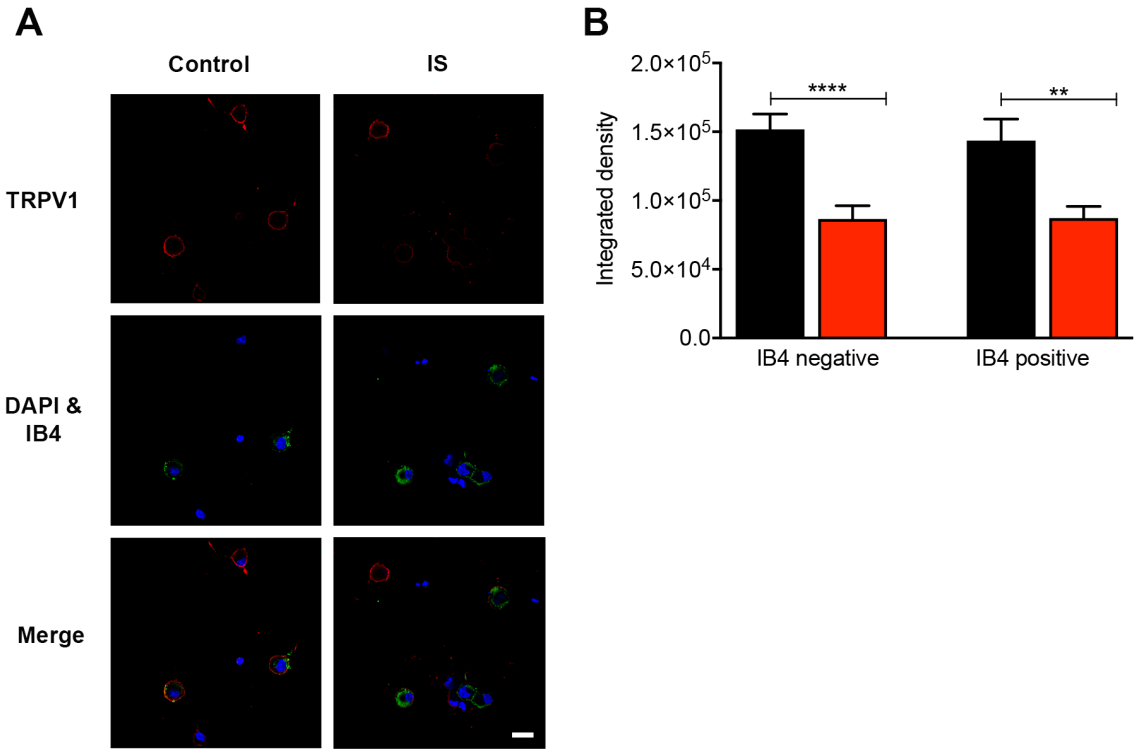

Figure 3.8 TRPV1 expression at the plasma membrane of IB4 positive and negative DRG neurones decreases after treatment with inflammatory soup.
Isolated DRG neurones were cultured for 24 h and incubated with inflammatory soup for 6 h before fixing with paraformaldehyde. Immunocytochemistry was performed to identify expression of TRPV1(red) close to the plasma membrane of treated and untreated neurones with inflammatory soup. DRG neurones were also probed for IB4 (green) to identify the peptidergic population (IB4 negative) and DAPI (blue) to identify nuclei. (A) Representative images of TRPV1 expression. Images were acquired using a confocal microscope. Scale bar shows 20 μm. (B) Quantification analysis of TRPV1's expression in IB4 positive and negative DRG neurones. Integrated density was calculated using ImageJ and JaCOP plug in. Mean values are plotted and error bars show SEM (IB4 negative n=66, IB4 positive n=54, N=2). **p=0.00489 ****p<0.0001 One-way ANOVA

3.2.6 Inflammatory soup incubation (6 h) does not alter VGSC protein expression of Nav1.7

To further understand the effects of the inflammatory soup incubation on Nav1.7 and Nav1.9 expression in DRG neurones, DRG cultures treated and untreated with IS were lysed and their proteins separated by electrophoresis (Figure 3.9 A). The rationale behind these experiments was to evaluate the

impact of the IS on Nav1.7 and Nav1.9 protein expression given the contradictory results of the immunocytochemistry data, which suggest a downregulation of the channel. Due to technical issues, the Nav1.9 signal could not be detected. Thus, only Nav1.7 was quantified over 3 different cultures from 3 different mice (Figure 3.9 B). Nav1.7 protein bands were normalised to the respective β-III tubulin band. Statistical analysis, paired t-test, showed no significant difference between the lysates. Thus, it suggests the IS altered the Nav1.7's location but not their expression.

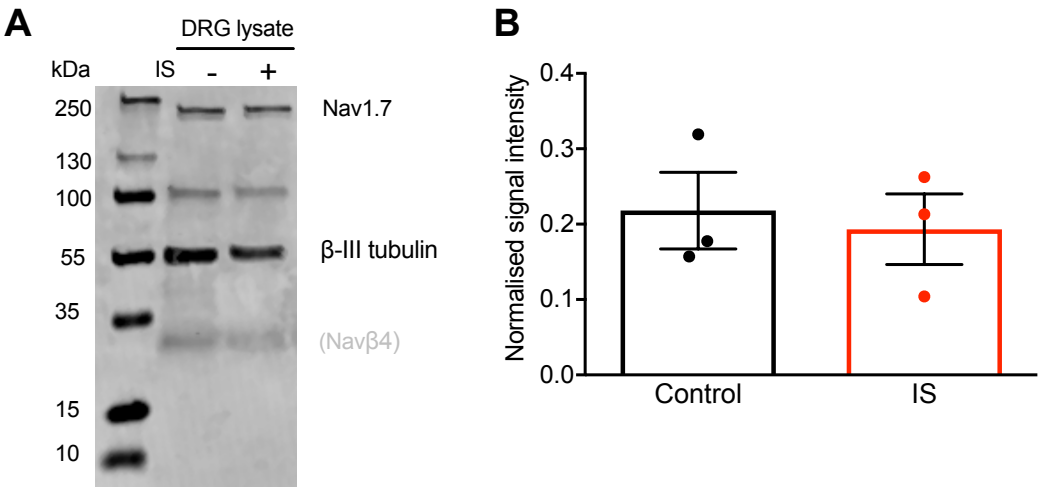

Figure 3.9 Quantification of VGSC Nav1.7 expression in isolated DRG neurones treated and untreated with inflammatory soup.
(A) Representative immunoblot depicting Nav1.7 expression (~200 kDa) and β-III tubulin. This particular immunoblot was also probed for Navβ4 subunit hence the band at ~30 kDa. (B) Quantification of 3 separate immunoblots of 3 different mice cultures treated and untreated with inflammatory soup (IS). The median intensity of Nav1.7 was normalised to the β-III tubulin loading control. Data not significantly different paired t-test. Error bars show SEM.

3.3 Discussion

The main goal of this chapter was to establish an *in vitro* model of inflammation that would induce hyperexcitability and could subsequently be used to test the role of SNARE proteins and toxins targeting these proteins in pain. The IS induced hyperexcitability from 6 h, decreasing the threshold for firing and increasing the frequency of action potentials. Further characterisation of the effects of the IS showed a significant increase in TTX-R Na^+ current, suggesting modulation and/or changes in the expression of Nav1.8 and Nav1.9. Analysis of the expression of these channels revealed a decrease in

the expression of Nav1.7 and Nav1.9 at the soma plasma membrane. Changes in the density and subcellular location of VGSCs have previously been proposed to induce hyperexcitability in DRG neurones (Matzner and Devor 1992, Devor, Govrinlippmann and Angelides 1993). Thus, suggesting that changes are occurring at the level of the neurites or potentially the regulation of other channels responsible for effects on excitability.

3.3.1 Inflammatory soup induces hyperexcitability in DRG neurones

Increased pain response from inflamed tissue results from exposure of inflammatory mediators released at the site of injury and consequent nociceptor sensitisation (Ji and Strichartz 2004). In the context of hyperalgesia (subject response), these are characterised by decreased pain threshold, increased pain in response to suprathreshold stimuli and spontaneous pain (Meyer and Campbell 1981). On the other hand, the sensitisation of nociceptors (fibre response) is characterised by a decrease in the threshold for action potential firing, increased firing to suprathreshold stimuli and spontaneous activity (Cummins et al. 2009). Hence, in this *in vitro* model of inflammation, these parameters were evaluated as hallmarks for hyperexcitability.

Many of the inflammatory mediators included in the IS have been shown to act directly on DRG neurones and alter excitability (section 1.5). Indeed, in Figure 3.1 the IS induced hyperexcitability in DRG neurones (Figure 3.1). One of the inflammatory modulators that have been more studied is PGE_2. PGE_2 has been shown to modulate Nav1.8 currents, HCN current and suppress K^+ conductance (Momin and McNaughton 2009, Gold et al. 1998, Nicol et al. 1997). These phenomena are believed to occur via cAMP-PKA-PKC signalling cascades (England et al. 1996, Evans, Vasko and Nicol 1999, Gold et al. 1998). PKC inhibitors have been shown to decrease the TTX-R Na^+ density, although, there is some debate towards the contribution of TTX-R in DRG excitability *in vivo* as PKA and PKC may serve as a common signalling for the

modulation of other physiological processes (Gold et al. 1998, Zheng et al. 2007). In fact, it has been demonstrated that changes in sodium currents only play a minor role and that PGE_2's main effect on firing frequency is via enhanced hyperpolarisation-activated inward current through cAMP modulation. PGE_2 changes shifts the voltage sensitivity to a more positive voltage which essentially enhances the inward current between the resting membrane potential and action potential threshold. Thus, neurones are thought to depolarise more regularly (Matsutomi et al. 2006). In my data set, I recorded from IB4-negative DRG neurones, and there is evidence to suggest PGE_2 receptors are expressed in this subgroup (Usoskin et al. 2015, Lin et al. 2006, Ng et al. 2013). Hence, it is likely that modulation by PGE_2 contributes to increased excitability. Likewise, IB4-negative DRG neurones express TrkA, the NGF receptor. In culture, NGF supplementation has also been shown to alter DRG excitability. Overnight incubation with 100 ng/mL NGF has been demonstrated to induce hyperexcitability (in this thesis IS: 50 ng/mL NGF) which is observed for up to 8 days (Kitamura et al. 2005). NGF is a known modulator of TTX-R currents (Fjell et al. 1999a, Leffler et al. 2002, Okuse et al. 1997, Kerr et al. 2001, Gold et al. 1996, Zhang et al. 2002) and these have been shown to be the main component in action potential generation (Matsutomi et al. 2006). Furthermore, serotonin incubation has been demonstrated to induce excitability DRG neurones. Multiple studies have confirmed its role on TRPV1 sensitisation, but 5-HT_{2C} receptor activation has also shown modulation of calcium-activated Cl^- channels (Salzer et al. 2016). However, these were acute applications of serotonin (60 s), and in this data set, incubations were set for 22h. If these mechanisms are contributing to the hyperexcitability observed is not known. Moreover, addition of bradykinin to DRG cultures has also been shown to depolarise DRG neurones (Jeftinija 1994, Rang and Ritchie 1988) and to primarily affect IB4-negative neurones (Devesa et al. 2014), and addition of ATP to increased DRG excitability via P2Y receptors (Malin and Molliver 2010, Yousuf et al. 2011). One significant difference in this thesis is that these mediators were added together to the DRG cultures and thus these represent a combined effect of these inflammatory mediators.

Previous *in vitro* studies have established that treatment of nociceptors with an inflammatory soup increases neuronal excitability (Maingret et al. 2008, Zhao et al. 2010). Maingret et al. 2008 have used gene targeting and computer modelling to identify Nav1.9 channel current signature and its impact on DRG excitability in acutely dissociated DRG neurones. They report increased Nav1.9 current after 3 min of continuous incubation with inflammatory mediators (50 nM bradykinin, 500 nM prostaglandin E2, 1 μM histamine, 500 nM noradrenaline and 2 μM ATP) which remains until the last measured time point, 12 min. They demonstrate via knockout mice that TTX-R current increase is via Nav1.9 and not Nav1.8. Interestingly, they also report that only when the inflammatory soup components are applied together, and not each element individually, the Nav1.9 current increases. Thus, the cocktail of inflammatory mediators acted synergistically to modulate Nav1.9. The authors suggest a converging action of PKA and PKC pathways behind the enhanced excitability but also a minor inhibition of K^+ currents (Maingret et al. 2008). This increase in Nav1.9 mediated Na^+ current contributes to subthreshold amplification and increased excitability. In a different set of experiments, Zhao et al. 2010 showed that incubation with an inflammatory soup that contained bradykinin, prostaglandin E2, histamine, ATP, and 5-HT induced increased excitability in wild-type DRG neurones but not in dicer null Nav1.8 positive neurones. Dicer enzyme controls multiple gene transcripts, and their study identifies a role in altering pain thresholds (Zhao et al. 2010).

Increases in channel currents and excitability may also result from increased trafficking and membrane insertion of channel proteins into the plasma membrane. In support of such a mechanism, a recent report by Huang et al. 2016 provided evidence that inflammatory mediators increased recruitment of Cav3.2 to the plasma membrane. Overnight incubation with 2 μM ATP and 100 nM bradykinin has revealed an increase in T-type Ca^{2+} channels in DRG neurones. The authors suggest these inflammatory mediators trigger the recruitment of a reserve pool of Cav3.2 (Huang et al. 2016). In this chapter's IS 2 μM ATP and 50 nM bradykinin were included in the inflammatory insult

hence it is possible that a similar mechanism is occurring but whether this plays a part in IS induced hyperexcitability is unknown. While mechanisms for hyperexcitability are expected to be similar to Maingret et al. 2008, due to similar inflammatory soup recipes, it is likely that second messenger events are happening. For example, the release of further inflammatory mediators from paracrine interaction, and an interplay between non-neuronal cells (e.g. satellite glial cells) are contributing to the hyperexcitability induced by IS.

One component that contributed to IS-induced hyperexcitability is the reduction of action potential threshold (Figure 3.1 C). The contribution to the threshold of action potential firing in DRG neurones is thought to be mainly via Nav1.9 and Nav1.7. Extensive evidence supports that VGSC Nav1.9 currents are heavily modulated in inflammation and can crucially change firing thresholds in small diameter nociceptors (Rush and Waxman 2004, Maingret et al. 2008, Baker et al. 2003, Coste et al. 2004). Nav1.9 null mice have been shown to have reduced PGE_2 hypersensitivity (Priest et al. 2005) and reduced sensitivity to inflammatory mediators such as PGE_2, bradykinin, serotonin, and ATP but not NGF (Amaya et al. 2006). In this data set, small diameter DRG neurones were chosen, and these have been shown to express Nav1.9 (Dib-Hajj et al. 1998). A common second messenger of GPCRs activated by PGE_2, ATP, and 5-HT is GTP, and it has been shown to up-regulate Nav1.9 persistent currents and induce repetitive firing (Baker et al. 2003, Ostman et al. 2008). On the other hand, Nav1.7 is also thought to set the threshold of action potentials in nociceptors. Nav1.7's role is supported by knockout and shRNA studies where hyperalgesia is reduced (Nassar et al. 2004, Yeomans et al. 2005), and loss-of-function mutations associated with congenitive insensitivity to pain (Cox et al. 2006, Goldberg et al. 2007). Importantly, Nav1.7 is upregulated in models of inflammatory pain (Tanaka et al. 1998, Black et al. 2004). Furthermore, serotonin has been reported to reduce action potential threshold and increase excitability via cAMP coupled to TTX-R currents, those mediated by Nav1.8 and Nav1.9 (Cardenas et al. 2001). Hence, it is possible that the changes in threshold are due to Nav1.9 persistent current,

Nav1.7/Nav1.9 channel upregulation or direct modulation by second messengers such as PKA, PKC and GTP.

3.3.2 Inflammatory soup does not significantly alter action potential properties but alters timing of the first action potential at rheobase.

Action potentials result from an interaction of multiple voltage-dependent conductances expressed by neurones. In the mammalian brain these commonly include components of voltage-dependent Na^+ currents, voltage-dependent Ca^{2+} currents, voltage-activated K^+ currents, calcium-activated K^+ currents and the hyperpolarisation-activated current (Bean 2007). Because the IS induced hyperexcitability in isolated DRG neurones (Figure 3.1) it would be expected that one of the action potential voltage-dependent conductances, which led to increased excitability, would be altered and thus detected in the action potential threshold measurements. Current clamp data showed a significant reduction in current necessary for action potential firing (Figure 3.1 C), but individual analysis of each action potential from each recorded neuron did not (Figure 3.2 A).

Other studies have reported changes in action potential shape in the context of inflammation and hyperexcitability. In a rat CFA model of inflammation, NGF sequestration reduced the effects of inflammation on *in vivo* action potential duration at base and firing frequency (Djouhri et al. 2001). In Figure 3.2 F, IS also seems to decrease the action potential duration at rheobase. Axotomy, which is necessary for DRG culture, changes the excitability and action potential waveform of DRG neurones (Gurtu and Smith 1988, Devor and Wall 1990, Oyelese et al. 1997) so it limits the perspective of these action potentials to those acquired *in vitro*. It is, however, changes in latency, measured as the interval between the start of the protocol and peak of the action potential, that is significantly different (Figure 3.2 G). The IS significantly reduces the latency at twice rheobase for the generation of the action potential, suggesting changes in Nav1.9 activity. Similar findings were reported when inflammatory

mediators were added acutely to DRG neurones in Nav1.9 -/- and WT. This reduction in latency is likely due to Nav1.9 current potentiation (Maingret et al. 2008).

3.3.4 Inflammatory soup (6 h) increases TTX-R sodium currents

As previously mentioned, inflammatory mediators have been shown to increase TTX-R currents in DRG neurones in both *in vivo* and *in vitro* studies (Gold et al. 1996, Maingret et al. 2008, Omri and Meiri 1990). Hence, these results were expected. What it was not known was whether a single inflammatory insult would have such impact even after 6 h. As Maingret and colleagues reported, it is likely that a mechanism involving both PKA and PKC underlies the upregulation of Nav1.9 TTX-R currents seen during acute applications. Hence, it is not clear if these changes depicted in Figure 3.6, incubation with IS for 6 h as opposed to acute, are due to modulation of the channel's activity or increased channels at the plasma membrane. There is no current direct evidence of trafficking of Nav1.9 as an effect of the inflammatory soup *in vitro*.

In contrast, no significant changes were observed in TTX-S sodium current. Nav1.7, a TTX-S channel, has been linked to inflammatory conditions (Nassar et al. 2004, Abrahamsen et al. 2008). The absence of TTX-S current increase may reflect a limitation of the *in vitro* model or of the data acquisition. It has been previously reported in a combined voltage and current clamp study that TTX-R/slow Na^+ current plays a major role in action potential generation evoked by current injection protocols but from a resting membrane potential of -70 mV. The TTX-S component in action potential generation was only detected when the membrane was held at -100 mV (Matsutomi et al. 2006). In this thesis the DRG neurones were held at -70 mV as small mouse DRG neurones have a typical resting membrane potential of -70 to -50 mv at the soma, only in certain pathological conditions the membrane may be excessively hyperpolarised (Matsutomi et al. 2006).

3.3.5 Does Inflammatory (6 h) soup induce trafficking of VGSC to the plasma membrane?

There are nine VGSC (Nav1.1 – Nav1.9), but only three sodium channels (Nav1.7, Nav1.8 and Nav1.9) are associated with DRG neurones and pain disorders (Eijkelkamp et al. 2012). In addition to Nav1.7-Nav1.9, the Navβ4 subunit was also included due to its role in the regulation of fast-resurgent currents and excitability in DRG neurones (Barbosa et al. 2015). Interestingly, the IS induced changes in the expression of VGSC, the Nav1.7's and Nav1.9's expression levels at the soma plasma membrane decreased (Figure 3.5, 3.6 and 3.7). At first, these changes were the opposite of what was expected, an increase in VGSC expression at the plasma membrane or the expression to remain the same, as current clamp recordings depicted increased excitability (Figure 3.1). I hypothesised that if there were changes induced by the IS regarding expression, it would be an increase in expression. However, location is also critical. Changes in the density and subcellular location of VGSCs have previously been proposed to induce hyperexcitability in DRG neurones (Matzner and Devor 1992, Devor et al. 1993, Waxman and Ritchie 1985).

Previous studies support this view of the increased expression of VGSC following inflammation (Black et al. 2004, Tanaka et al. 1998, Strickland et al. 2008). There is evidence to suggest inflammation induced upregulation *in vivo* of both TTX-R and TTX-S VGSCs. Therefore, these results could indicate that the time window of observation chosen is a period of desensitisation. For instance, in the context of long-term potentiation, central neurones adapt by changing the composition of the plasma membrane and internalise some receptors (Collingridge, Isaac and Wang 2004). Current clamp data depicts hyperexcitability at 6 h (Figure 3.3). In other pain syndromes such as nerve injury, TTX-R VGSCs have been shown to be downregulated in parallel with TTX-S VGSCs upregulation (Cummins and Waxman 1997). It is possible that the biophysical properties of the DRG neurones have changed via other mechanisms such as activation of M channels (Du et al. 2014).

The effects of IS on TRPV1 plasma membrane expression were also assessed (Figure 3.8). Likewise, the expression of TRPV1 is significantly reduced after 6 h incubation with IS. In line with VGSCs, previous studies on TRPV1 regulation have also described an increase in expression in animal models of inflammation (Yu et al. 2008), and fusion of vesicles containing TRPV1 following bradykinin (Mathivanan et al. 2016) or ATP (Devesa et al. 2014) in a SNARE regulated process. Hence, these data (Figure 3.7 and Figure 3.8) seem to contradict what has been described. However, as with VGSCs, the location of TRPV1 is also important. In an *in vivo* setting, these would be found mainly in the free nerve endings in the skin (Szallasi and Blumberg 1999). In the study by Mathivanan et al. 2016, exocytosis of TRPV1 channels driven by 1 μM bradykinin was impaired by the peptide DD04107, which impairs regulated exocytosis. Whole-cell recordings of IB4-negative neurones showed acutely the effects of this peptide (Mathivanan et al. 2016). Technically, soma whole-cell recordings clamp the whole cell, but there may be some current flowing between neurites that is not detected so this exocytosis effect must be at the level of the soma. Given that these are acute observations it is possible that in this thesis' inflammation model, the fusion of primed vesicles, such as those in Mathivanan 2016, do occur in the first instance. However, given a longer period of incubation, these vesicles might relocate, if initially found at the soma, to the neurites of the neurones, which is where they are mainly found in vivo (Szallasi and Blumberg 1999) or the combined effects of this thesis' IS lead to receptor desensitisation and internalisation. One possible approach to follow these experiments is to add tumour necrosis factor - α (TNF-α) to DRG neurones. A recent study has described TRPV1 upregulation in the soma of trigeminal ganglion neurones after 24 h incubation with 100 ng/mL TNF-α (Meng et al. 2016).

3.3.6 Inflammatory soup incubation (6 h) does not alter VGSC protein expression

Following the unexpected results on the expression of VGSCs, I hypothesised that this decrease in the expression of Nav1.7 and Nav1.9 at the level of the

soma was a consequence of subcellular redistribution. Although it does not address this hypothesis directly, I set out to analyse changes in protein expression of both Nav1.7 and Nav1.9 following the *in vitro* incubation with IS to evaluate possible transcriptional regulation changes. No significant changes were seen in the protein expression of Nav1.7. Regrettably, technical issues did not permit the detection of Nav1.9. Thus, the IS incubation induced hyperexcitability of IB4 negative DRG neurones (Figure 3.3) while maintaining the same level of Nav1.7 expression (Figure 3.9). Yet, channel's expression at the plasma membrane of DRG soma is significantly reduced in IB4-negative neurones.

Nav1.7, Nav1.8 and Nav1.9 are distributed across the soma and the neurites of DRG neurones (Black et al. 2012, Fukuoka et al. 2008). As previously mentioned, action potential shape of neurones may vary if recorded at the level of processes or soma. Evidence suggests nociceptor afferents have a resting membrane potential (V_{rest}) of -40 mV and at the soma between -50 and -75 mV (Baccaglini and Hogan 1983, Gold et al. 1996). Furthermore, computer modelling has shown that increased VGSC density may cause hyperexcitability (Matzner and Devor 1992) and that VGSCs accumulate at the site of injury (Matzner and Devor 1994, Devor et al. 1993). Thus, it is possible that Nav1.7 and Nav1.9 are redistributed following incubation with IS. Although the experiments in this chapter did not test this hypothesis directly there is evidence that this occurs in nerve injury (England et al. 1994, Devor et al. 1993, Lombet et al. 1985) and in CFA models of inflammatory pain, for voltage-gated Ca^{2+} channels (Lu et al. 2010).

3.3.7 General discussion and future directions

The inflammatory mediators in the IS induced hyperexcitability in DRG neurones. Though, there is a major caveat to these experiments. These recordings were clamped at the level of the soma, and thus demonstrate that TTX-R Na^+ currents are increased at the level of the soma following the incubation with these inflammatory mediators. The functional relevance of somatic depolarisation of DRG neurones is still not completely understood.

There is evidence that somatic depolarisation is involved in nociceptor sensitisation and ectopic activity (Amir and Devor 1996, Shinder, Amir and Devor 1998, Liu, Amir and Devor 1999, Utzschneider, Kocsis and Devor 1992) but the function of TTX-R Na^+ currents during axonal propagation of action potentials is disputed. *In vitro*, somatic TTX-R Na^+ currents have been shown to be a major component of the action potential (Matsutomi et al. 2006), and there is evidence of TTX-R Na^+ currents in axons in C-fibres (Quasthoff et al. 1995). However, axonal propagations are blocked by TTX (Ritter and Mendell 1992, Villiere and McLachlan 1996) but only 15% of C-fibres. However, when all the experiments of this chapter are considered, IS induces hyperexcitability and increase in TTX-R but Nav1.7 and Nav1.9's expression decreases at the soma plasma membrane. Thus, suggesting that subcellular location of these channels is likely having an impact. In a recent study by Branco et al. 2016, they demonstrated that synaptic integration by Nav1.7 is critical in hypothalamic neurones. A persistent current by Nav1.7 specifically prolonged the excitatory postsynaptic potentials making the synaptic integration by these cells unique. However, knockdown of Nav1.7 observed no changes in threshold for action potential or transient Na^+ current recordings, suggesting a dendritic location of Nav1.7 (Branco et al. 2016).

Following up these results, it would be beneficial to characterise pharmacologically (e.g. Protoxin II, Nav1.7 antagonist) the components of the currents measured in voltage-clamp and further understand the contribution of each α-subunit. Likewise, analysis of the expression of each α-subunit at the level of the neurites via immunocytochemistry. Overall, the signalling pathways and the effects of the inflammatory soup are not yet well characterised, but further understanding might reveal interesting targets regulating the subcellular location and density of VGSCs for the development of inflammatory pain treatments.

4 – VAMP expression in DRG neurones

4.1 Introduction

SNARE proteins mediate the ubiquitous phenomenon of vesicular fusion. This phenomenon is crucial for the transport of cargo within the cell, cargo release to the extracellular medium, and for plasma membrane maintenance (Schoch et al. 2001, Rao et al. 2004, Jurado et al. 2013). The SNARE family has been mainly studied in the central nervous system (CNS) in the context of neurotransmitter release. In the brain, VAMP2 is an abundant v-SNARE protein interacting with t-SNARE proteins such as syntaxin-1 and SNAP-25 (Takamori et al. 2006). Nevertheless, other v-SNAREs such as VAMP7 have also been shown to participate in neurotransmission in the CNS (Bal et al. 2013). Evidence suggest different v-SNAREs might be segregating different vesicular pools (Deitcher et al. 1998, Hua et al. 1998, Sara et al. 2005, Revelo et al. 2014).

In DRG neurones, vesicular fusion at nerve endings and in the spinal cord is crucial for nociception. During inflammation and pain processing not only is there the release of neurotransmitters and inflammatory mediators, but several ion channels and receptors may also be delivered to the plasma membrane (Black et al. 1999, Tanaka et al. 1998, Garry and Hargreaves 1992, Karanth et al. 1991, Kilo et al. 1997, Meng et al. 2016). Hence, identifying the v-SNAREs mediating vesicular fusion in DRG neurones will substantially improve our basic understanding of how vesicular trafficking is organized and regulated in nociception but also provide insight to the development of new drugs that may target specific vesicular trafficking pathways contributing to the establishment of a chronic pain state.

Previous studies have indicated mRNA expression of all seven VAMP isoforms in DRG neurones (Chiu et al. 2014, Thakur et al. 2014, Usoskin et al. 2015).

In addition, Rouwette et al. 2016a have profiled 3067 proteins expressed in DRG, and found evidence for seven VAMP proteins (Rouwette et al. 2016b). VAMP-1 and -2 have been described in regulated secretion of CGRP in rat trigeminal ganglia. They were found on CGRP-containing vesicles but forming different SNARE complexes (Meng et al. 2007). At the start of my project, major DRG profiling studies were still unpublished thus the aim of the work described in this chapter was to identify the VAMP isoforms in DRG neurones.

4.2 Results

4.2.1 Isolated DRG cultures express mRNA for all VAMP isoforms

DRG neurones were isolated and cultured for 72 h (N=2) (experiments by Drs Seward, Bauer and Nassar). Total RNA was extracted and processed by Paul Heath form Sheffield Institute for Neuroscience (details section 2.8). Statistical analysis was accomplished by Dr Marta Milo. Due to the low number of samples, probability of positive log-ratio (%) was calculated and indicates the presence of all VAMP isoforms in isolated DRG neurones (Figure 4.1).

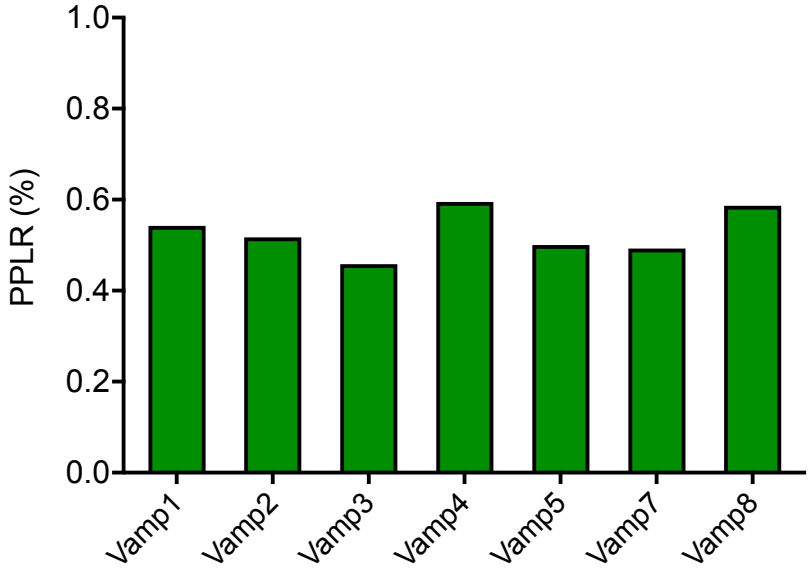

Figure 4.1 RNA expression in mouse DRG neurones.
Isolated DRG neurones were cultured for 3 days in standard cultured medium and harvested for mRNA identification (These experiments were conducted by Drs Seward, Bauer and Nassar, and statistical analysis by Dr Marta Milo).

4.2.2 Whole DRG express VAMP-1, -2, -3, -4, -5, and -7

Since the microarray results strongly suggest that all isoforms were being expressed at mRNA level (Figure 4.1) further experiments were necessary to confirm this at the protein level. Thus, western blotting was performed to identify the VAMP proteins on whole DRG lysate. Since the majority of the literature has demonstrated the presence of VAMP proteins in the CNS, brain lysates were added for comparison (Figure 4.2). All isoforms but VAMP8 were detectable in DRG neurones by western blot and were identified within the predicted molecular size for each isoform (VAMP-1, -2, -3, -5 and -8 close to 12 kDa and VAMP7 close to 25 kDa, see table 1.2). After quantifying 3 repeats, VAMP-1 and -2 were found to have a lower expression level than brain lysate (0.39 ± 0.07 and 0.03 ± 0.007, respectively); in contrast, VAMP-3, -4, -5 and -7 were highly expressed in DRGs when compared to the brain (12.3 ± 11.04, 5.03 ± 1.05, 4.5 ± 0.7 and 5.59 ± 0.63, respectively, Figure 4.3).

Lysates from other tissues were used to evaluate the antibodies' selectivity. Tissues selected had previously been reported to be enriched with a specific isoform. Namely, spleen is enriched with VAMP3 (McMahon et al. 1993), heart with VAMP5 (Zeng et al. 1998), and lung with VAMP7 (Braun et al. 2004). In addition, a HeLa cell line lysate was used to confirm anti-VAMP8 antibody sensitivity (Wong et al. 1998). Several concentrations of brain and DRG lysate were used to detect VAMP8 and the highest (58 μg) is shown on figure 4.2. Nevertheless, VAMP8 could not be detected by western blot. In addition, non-commercial antibodies (VAMP4, -7, and-8) were previously tested against knockout samples and shown to be specific (data not shown, Dr Andrew Peden's lab, The University of Sheffield)

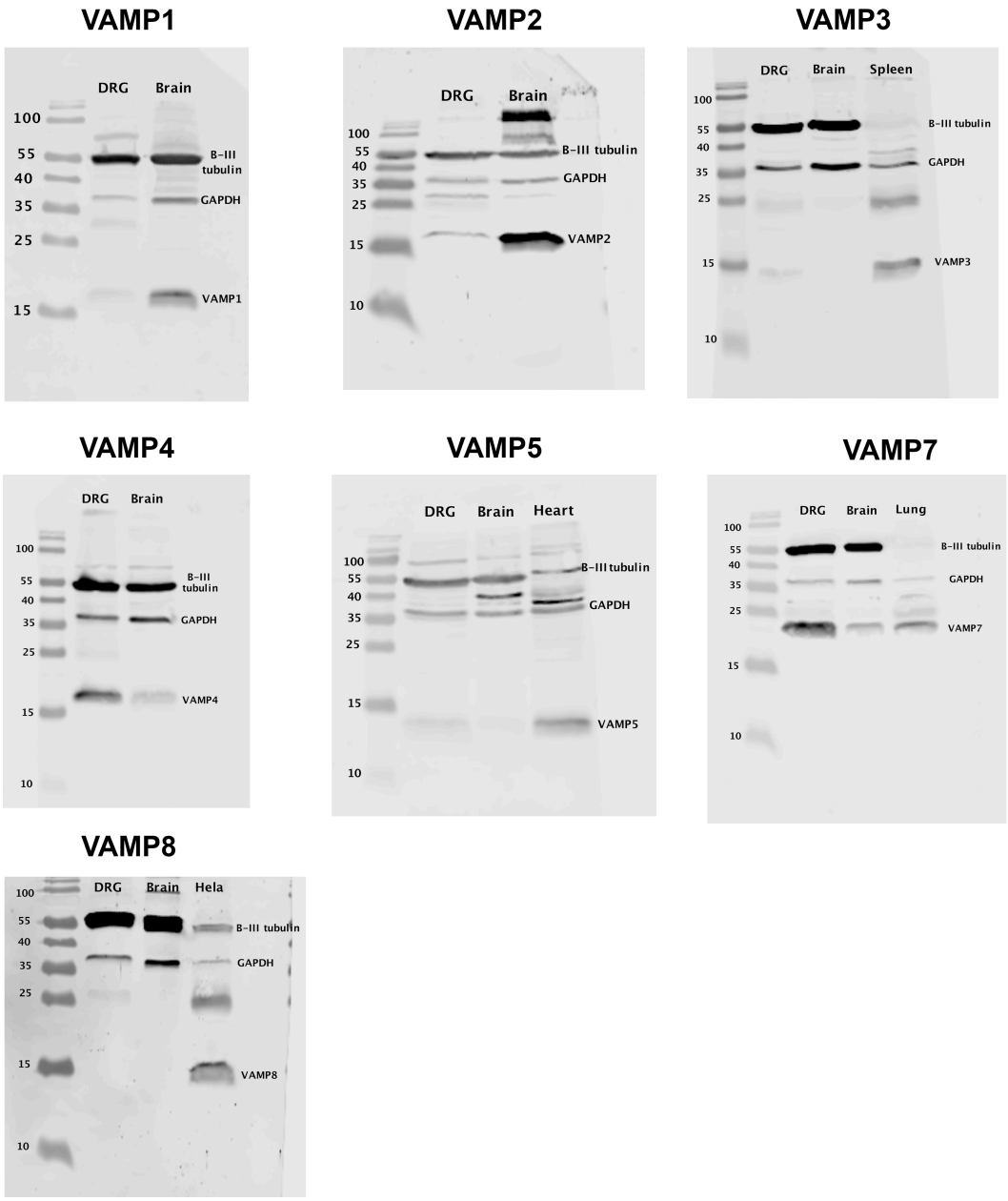

Figure 4.2 Western blots depicting protein expression of VAMP isoforms.
Lysates were obtained from whole dorsal root ganglia (not cultures). Other mouse tissues were also lysed and used as positive controls (brain, spleen, heart and lung) as well as HeLa samples. All blots were probed for GAPDH and β-III tubulin in addition to VAMP isoforms. All isoforms except VAMP8 were detected in DRG samples. All immunoblots were repeated at least 3 times. HeLa samples were kindly donated by Dr Selvambigai Manivannan.

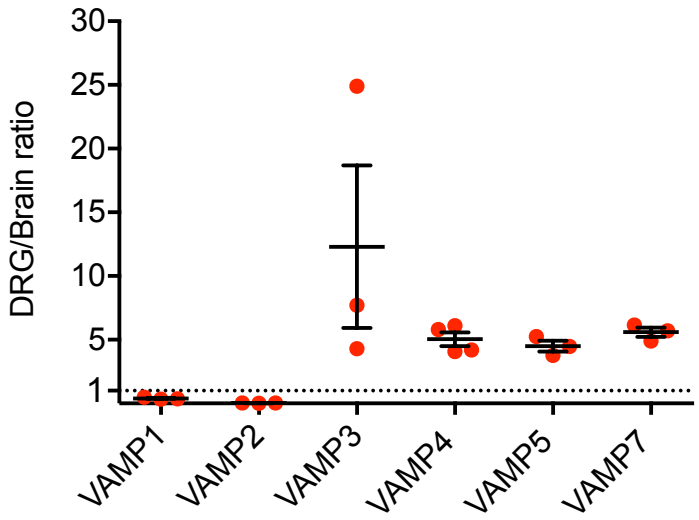

Figure 4.3 The expression ratio of the different VAMP isoforms in DRG compared to brain.
The median intensity of the immunoblot bands indicating VAMP expression in DRG was divided by the median intensity of the respective bands in the brain lysate. VAMP1 and VAMP2 were found to have a lower expression when compared to the brain whereas VAMP-3, -4, -5 and -7 had a higher expression. Error bars show SEM (n_{VAMP1}=3, n_{VAMP2}=3, n_{VAMP3}=3, n_{VAMP4}=4, n_{VAMP5}=3, n_{VAMP7}=3).

4.2.3 VAMP-1, -2, -3, -4, -5, -7 and -8 are expressed in the soma of isolated DRG neurones. VAMP-1, -2 and -7 in the neurites.

Both mRNA microarray and western blotting experiments demonstrated the presence of VAMP isoforms in DRG neurones. With the exception of VAMP8 all were detected in the immunoblots. However, the samples used for lysing were from either mixed cultures (microarray) or whole DRG lysates (western blot). It was still possible that the mRNA or protein detected was from non-neuronal cells. Hence, isolated DRG neurones were cultured for 24h, fixed and probed against all VAMP isoforms and the pan neuronal marker β-III tubulin used to identify the subcellular location (Figure 4.4).

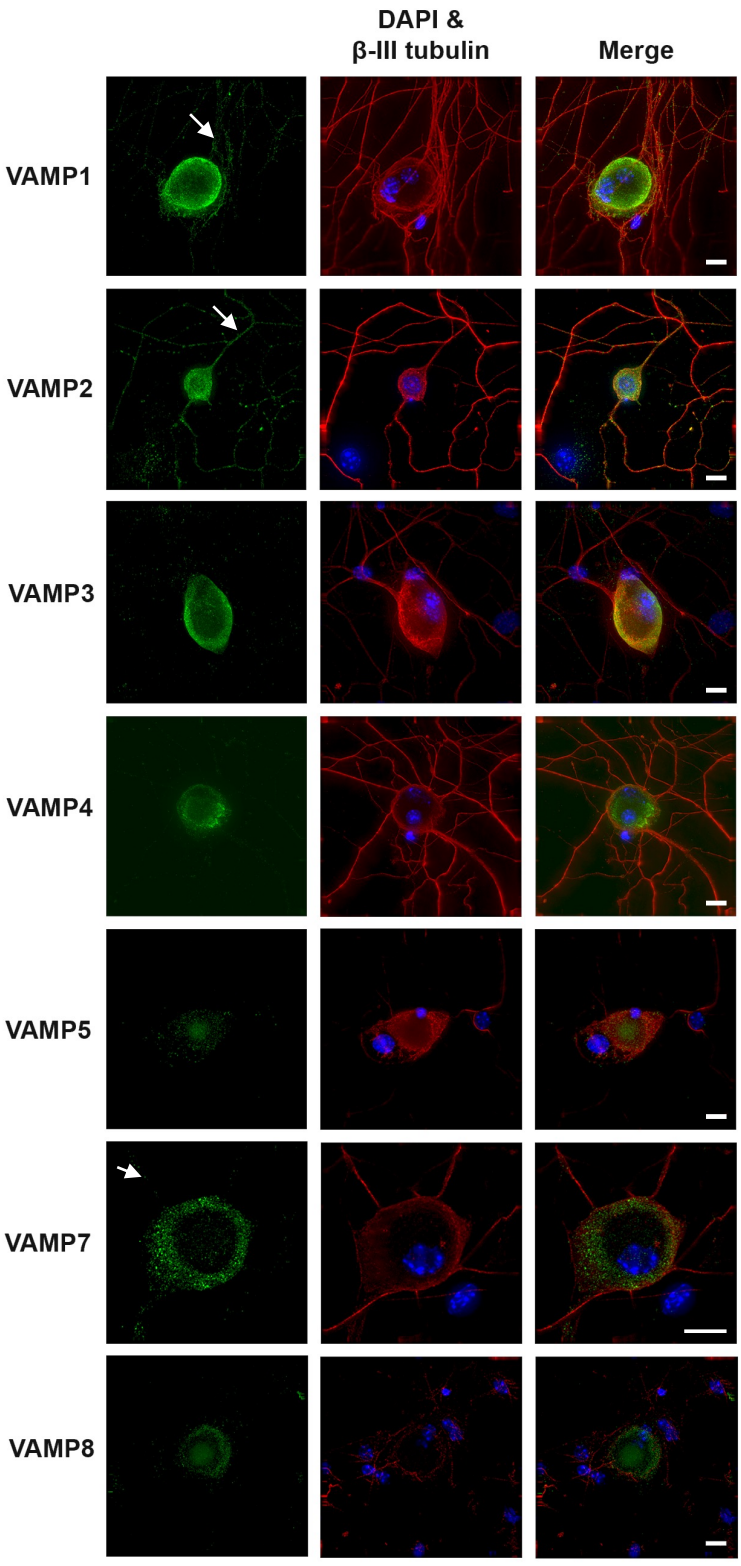

Figure 4.4 Representative images of VAMP expression in DRG neurones in culture. Isolated DRG neurones were cultured for 24 h. Immunocytochemistry was performed to identify the subcellular location of VAMP isoforms (green) in DRG neurones positive for β-III tubulin(red) and DAPI for nuclei (blue). Details of the antibodies used can be found at section 2.4.1. Images were acquired using "Deltavision RT system" (Applied Precision, Issaquah, Washington) and were further processed by deconvolution. No primary antibody controls were

used to account for DRG neurones' autofluorescence by adjusting acquisition settings. Images shown are the maximum intensity of the respective z-stack. Scale bars show 20 μm and arrows indicate VAMP staining in neurites.

Interestingly, all VAMP isoforms were detected in the immunocytochemistry of DRG neurones, even VAMP8 (Figure 4.4). Most of the staining for VAMP isoforms could be seen in the soma of the DRG neurones. Exceptionally, VAMP-1, -2 and -7 were also seen in the neurites of DRG neurones (Figure 4.4 arrows). On the other hand, most of the isoforms were detected in β-III tubulin negative cells with the exception of VAMP7 (data not shown). VAMP4 was found close to the nucleus and it is in agreement with its previously described role in the trans-Golgi network (Peden et al. 2001).

To further understand the proportion of DRG neurones expressing VAMP isoforms, an automated system was used to quantify expression. Of a total of 5515 isolated DRG neurones analysed 90 ± 8 % expressed VAMP8, 82 ± 8 % VAMP3, 90 ± 160 % VAMP1, 78 ± 12 % VAMP2, 71± 12 % VAMP4, 50 ± 16 % VAMP5 and 35 ± 12 % VAMP7 (Figure 4.5 B). Hence, VAMP5 and VAMP7 seem to be expressed only in a portion of isolated DRG neurones.

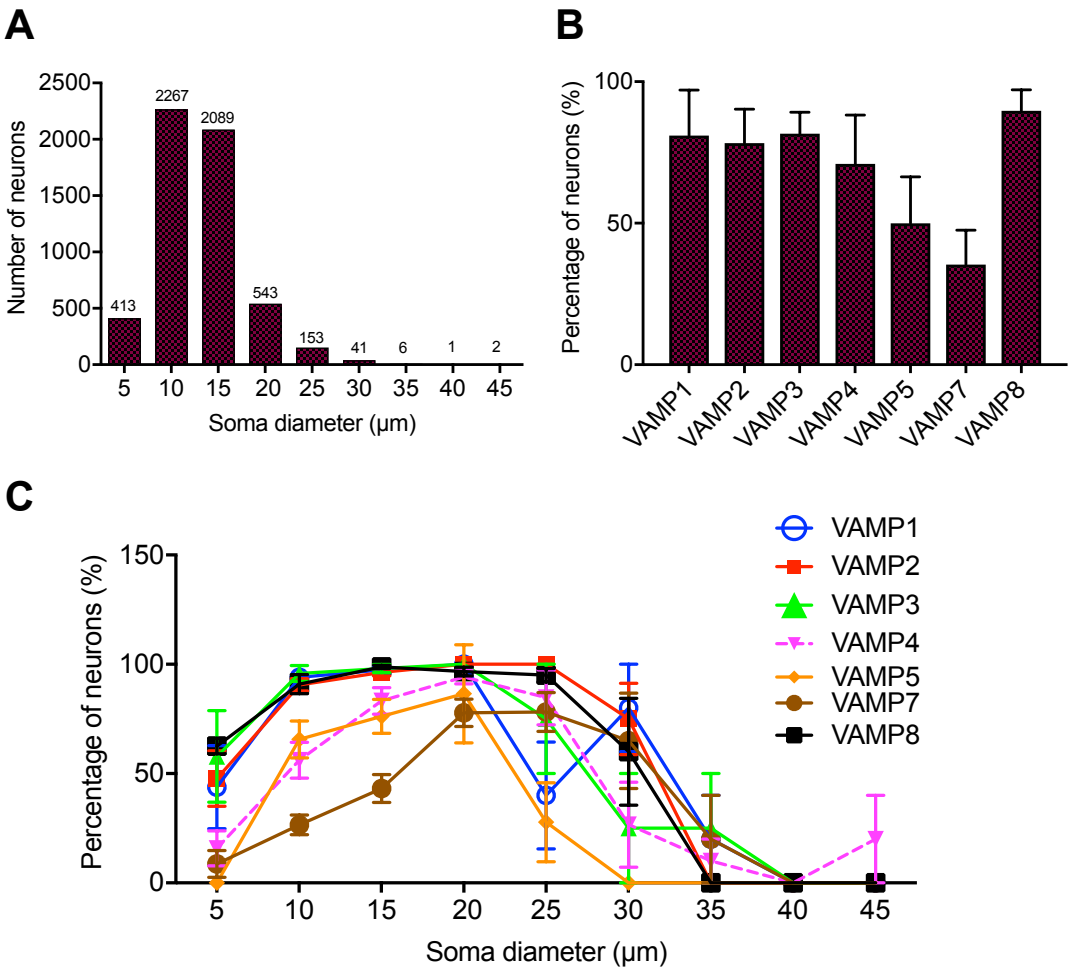

Figure 4.5 Quantification of VAMP expression across soma diameters.
Isolated DRG neurones were cultured for 48h. Immunocytochemistry was performed to identify VAMP isoforms in β-III tubulin positive DRG neurones in culture. An automated system, InCell analyser 2200 (GE healthcare), was used to quantify the number of DRG neurones positive for each VAMP isoform and each DRG neurone's soma diameter was measured. (A) Histogram summarising the distribution of soma sizes measured (n=5515). (B) The percentage of DRG neurones positive for each VAMP isoform. (C) The percentage of DRG neurones positive for each VAMP isoform across different soma diameters. Error bars show SEM.

4.2.4 VAMP isoform expression is consistent across soma diameter

DRG neurones may be subdivided according to distinct response characteristics, chemical markers, modalities of stimulation and soma diameter (Lawson and Waddell 1991, Stucky and Lewin 1999, Slugg et al. 2000). Nociceptors have been demonstrated to have a smaller mean soma diameter compared to other primary fibres (Lawson and Waddell 1991).

Hence, VAMP expression was also analysed against soma diameter (Figure 4.5 C). Each cell body was measured according to β-III tubulin staining and an average diameter (Feret's analysis) per neurone was calculated. It is worth noting that these data derive from isolated DRG neuronal cultures. Thus, larger soma diameters are less well represented in culture as these are more difficult to isolate (Figure 4.5 A). Taken together these data demonstrate ubiquitous expression of VAMP-1, -2, -3, -4 and -8 across different DRG soma diameters. In contrast, VAMP7 expression profile depicts a trend towards higher soma diameters peaking at 25 μm and VAMP5 towards 20 μm.

4.2.5 Is Nav1.7 found within vesicles with specific VAMP isoforms?

Compelling evidence suggest the involvement of Nav1.7 in pain signalling (Ahmad et al. 2007, Cox et al. 2006, Goldberg et al. 2007). To date the SNAREs, including VAMPs, involved in Nav1.7 trafficking remain unknown. Thus, DRG neurones were isolated and probed with anti-Nav1.7 and anti-VAMP in the process of immunocytochemistry (Figure 4.6). As expected Nav1.7 fluorescence can be seen in the neurites and at the plasma membrane of DRG neurones. The aim was to identify vesicles containing the α-subunit Nav1.7. Yet, statistical analysis did not indicate a specific VAMP isoform to co-localise with Nav1.7 and thus likely involved in the channel's trafficking in DRG neurones (Figure 4.7).

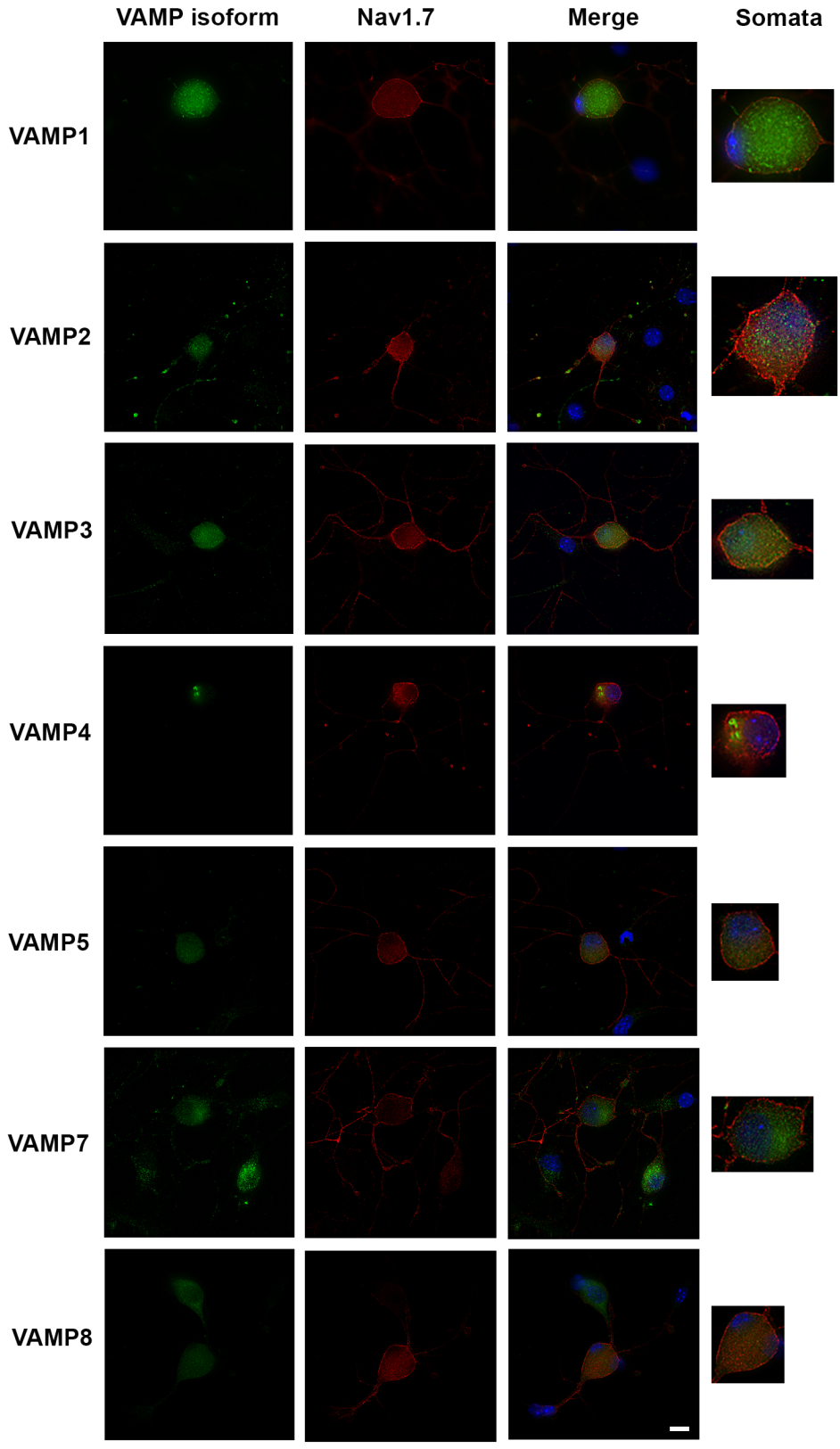

Figure 4.6 Representative images of VAMP expression and Nav1.7 in DRG neurones. Isolated DRG neurones were cultured for 24h. Immunocytochemistry was performed to assess the co-localisation of VAMP isoforms (green) and the voltage-gated ion channel Nav1.7 (red). DAPI was used to identify nuclei (blue). Images were acquired using "Deltavision RT system"

(Applied precision, Issaquah, Washington) and z-stack of each cell were further processed by deconvolution. No primary antibody controls were used to account for DRG neurones' autofluorescence by adjusting acquisition settings. Scale bar shows 20 μm.

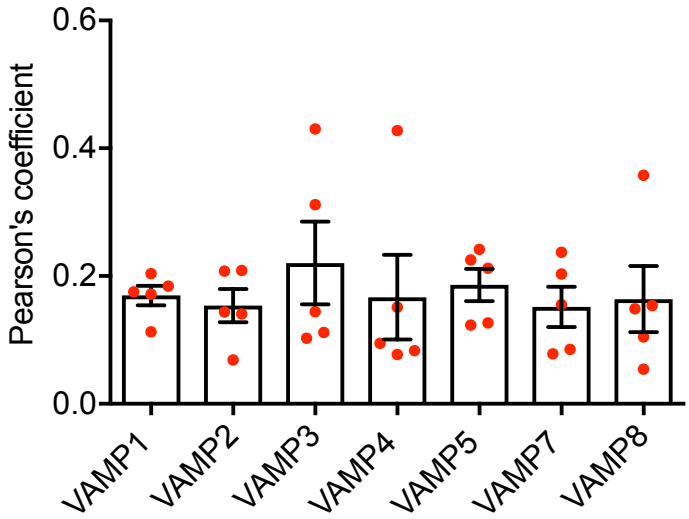

Figure 4.7 Quantification of the co-localisation of VAMP isoforms with Nav1.7 by Pearsorn's coeffiecient analysis.
A selection of at least 10 somata per mouse per isoform were analysed with ImageJ's co-localisation analysis plug in JACoP (N=5). Background was subtracted by analysing a flipped imaged of the same soma. Data not significantly different (One-way ANOVA). Error bars show standard error of the mean.

4.3 Discussion

Vesicular fusion is a key event for pain signalling as it is the mechanism underlying neurotransmitter release and ion channel trafficking (Garry and Hargreaves 1992, Karanth et al. 1991, Martling et al. 1988, Suedhof 2013). For instance, increased expression of voltage-gated ion channels at the plasma membrane changes excitability of DRG neurones (Black et al. 1999, Tanaka et al. 1998). Hence, these vesicular fusion events are important for the fine tuning of the pain signalling. Evidence suggests v-SNAREs may participate in differentiating vesicular populations within the cell. Thus, to further understand the role of v-SNAREs in DRG neurones, experiments in this chapter were designed to identify and characterise the expression of VAMP isoforms. Firstly, a microarray analysis of the mRNA was performed in isolated DRG neurones. Followed by western blotting analysis of protein expression and subcellular location by immunocytochemistry.

4.3.1 Isolated DRG cultures express mRNA for all VAMP isoforms

The microarray results in this chapter strongly suggest expression of VAMP1-8 (Figure 4.1). This is in agreement with recent studies published in the interim of this project which have also indicated a similar expression profile. Using single cell RNA-seq Usoskin et al. 2015 unbiasedly grouped DRG neurones according to their expression profile; Thakur et al. 2014 have used a novel application of magnetic cell sorting (MAC) to isolate nociceptors and compared them to other DRG neuronal subtypes, and Chiu et al 2014 have used two mouse reporter lines to identify and purify a subset of DRG neurones in combination with IB4 surface labelling. Importantly, these three studies have a common message regarding VAMP mRNA expression. They all identified the 7 isoforms but have used slightly different preparations. Usoskin et al. 2015 and Chiu et al. 2014 only included in their analysis L4-L6 ganglia whereas Thakur et al. 2014 pooled from all the ganglia. This can be a limitation for both approaches. On one hand, by using a specific subset we learn the ganglia's specific set but caution should be used when extrapolating it for other ganglia. On the other hand, it has been suggested that certain anatomical regions are potentially more enriched for certain transcripts (e.g. lumbar vs cervical) and may introduce an error (Chiu et al. 2014). Nevertheless, it is important to mention that the results presented in this project are from a mixed culture of both neuronal and non-neuronal cells from all regions. Although it is possible to 'enrich' DRG cultures with neurones with the use of mitotic inhibitors and extended cultures (more than a week) these are often not used as off-target effects on neurones by inhibitors and changes in protein expression over the course of prolonged culture are a concern (Buschmann et al. 1998, Malin, Davis and Molliver 2007, Wallace and Johnson 1989, Scott and Edwards 1980). Ideally, approaches used by other labs such as unbiased RNA-seq or MACS sorting could have been used to improve these results but it was not a possibility. Hence, the "impurity" of DRG cultures is a significant limitation of these results. Taken together these studies (Chiu et al. 2014, Thakur et al.

2014, Usoskin et al. 2015) and the results discussed here strongly support the idea of a complete mRNA VAMP expression by DRG neurones.

4.3.2 Whole DRG express VAMP-1, -2, -3, -4, -5, and -7

Immunoblot analysis showed expression of VAMP-1, -2, -3, -4, -5, and -7 (Figure 4.2). Given the results of the microarray (Figure 4.1) and what has now been published (Chiu et al. 2014, Thakur et al. 2014, Usoskin et al. 2015) it was expected that all isoforms would be detected. This was not the case for VAMP8. One possibility is that the preparation used might be altering the data set to a false negative. That is, there is the possibility that non-neuronal cells present in the lysate may be skewing the expression down or perhaps the expression level is below the detection level of the western blot technique. To confirm this, other techniques could be used such as mass spectrometry. Indeed, in the proteomics study by Rouwette et al. 2016 they demonstrated the expression of the VAMP8 protein in DRG neurones.

Another interesting observation is the varying levels of expression of each isoform (Figure 4.3). When compared to the brain lysate, VAMP-1 and -2 had a lower expression level. These are two known abundant SNAREs in the CNS tightly linked to vesicular fusion with the plasma membrane (Schoch et al. 2001, Raptis et al. 2005, Takamori et al. 2006). Both have been described in slightly different areas and associated with different vesicular fusion events. For instance, NMDA receptor trafficking to plasma membrane is mediated by VAMP1 in hippocampal neurones (Gu and Huganir 2016) and VAMP2 mediates BDNF release in cortical neurones (Shimojo et al. 2015). The other VAMP isoforms, VAMP-3, -4, -5, -7 and -8, had a higher expression in DRG when compared to the brain lysate. One possible explanation, is that brain tissue used includes the neurones and supporting cells with their synapses whereas dorsal root ganglia lysate does not have its synapses to the spinal cord or the nerve endings at the dermis and other innervating organs. Hence, subcellular locations expected to be enriched with neurotransmitters may have not been included. That is, assuming that the same v-SNAREs are mediating the neurotransmitter release in DRGs. For instance, VAMP1 and VAMP2 have

been described in CGRP secretion from trigeminal neurones (Meng et al. 2007). Furthermore, differences in neuronal density between the tissues might influence the data. For example, neuronal density has been reported to vary between different cortical areas (Collins et al. 2010)

To confirm the antibodies specificity positive control tissues were used in parallel. Spleen due to its high levels of VAMP3 (McMahon et al. 1993), heart of VAMP5 (Zeng et al. 1998), lung of VAMP7 (Braun et al. 2004) and HeLa cells of VAMP8 (Wong et al. 1998). This proved particularly useful for detecting VAMP8 as DRG lysates used did not show any immunoreactivity. It demonstrates that the antibody used for VAMP8 was by definition working and it appears to be specific. The detection of VAMP8 was expected given the detection by the microarray mRNA analysis but perhaps the expression levels of VAMP8 in both DRG and brain are not within detection levels of western blotting. VAMP8 is associated with early endosomes (Wong et al. 1998) and in the kidney it regulates the fusion of aquaporin 2. So, it theoretically it could mediate the degradation of plasma membrane VGSCs in regulated endocytosis.

4.3.3 VAMP-1, -2, -3, -4, -5, -7 and -8 are expressed in the soma of isolated DRG neurones. VAMP-1, -2 and -7 in the neurites.

Following the results of the microarray and western blotting it was important to identify the source of the VAMP proteins in the lysates. Immunocytochemistry of isolated DRG neurones depicted punctate and widespread expression of the seven isoforms in DRG neurones' soma.

VAMP-1 and -2 have been linked to neurotransmitter release (Borisovska et al. 2005) and described in trigeminal ganglion neurones as mediators of CGRP secretion (Meng et al. 2007). In this thesis' immunocytochemistry both VAMP1 and VAMP2 were observed in the soma and in the neurites. Although, DRG neurones do not form physiological relevant synapses in culture (Gupton and

Gertler 2010), they do growth neurites and are believe to form ‘synapses’ with other neurones in culture. To confirm their role in synaptic transmission, further experiments could explore co-localisation with CGRP, substance P and VGLUT2. In chapter 5, I have explored the role of VAMP1/2/3 and SNAP25 with botulinum neurotoxin chimaeras.

VAMP3 is ubiquitously expressed and it has been associated with sorting/early and recycling endosomes (McMahon et al. 1993). In DRG neurones the staining was mainly observed in the soma and in some cells more intense closer to the plasma membrane. To further understand, the putative role of VAMP3 in endosomes, antibodies against EEA1 (endosome maker) could be used to elucidate its physiological role in DRG neurones.

Previous studies have stablished a role for VAMP4 in membrane trafficking in the transGolgi network, early/recycling endosomes (Peden et al. 2001, Mallard et al. 2002) and in hippocampal neurones asynchronous neurotransmitter release (Raingo et al. 2012). Here it is shown for the first time that VAMP4 is also expressed in DRG neurone somata and coherent with previous reports it appeared localized to nuclei and not in the neurites (Peden et al. 2001). To confirm this, further experiments could be performed with antibodies to synatxin 5 (Golgi) and calreticulum (endoplasmatic reticulum marker) to confirm the function of VAMP4 in sensory neurone biology.

VAMP5’s role may not be as clear. This SNARE is highly expressed in skeletal and cardiac muscle where it has been found at the plasma membrane and vesicles. It is also known as myobrevin due to its role in myogenesis (Zeng et al. 1998). In DRG neurones, the staining was not as intense as other isoforms but it was also mainly found in the soma.

VAMP7 has been described in neurite growth (Gupton and Gertler 2010), spontaneous neurotransmitter release in hippocampal neurones (Bal et al. 2013), and linked to phagocytosis in macrophages (Braun et al. 2004). Interestingly, VAMP7 was only found to be expressed on DRG neurones which

could be highlighting a neuronal specific role. Since DRG neurones in culture are known not to form synapses with relevant/physiological tissues (Zarei, Toro and McCleskey 2004) unlike hippocampal/cortical neurones (Bal et al. 2013) a role in synaptic transmission in DRG seems unlikely. On the other hand, DRG neurones in culture, particularly those treated with NGF, as I used, are known to rapidly extend neurites and thus it is seems likely that the VAMP7 vesicles observed in my study could be involved in neurite expansion. This could be assessed with antibodies against growth associated protein 43, a nerve-specific protein that has been linked to the development and restructuring of axons (Dani, Armstrong and Benowitz 1991).

Finally, VAMP8 is also believed to be ubiquitously expressed but enriched in epithelial cells in the lung, pancreas, intestine and kidney. It mediates homotypic fusion of early and late endosomes (Antonin et al. 2000b). In DRG neurones, the staining against VAMP8 was very broad but close to the plasma membrane. Co-localisation studies with EEA1 could further the understanding of this isoform in DRG neurones.

4.3.4 VAMP isoform expression is consistent across soma diameter

Nociceptors have been demonstrated to have a smaller mean diameter compared to other primary fibres (Lawson and Waddell 1991). These results (Figure 4.5) suggest a ubiquitous distribution of the isoforms throughout different soma diameters. Exceptionally, VAMP7 expression shows a shift towards 25 μm and VAMP5 to 20 μm. Hence, the cells falling within the smaller diameter range (<20 μm) are likely to be nociceptors and expressing VAMP-1, -2, -3, -4, -5, and -8. On the other hand, larger diameter (>30 μm) neurones associated with A-α and β fibers (Lawson and Waddell 1991) will likely express VAMP-1, -2, -3, -4, -7 and -8. Of all the VAMP isoforms, VAMP-1, -2, -3, 7 and 8 are known to mediate vesicle fusion with the plasma membrane (Hasan et al. 2010). VAMP5 is mainly found in skeletal and cardiac muscle and its expression increases during myogenesis. SNARE mediated fusion analysis

has shown that VAMP5 does not form complexes with SNAP25/syntaxin 1 or SNAP25/syntaxin 5 so it is not believed to be involved in regulated exocytosis (Hasan et al. 2010). In contrast, VAMP7, the other divergent VAMP between small and large diameter DRG neurones, mediates vesicular transport from endosomes and lysosomes in PC12 cells (Advani et al. 1999), regulates secretion of interleukin-12 in dendritic cells (Chiaruttini et al. 2016) and a reelin sensitive vesicle pool in hippocampal neurones that augments spontaneous transmission (Bal et al. 2013). Thus, it could indicate a unique secretory pathway in this subset of DRG neurones.

4.3.5 Is Nav1.7 found within vesicles with specific VAMP isoforms?

Recent studies indicate that specific subsets of SNARE proteins are involved in the delivery of ion channels and receptors to the plasma membrane. For instance, NMDA receptor delivery to the plasma membrane of hippocampal neurones is mediated by SNAP25-VAMP1-syntaxin4 complex (Gu and Huganir 2016). In PC12 cells, N-type Ca^{2+} channels have been shown to be translocated to the plasma membrane via secretory vesicles after stimulation by high KCl solutions and ionomycin. In contrast, VAMP2 has been identified for trafficking AMPA receptors (Jurado et al. 2013) and TRPC3 channels (Singh et al. 2004). Hence, there is evidence for SNARE-mediated delivery of channels and receptors to the plasma membrane as opposed to constitutive secretion (section 1.4.9). In the context of pain processing, the co-trafficking of TRPV1 and TRPA1 induced by TNF-α has been described by the Oliver Dolly group as being mediated by SNAP25-VAMP1-syntaxin1. These vesicles containing VAMP1, TRPA1 and TRPV1 contained CGRP, which suggests a dual role on neurotransmission and potentiation (Meng et al. 2016). Hence, it was postulated that a subset of VAMPs would co-localise with Nav1.7 in DRG neurones.

Surprisingly, these data do not indicate or suggest a possible isoform mediating the trafficking of Nav1.7. This is likely to be a false negative. Newly

synthesised proteins are strongly believed to be delivered to the plasma membrane via SNARE regulation (section 1.4.9)(Jahn and Scheller 2006). It is possible that this question falls beyond the sensitivity of the method used. Each pixel in the images acquired is equivalent to 200 nm which far greater than a large dense core vesicle (Burgoyne and Morgan 2003). Other techniques such proximity ligation assay or higher resolution imaging such as OMX or Stochastic Optical Reconstruction Microscopy (STORM) could be used to explore this hypothesis. Another possibility is that the images were not acquired at the right time point. That is, most of the Nav1.7 staining was observed at the membrane. So, the percentage of the channel being trafficked at the time of fixation might be too low for detection. Therefore, the use of a stimulant associated with increased trafficking events of Nav1.7 could improve the detection and aid identification of the SNARE proteins leading to membrane delivery of Nav1.7. For example, exploring the effects of PKA or PKC modulators, second messengers of inflammatory mediators known to upregulate Nav1.7 currents (Black et al. 2004, Gould et al. 2004) or adding the inflammatory mediators to DRG cultures to increase Nav1.7 trafficking.

4.4 General discussion

These are the first set of results to describe and characterise VAMP isoforms in DRG neurones by western blotting and immunocytochemistry. Even though, further experiments such as co-localisation with peptides or other markers, and functionally analysis of SNARE complexes are necessary to confirm suggestions of functional roles made by these results. They provide an important foundation for further investigation of DRG neurones' secretory pathways.

5 – Investigating the potential of Botulinum neurotoxin chimaeras to regulate ion channel trafficking and excitability in DRG neurones

5.1 Introduction

Therapeutic indications for botulinum neurotoxins have been progressively expanding (Abrams and Hallett 2013). BoNT/A has been useful for pathological conditions involving excess muscle contractions but also in the treatment of chronic migraine (Jackson, Kuriyama and Hayashino 2012). BoNT/A and BoNT/B have very defined molecular targets. BoNT/A cleaves SNAP25 (Matak and Lackovic 2014) and BoNTB VAMP1/2/3 (Schiavo et al. 1992) and as a consequence prevent vesicular fusion. Hence, not only are they useful in a clinical setting but they are also valuable experimental tools. Botulinum neurotoxins have been used to further understand CGRP secretion from trigeminal ganglia and DRG neurones. For instance, trigeminal ganglia neurones have been demonstrated to require VAMP1 for CGRP secretion (Meng et al. 2007) and 100 nM BoNT/A pre-incubation significantly delayed CGRP release from trigeminal ganglia neurones *in vitro* (Meng et al. 2009). To better select the subpopulation of DRG neurones, those that are IB4 negative, botulinum neurotoxin chimaeras were used in this chapter.

Botulinum neurotoxin chimaeras, tetbot A and tetbot B, contain the *tetanus* toxin binding domain stapled with the proteolytic domain of botulinum neurotoxin A and B, respectively. The main difference between these chimaeras and the native toxins is that they are design to target IB4-negative DRG neurones, cleaving SNAP25 (tetbot A) (Ferrari et al. 2013) and VAMP2 (tetbot B) (Appendix 2 & 4). Thus, targeting mainly peptidergic DRG neurones while maintaining the same proteolytic activity of the native toxins. Hence, in this chapter I aimed to explore the potential of these engineered toxins, tetbot

A and tetbot B, to regulate peptide secretion and inhibit excitability changes induced by IS.

5.2 Results

5.2.1 Tetbot A cleaves SNAP25 in IB4-negative DRG neurones within 24 h incubation

Tetbot A has been demonstrated to successfully cleave SNAP25 in hippocampal neurones and to be selective to IB4-negative DRG neurones (Ferrari et al. 2013). To assess the ability of tebot A to cleave SNAP25 in mouse DRG neurones *in vitro,* isolated DRG neurones were treated with 10 nM tetbot A (concentration previously described in Ferrari et al. 2013) for 24 h and 65 h. Confocal microscopy of DRG neurones pre-treated for 24 h revealed robust staining of cleaved SNAP25 (cSNAP25) in IB4-negative DRG neurones' soma and neurites (Figure 5.1 A). IB4-negative neurones were identified with IB4-FITC and cSNAP25 was identified by an in-house antibody selective only to the cleaved form of SNAP25 (Mangione et al. 2016). Western blotting further confirmed cleavage of SNAP25 within 24 h and 65 h (Figure 5.1 B). Clearly denoting two bands for SNAP25 and cSNAP25.

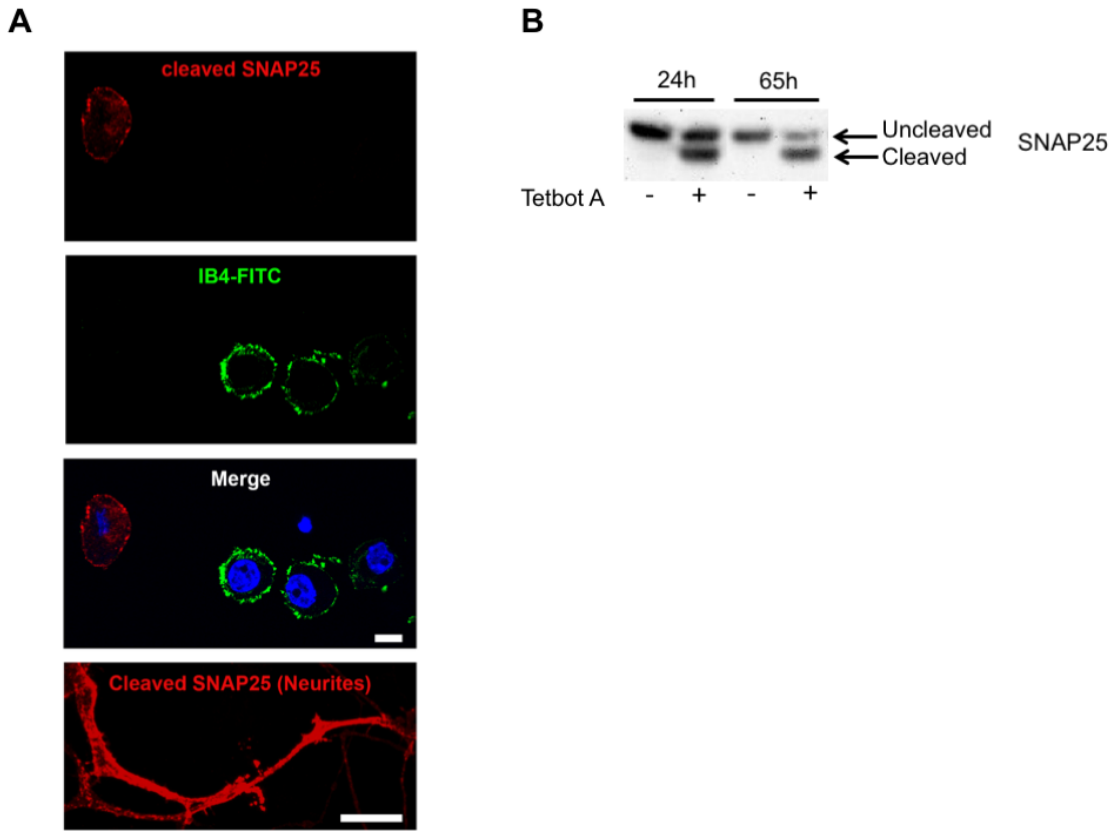

Figure 5.1 Tetbot A selectively cleaves SNAP25 in mostly peptidergic DRG neurones. (A) Immunocytochemistry illustrating the selectivity of Tetbot A to IB4-negative DRG neurones. Cleaved SNAP25 signal was detected in the soma and neurites. (Blue) DAPI, identifying the nuclei, (Green) IB4, identifying non-peptidergic DRG population and (Red) cSNAP25. Scale bars show 10 μm. (B) Western blot depicting cleaved SNAP25 (with an anti-SNAP25 antibody with an epitope common to both cSNAP25 and SNAP25) in lysates recovered from matched cultures of DRG neurones treated for 24 h and 65 h with 10nM Tetbot A. Marta Alves Simões generated the western blot samples and Dr Charlotte Leese performed the western blot.

5.2.2 Tetbot A reduces CGRP secretion

To further understand the functional consequences of SNAP25 cleavage by tetbot A on DRG neurones, CGRP secretion was quantified from DRG neurones pre-incubated with 10 nM tetbot A and BoNT/A for 65 h (Figure 5.2 A). Due to manufacture requirements tetbot A was dissolved in 0.4% n-octylglucoside detergent (OG). Thus, all other groups were also incubated with the same concentration of OG. Conditions were optimised to trigger CGRP release specifically from IB4-negative neurones (capsaicin) versus CGRP release from unselected neurones (60 mM KCl) (further details Appendix 3). As shown in Figure 5.2, both stimuli effectively and significantly evoked CGRP

secretion (capsaicin, p=0.0095, N=6; KCl p<0.0001, N=3). In line with previous reports (Meng et al. 2009), I observed KCl to evoke more CGRP secretion than capsaicin; whether this was due to recruitment of peptidergic neurones not expressing the capsaicin receptor TRPV1 (Usoskin et al. 2015), or attenuated secretion caused by rapid desensitisation of the TRPV1 receptor under our experimental conditions (Jancso, Jancsoga.A and Szolcsanyi 1967) or more effective peptide secretion due to increased presence of full fusion events by KCl was not determined here. However, importantly for the purposes of my study, pre-incubation with 10 nM tebot A significantly reduced KCl evoked CGRP secretion (p=0.0001, N=3) but not that induced by capsaicin (p=0.1388, N=4; Figure 5.2). Likewise, 10 nM BoNT/A did not reduce CGRP release induced by 1 μM capsaicin (p= 0.1372, N=4, one-way ANOVA with Fisher's LSD). No significant changes were seen in basal release.

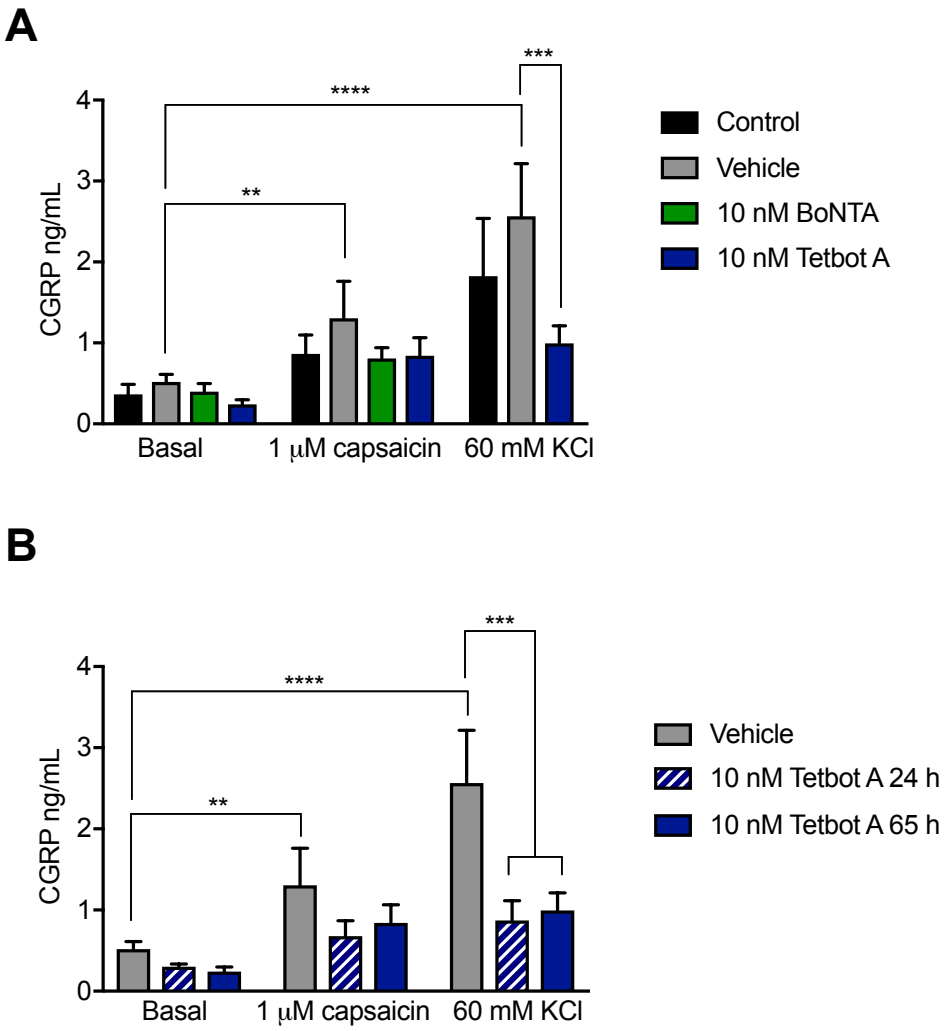

Figure 5.2 Tetbot A reduces CGRP secretion from DRG neurones.
Isolated DRG neurones were incubated with 1 μM capsaicin or 60 mM KCl in external recording solution for 30 min. The supernatant was used to detect CGRP levels using a commercial ELISA kit by Phoenix, USA. (A) DRG neurones in control conditions and pre-incubated with vehicle (n-octylglucoside), 10 nM Tetbot A, and 10 nM BoNT/A. (B) DRG neurones pre-incubated with vehicle, Tetbot A for 24 h, and Tetbot A for 65h. One-way ANOVA with uncorrected Fisher's LSD. [**p=0.0095 ***p=0.0003 (24 h) ***p=0.0001(65 h) ****p<0.0001] (N=3-6 for each data column). Error bars show SEM.

Next, a time-course analysis of 24 h and 65 h incubations was investigated (Figure 5.2 B). Pre-incubation with 10 nM tetbot A for 24 h and 65 h significantly reduced CGRP release induced by 60 mM KCl (24 h: p=0.0003, N=3; 65 h: p=0.0001, N=4). Surprisingly, no significant changes were seen with 1 μM capsaicin (24 h: p=0.085, N=3; 65 h: p=0.1388, N=4) when compared with basal release from cultures similarly pre-incubated with the toxins (24 h: p=0.5513, N=3; 65 h: p=0.3459, N=4; one-way ANOVA with Fisher's LSD).

Hence, these data suggest that 10 nM tetbot A pre-incubation for 24 h is enough time for cleavage of SNAP25 that affects CGRP release. This could indicate that another t-SNARE is involved in secretion of CGRP (e.g. SNAP23) or that TRPV1 receptor is no longer coupled to the CGRP release.

5.2.3 SNAP25 cleavage does not prevent hyperexcitability of DRG neurones in an *in vitro* model of inflammation

After establishing that 10 nM tetbot A cleaves SNAP25 and inhibits CGRP release evoked by KCl within 24 h, I investigated whether the increased excitability induced by IS (Chapter 3) is also affected by SNAP25 cleavage. Hence, isolated DRG neurones were pre-treated with 10 nM tetbot A and control neurones with OG, followed by IS incubation for 6 h (Figure 5.3 A). Comparable to results reported in chapter 3 (Figure 3.3), the frequency of action potentials at rheobase and twice rheobase was assessed for the four groups (vehicle, IS, tetbot A, tebot A + IS) from IB4-negative DRG neurones (Figure 5.3). Surprisingly, vehicle treated DRG neurones showed an increase in baseline excitability together with DRG neurones pre-treated with tetbot A only, which is likely to be a vehicle (OG) effect.

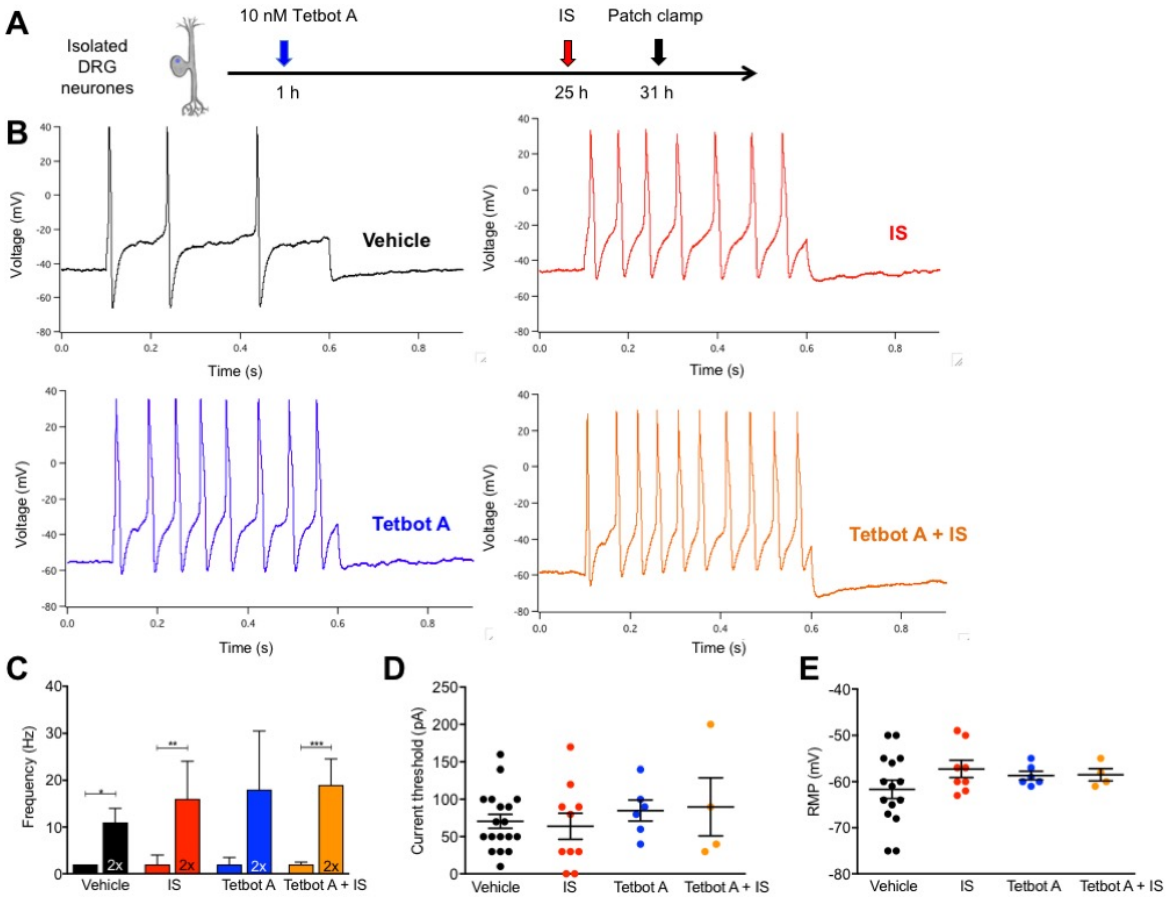

Figure 5.3 SNAP25 cleavage does not prevent hyperexcitability following inflammatory soup.

(A) Isolated DRG neurones were pre-incubated with Tetbot A before adding the inflammatory soup (IS). (B) Representative traces of current clamp recordings at twice rheobase of DRG neurones of each condition. (C) Frequency of action potentials at rheobase and twice rheobase, (D) current threshold, and (E) resting membrane potential. Error bars show SEM in E and interquartile range for C and D. Each data point corresponds to a DRG neurone from up to five mice. *p<0.05 **p<0.01 ***p<0.001 kruskal-wallis test ($n_{vehicle}$=20, n_{IS}=9, $n_{TetbotA}$=6, $n_{TetbotA+IS}$=4, N=2-5).

Tetbot A did not prevent hyperexcitability induced by IS. For all groups, with the exception of tetbot A only group, an increase excitability at twice rheobase was observed (Figure 5.3 C) (Median - vehicle rheobase: 2 Hz, vehicle twice rheobase: 11 Hz, p<0.05; IS rheobase: 2 Hz, IS twice rheobase: 16 Hz, p<0.01; tetbot A rheobase: 2 Hz, tetbot A twice rheobase: 19 Hz, p>0.05; tetbot A + IS rheobase: 2 Hz, tetbot A + IS twice rheobase: 18 Hz, p<0.001; Kruskal-Wallis test, $n_{vehicle}$=20, n_{IS}=9, $n_{tetbot\ A}$=6, $n_{tetbot\ A\ +\ IS}$=4, N=2-5). In addition, no changes were seen in current threshold (Median - vehicle: 60 pA, IS: 55 pA, tetbot A: 85 pA, tetbot A + IS: 65 pA; kruskal-wallis test) (Figure 5.3 D) or resting membrane potential (vehicle: -61.67 ± 7.77 mV, IS: -57.25 ± 5.23 mV,

tetbot A: -58.67 ± 2.25 mV, tetbot A + IS: -58.5 ± 2.64 mV; one-way ANOVA) (Figure 5.3 E). Taken together, these data seem to suggest SNAP25 does not have a role in reducing or altering the effects of IS.

5.2.4 The effects of tetbot B on VAMP1, VAMP2, and VAMP3 protein expression

Another botulinum chimaera developed by the Davletov lab is tetbot B. Similar to tetbot A it also targets IB4-negative DRG neurones as it has the same receptor binding domain but instead has the proteolytic domain of BoNT/B (VAMP1/2/3 cleavage) and not BoNT/A. Previous unpublished lab data on cortical neurones has shown significant reduction in VAMP2 expression with 10 nM Tetbot B (Appendix 2). To assess the effects of tetbot B on VAMP1, VAMP2 and VAMP3 protein levels in DRG neurones *in vitro,* isolated DRG neurones were incubated for 24 h and 65 h (Figure 5.4). Due to manufacture requirements tetbot B was also dissolved in 0.4% OG. Thus, control samples were also incubated with the same concentration of OG for 65 h.

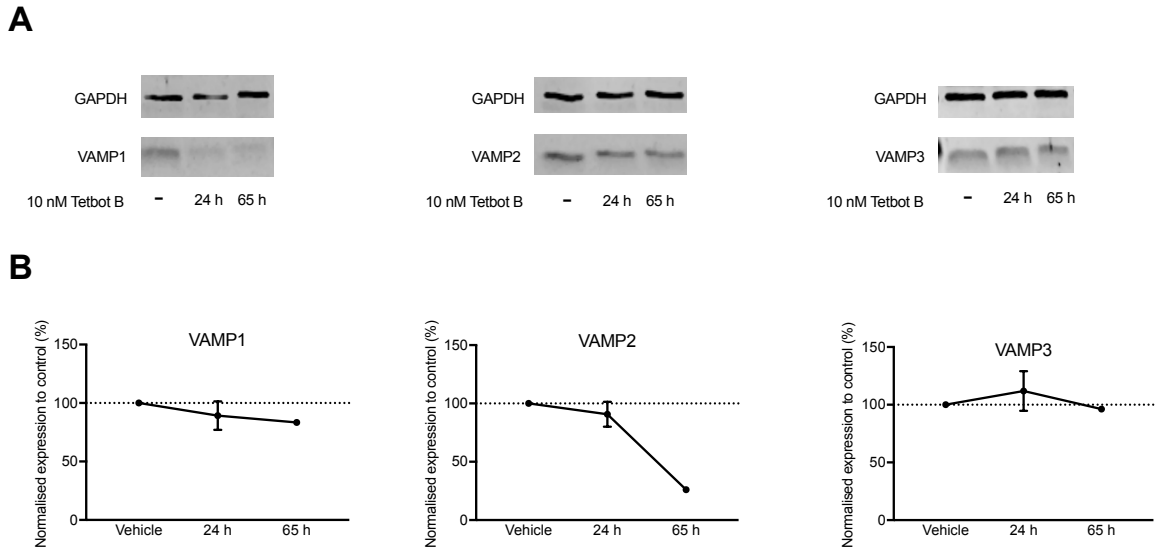

Figure 5.4 Tetbot B does not seem to significantly reduce VAMP1, VAMP2 or VAMP3 after 24 h incubation.
Isolated DRG neurones were incubated with 10 nM Tetbot B for 24 h and 65 h. (A) Representative immunoblots for VAMP1, VAMP2 and VAMP3. (B) Normalised expression to GAPDH loading control. The median intensity of the immunoblot bands indicating VAMP expression in DRG was divided by the median intensity of the respective loading control and then normalised to the experimental control (vehicle samples). VAMP1 – $n_{vehicle}$=3, n_{24h}=3, n_{65h}=2; VAMP2 – $n_{vehicle}$=4, n_{24h}=4, n_{65h}=2; VAMP3 – $n_{vehicle}$=3, n_{24h}=3, n_{65h}=2. Error bars show SEM, no error bars were added to 65 h data points as the n number is insufficient.

Changes in protein levels were assessed by western blot via changes in band integrated density (Figure 5.4 A). The rationale behind these experiments was if Tetbot B cleaves VAMP1/2/3, the cleaved VAMP isoforms will be degraded by the cell and a decrease in protein expression may be detected via western blotting. At 24 h there were no significant changes detected (paired t-test; N_{VAMP1}=3, p=0.471; N_{VAMP2}=4, p=0.452; N_{VAMP3}=3, p=0.561). At 65 h, both VAMP1 and VAMP2 seem to decrease in expression to 83% and 26% respectively but low N numbers did not allow to do further statistics (N=2) (Figure 5.4).

5.2.5 Tetbot B does not impair CGRP secretion

To evaluate tetbot B's effects on CGRP secretion from DRG neurones, these were pre-incubated with 10 nM tetbot B or 10 nM BoNT/D (also VAMP cleaving) for 65 h and stimulated with 1 μM capsaicin or 60 mM KCl (Figure 5.5 A). Akin to experiments with tetbot A, our control set significantly increased. That is, 1 μM capsaicin significantly increased the concentration of CGRP detected in vehicle treated DRG neurones' supernatant (p=0.0095, N=6) as well as 60 mM KCl (p<0.0001, N=3), demonstrating that the stimuli are working. However, this increase was not prevented by pre-incubation with 10 nM tebot B or 10 nM BoNT/D (1 μM capsaicin – control: 0.863 ± 0.572 ng/mL, vehicle: 1.2 ± 1.121 ng/mL, BoNT/D: 0.942 ± 0.257 ng/mL, tetbot B: 0.994 ± 0.379 ng/mL) (60 mM KCl - control: 1.826 ± 1.235 ng/mL, vehicle: 2.565 ± 1.124 ng/mL, tetbot B: 2.341 ± 1.176 ng/mL) (Figure 5.5 A), suggesting that cleavage of VAMP1/2/3 does not significantly impair CGRP secretion or that tetbot B was insufficiently effective in cleaving VAMP1/2/3.

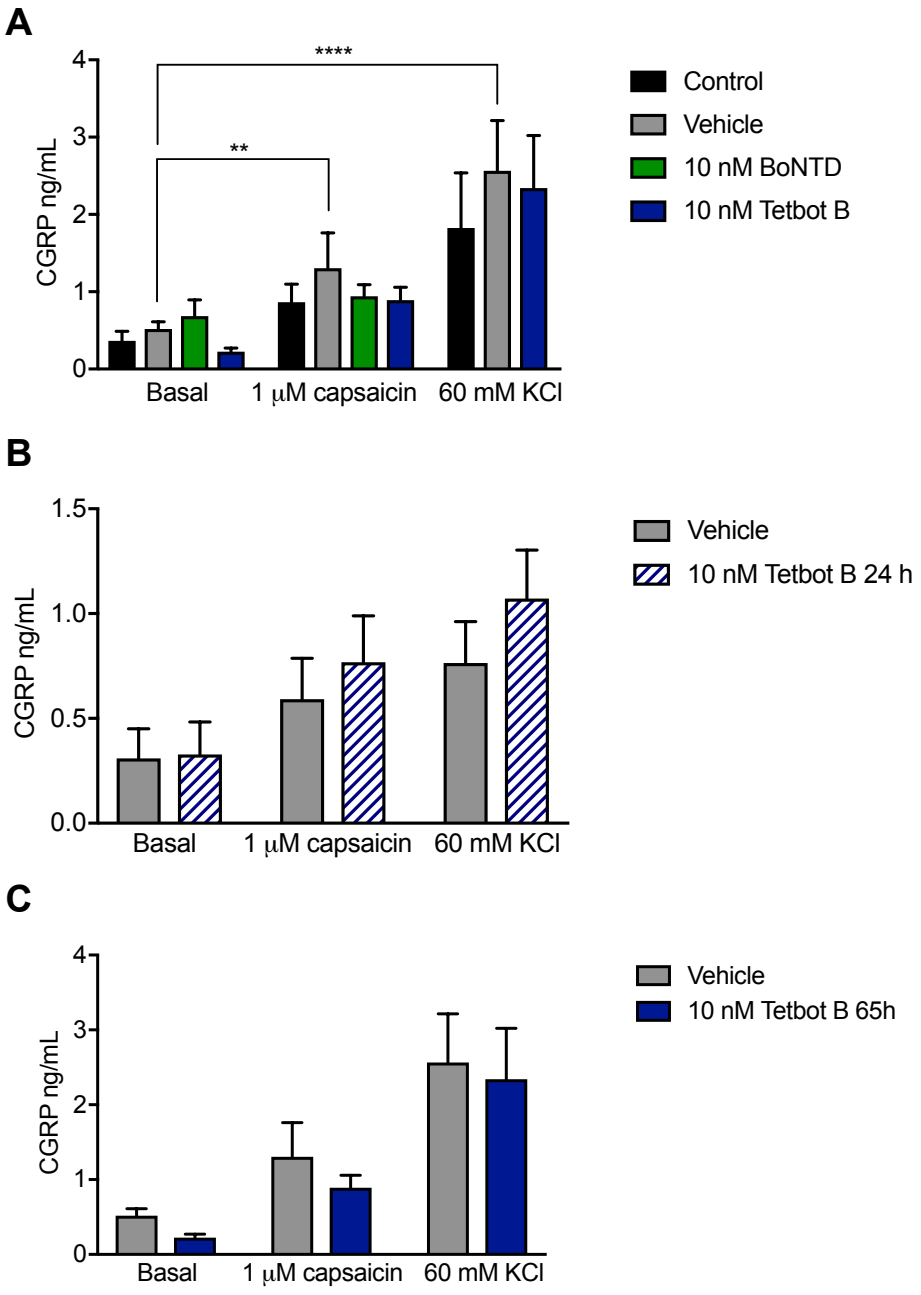

Figure 5.5 Tetbot B does not impair CGRP secretion from DRG neurones.
Isolated DRG neurones were incubated with 1 μM capsaicin or 60 mM KCl in external recording solution for 30 min. The supernatant was used to detect CGRP levels using a commercial ELISA kit by Phoenix, USA. (A) DRG neurones in control conditions and pre-incubated with vehicle (n-octylglucoside), 10 nM Tetbot B, and 10 nM BoNT/D. (B) DRG neurones pre-incubated with vehicle and Tetbot B for 24 h. (C) DRG neurones pre-incubated with vehicle and Tetbot B for 65h. One-way ANOVA with uncorrected Fisher's LSD *p=0.0095 ****p<0.0001(N=3-6 for each data column). Error bars show SEM.

Further analysis of CGRP secretion with tetbot B pre-incubation for 24 h and 65 h (Figure 5.5 B and C) also showed no significant reduction for 24 h (1 μM capsaicin – vehicle: 0.591 ± 0.339 ng/mL, tetbot B: 0.767 ± 0.382 ng/mL, Tukey

post hoc, p=0.998, N=3) (60 mM KCl – vehicle: 0.764 ± 0.343 ng/mL, tetbot B: 1.07 ± 0.4 ng/mL, Tukey post hoc, p=0.963, N=3) and 65 h (1 μM capsaicin – vehicle: 1.2 ± 1.121 ng/mL, N=6, tetbot B: 0.994 ± 0.379 ng/mL, N=5, Tukey post hoc, p=0.188) (60 mM KCl – vehicle: 2.565 ± 1.124 ng/mL, tetbot B: 2.341 ± 1.176 ng/mL, Tukey post hoc, p=0.594, N=3). Thus, it suggests tetbot B has no effect on CGRP secretion form isolated DRG neurones when incubated for 24 h or 65 h.

5.2.6 Tetbot B does not reduce hyperexcitability of DRG neurones in an *in vitro* model of inflammation

To further investigate the effects of tetbot B and the possible impact of VAMP1/2/3 cleavage on IS-induced hyperexcitability, I investigated the effects of tetbot B on DRG excitability (Figure 5.6 A). As reported earlier, vehicle treated DRG neurones had an unexpected high baseline excitability (Figure 5.6 B and C) (rheobase: 2 Hz, twice rheobase: 11 Hz). Action potential frequency was significantly increased at twice rheobase (Kruskall-wallis with Dunn's multiple comparisons test, $p<0.05$), defining them as hyperexcitable. IS alone and tebot B + IS also induced hyperexcitability characteristics (IS - rheobase: 2 Hz, twice rheobase: 16 Hz, Kruskall-wallis with Dunn's multiple comparisons test, $p<0.01$) (Tetbot B + IS - rheobase: 2 Hz, twice rheobase: 15 Hz, Kruskall-wallis with Dunn's multiple comparisons test, $p<0.05$) (Tetbot B - rheobase: 2 Hz, twice rheobase: 12 Hz, Kruskall-wallis with Dunn's multiple comparisons test, not significant). As with previous experiments with tetbot A no changes were also observed in resting membrane potential of DRG neurones (vehicle: -61.67 ± 7.77 mV, IS: -58 ± 7.56 mV, tetbot B: -60.2 ± 7.48 mV, tetbot B + IS: -59.88 ± 8.23 mV; one-way ANOVA) (Figure 5.6 D) or current thresholds (Median - vehicle: 50 pA, IS: 50 pA, tetbot A: 95 pA, tetbot A + IS: 140 pA; kruskal-wallis test) ($n_{vehicle}=20$, $n_{IS}=9$, $n_{TetbotB}=8$, $n_{TetbotB+IS}=8$, N=6) (Figure 5.6 E).). Hence, these experiments may suggest that cleavage of VAMP1/2/3 does not have an impact on IS induced excitability but require further optimisation. Overall it suggests the toxins were ineffective over the time-course tested.

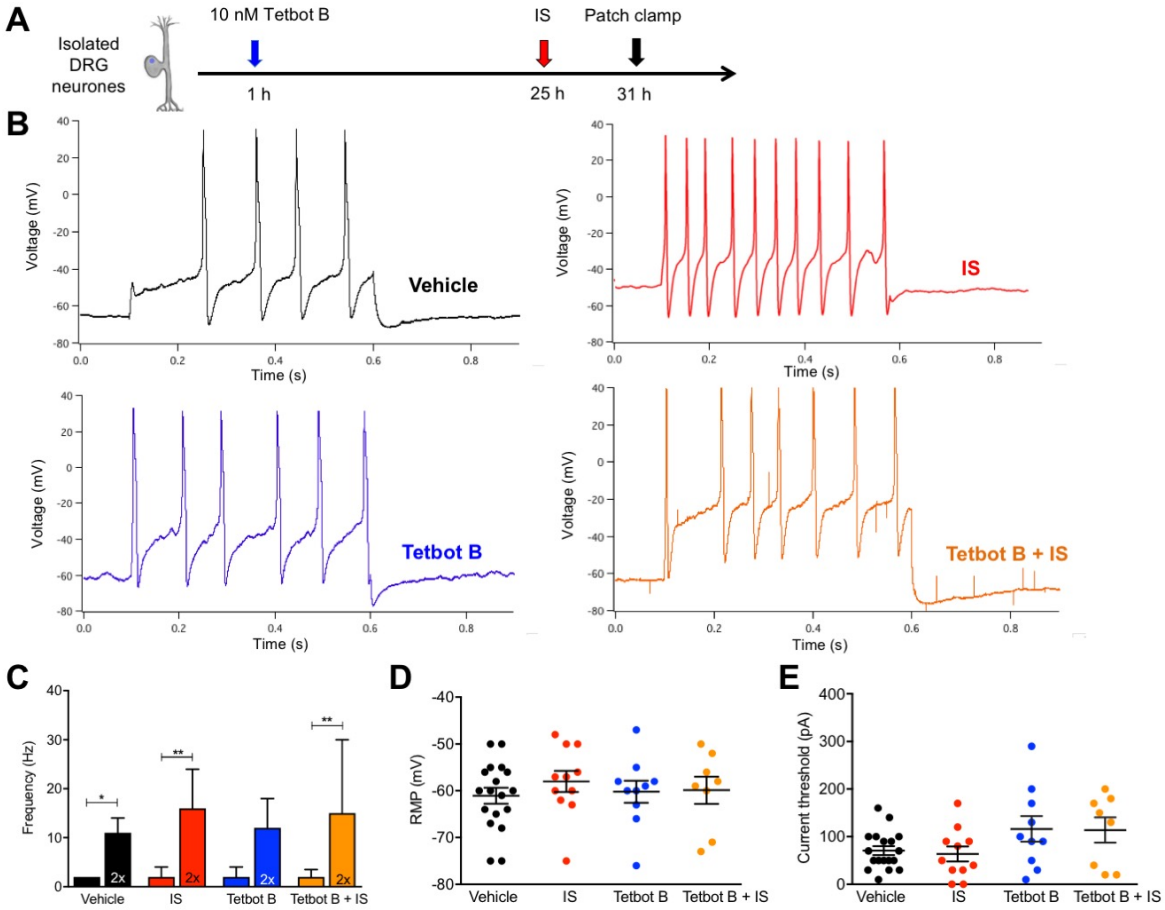

Figure 5.6 Pre-incubation with 10 nM Tetbot B does not prevent IS-induced hyperexcitability.

(A) Timeline for the experimental protocol. Isolated DRG neurones were pre-incubated 10 nM Tetbot B and with the inflammatory soup (IS) for 6 h or 10 nM Tetbot B only, IS or none. (B) Representative traces at twice rheobase for vehicle, IS, Tetbot B, and Tetbot B + IS. (C) Frequency of action potentials at rheobase and twice rheobase, (D) current threshold, and (E) resting membrane potential. Error bars show SEM except (C) where median with interquartile range is plotted. Each data point corresponds to a DRG neuron from six mice. *p<0.05 **p<0.01 kruskal-wallis with Dunn's multiple comparisons test ($n_{vehicle}$=20, n_{IS}=9, $n_{TetbotB}$=8, $n_{TetbotB+IS}$=8, N=6)

5.3 Discussion

The aims of this chapter were to evaluate the potential of these new chimaeras, tetbot A and tetbot B, to inhibit CGRP release and to impair IS-induced hyperexcitability. Using CGRP release as an assay to establish tetbot A and tetbot B functional effects, only tetbot A significantly reduced CGRP release within 24 and 65 h. Immunocytochemistry revealed strong staining for cSNAP25 in IB4-negative DRG neurones pre-incubated with tetbot A. Patch clamp analysis of the effects of pre-incubation of these chimaeras revealed no

significant changes in excitability. The DRG neurones incubated with either tetbot A or tetbot B had no significant changes in excitability parameters analysed. Vehicle effects were seen throughout patch clamping experiments that need to be addressed for further experiments.

5.3.1 Tetbot A cleaves SNAP25 in IB4-negative DRG neurones within 24 h incubation

These results further support previously published data (Ferrari et al. 2013) showing the efficacy and selectivity of tetbot A. Yet, this is the first time-course analysis done on DRG neurones. It strongly showed that 10 nM tetbot A cleaves SNAP25 within 24 h (Figure 5.1 A and B) which was maintained at 65 h (Figure 5.1 B). The two bands detected by the anti-SNAP25 antibody (Figure 5.1 B) are likely to be a consequence of the selectivity of tetbot A as it is only able to enter IB4-negative DRG neurones. Thus, the uncleaved SNAP25 band is probably from IB4-positive DRG neurones and some IB4-negative DRG neurones. SNAP25 can be observed in IB4 positive neurones in cultures treated with tetbot A (Figure 5.1 A).

5.3.2 Tetbot A reduces CGRP secretion

Meng and colleagues have shown previously that SNAP25 is necessary for CGRP secretion in trigeminal ganglia neurones (Meng et al. 2009). In this chapter, pre-incubation with tetbot A reduced CGRP release from DRG neurones when stimulated with 60 mM KCl. Tetbot A and BoNT/A, used by Meng and colleagues, differ in their receptor binding domain (Ferrari et al. 2013). Tetbot A has the receptor binding domain of the tetanus toxin, making it selective to mainly peptidergic DRG neurones, whereas BoNT/A does not selectively target this population. Unpublished lab data has shown that Tetbot A and BoNT/A overlap in their targeting DRG subpopulation but are not equal (due to different gangliosides). Hence, this would suggest that tetbot A has a higher degree of potency has it only targets mostly CGRP-secreting neurones. Yet, when 1 μM capsaicin was applied to both groups no significant changes were seen with pre-incubation of either these compounds. In similar

experiments by Meng et al. 2009, 10 nM BoNT/A pre-incubation has also been found to have limited effect in reducing CGRP secretion elicited by 1 μM capsaicin, around ~15%. Measurements obtained with tetbot A pre-incubation did not show a significant difference between 10 nM BoNT/A and 10 nM tetbotA. Both tendentially decrease, but it is not significant. Hence, these data suggest that changes in the receptor binding domain do not have an impact overall *in vitro* CGRP release. However, this is likely to be due the potency of this compound rather than its selectivity. Furthermore, CGRP secretion elicited by 60 mM KCl had a 60% reduction with pre-incubation of 10 nM BoNT/A (Meng et al. 2007). Regrettably, no data were acquired for BoNT/A in our data set but tebot A did in fact significantly reduce CGRP release of DRG neurones elicited by 60 mM KCl.

Usoskin and colleagues have shown that SNAP25 is present in peptidergic neurones expressing TRPV1 but only the subgroup PEP1 expresses both TRPV1 and CGRP (see introduction section 1.2.6). Hence, if tetbot A is able to enter these neurones it would cleave SNAP25 and impair SNAP25 mediated secretion in these neurones. Yet, the results in this chapter (Figure 5.2) do not show a significant reduction in CGRP secretion induced by capsaicin. If the expression analysis described by Usoskin et al. 2015 is true at the protein level it is possible that this assay is only targeting very small population and the results demonstrate a false negative. One possible improvement for this assay could be combined stimulation (capsaicin plus another stimulus) as half of the peptidergic population (PEP2) does not seem to express TRPV1. For instance, NGF has been shown to induce CGRP release from DRG neurones in culture (Park et al. 2010) and TrkA is expressed in both peptidergic subgroups. This might further explain why a significant reduction was seen only with unspecific stimulation (60 mM KCl) and not capsaicin.

5.3.3 SNAP25 cleavage does not prevent hyperexcitability of DRG neurones in an *in vitro* model of inflammation

The rationale behind these experiments was to explore the reduction in mechanical hypersensitivity seen *in vivo* with tetbot A (Ferrari et al. 2013) and the role of vesicular fusion in establishing inflammatory hyperexcitability induced in our *in vitro* model (chapter 3). These data suggest that SNAP25 has no role. One possible explanation would be that tetbot A may alter mechanosensitivity by decreasing the number of action potentials that lead to the release of neurotransmitters at the level of the spinal cord or by direct cleavage of vesicles containing neurotransmitters and ion channels at spinal cord synapses. In experiments with BoNT/A, pre-incubation with 10U/mL BoNT/A decreased the proportion of mechanosensitive DRG neurones showing slowly adapting currents (Paterson et al. 2014). In this *in vitro* model of inflammation, no changes in excitability were observed with the pre-incubation of tetbot A. These are similar findings to those using BoNT/A (Paterson et al. 2014). Given the previous results with CGRP ELISA (Figure 5.2) it is possible that the effects seen before (Ferrari et al. 2013) are mediated mainly by impaired neurotransmitter release at the level of the spinal cord from primary afferents and changes in mechanotransduction as seen with BoNT/A. Another possibility is that the targeting of mostly peptidergic DRG neurones by tetbot A *in vivo* impairs neurotransmitter release from IB4-negative DRG neurones at the level of the soma and that may affect mechanoceptors within DRG ganglia in a paracrine manner. DRG neurones have been shown to secrete substance P, glutamate, and ATP from their soma (Jung et al. 2013, Zhang et al. 2007, Harding, Beadle and Bermudez 1999). For instance, Zhang and colleagues (2007) have shown that ATP secreted from DRG somata activates P2X7 receptors in satellite glial cells. In turn, they secrete TNF-α which increases DRG excitability. Evidence also suggests that parts of the botulinum and tetanus neurotoxins may be transcytosed to other cells even after internalization (Restani et al. 2012b, Restani et al. 2012a). BoNT/A has been found to cleave SNAP25 in neurones that were at least two synapses

away from the local injection site (Restani et al. 2012b), suggesting it can remain catalytically active between transcytosis and transport between neurones. Hence, *in vivo* effects can result from multiple affected cells.

5.3.4 The effects of tetbot B on VAMP1, VAMP2, and VAMP3 protein expression

Following unpublished lab experiments on cortical neurones, it was important to understand the effects of tetbot B on DRG neurones. Experiments on cortical neurones showed high efficacy of VAMP2 cleavage for tetbot B at 10 nM after incubation for 65 h. Western blotting experiments on DRG neurones did not show a significant reduction in the intensity of either targeted VAMP. Regrettably, I did not acquire enough data points at 65 h but taken together it is likely that VAMP2 is cleaved by tetbot B at this time point in DRG neurones. This low N number was partially due to a high variability of data points collected for DRG neurones. Cortical neuronal preparations yield high number of neurones with a high concentration of VAMP2 (brain lysates versus DRG lysates in chapter 4, Figure 4.2) making it easier to prepare paired experiments (treated vs untreated). In addition, a higher expression of VAMP2 in cortical neurones may have contributed to more robust detection of changes with tetbot B with western blot experiments.

5.3.5 Tetbot B does not impair CGRP secretion

VAMP1 has been shown to mediate CGRP secretion of trigeminal ganglia neurones (Meng et al. 2007). Thus, given that tetbot B putatively targets IB4-negative DRG neurones it was expected to reduce CGRP secretion further when compared to BoNT/D. BoNT/B and BoNT/D both cleave VAMP1/2/3 but BoNT/D has been shown to be more potent due to its higher uptake efficiency by neurones (Schiavo et al. 1992, Eleopra et al. 2013). Surprisingly, CGRP secretion stimulated with 1 μM capsaicin triggered similar CGRP release in vehicle, tetbot B and BoNTD treated groups (Figure 5.5). BoNT/D has been shown to reduce 1 μM capsaicin-induce CGRP release by 40% in trigeminal ganglia neurones. Conversely, BoNTB pre-incubation on trigeminal ganglia

neurones showed similar results to tetbot B (which have the same proteolytic domain), no reduction was seen when CGRP secretion was stimulated by 60 mM KCl (Meng et al. 2007). Taken together, these data suggest possible differences in BoNT/D efficacy between trigeminal ganglia and DRG neurones. Experiments with increased concentrations of tetbot B will be useful to further determine its ability to cleave VAMP1/2/3 and affect CGRP release. However, there is still the underlying possibility that CGRP regulated exocytosis might be also mediated via other VAMP proteins. In chapter 4, all 7 isoforms were identified in DRG neurones and its further characterisation would be beneficial to understand if more than one VAMP drives CGRP release in DRG neurones.

5.3.6 Tetbot B does not reduce hyperexcitability of DRG neurones in an *in vitro* model of inflammation

Current clamp recordings suggest that cleavage of VAMP1/2/3 does not impact the effects of IS-induced excitability. Theoretically, this could be affected directly by altering the equilibrium of ion channels present at the plasma membrane responsible for DRG excitability. Or the impairment of neurotransmitter release by the targeted neurones could interfere with signalling and communication between the different cell types *in vitro* and affect the development of IS-induced hyperexcitability. However, no changes were observed. There were two major caveats to these experiments. There was significant effect of the vehicle used. It had an impact on the excitability of the DRG neurones and CGRP secretion. Thus, it makes it more difficult to filter the effects of tetbot B (and tetbot A) on DRG excitability. It is also possible that the efficiency of these chimaeras varies between cell types (cortical vs DRG neurones). The set concentration used for these experiments was originally established in cortical neurones (Appendix 2) and it could be that a higher concentration of tetbot B would be more suitable for DRG neurones. In fact, further experiments demonstrating the efficacy of this chimaera in DRG neurones should have been done at an earlier stage of the project to define better experimental conditions.

5.3.7 General discussion and future directions

BoNT/A has been shown to silence synaptic transmission by cleaving SNAP25 (Abrahamsen et al. 2008) and prevent trafficking of TRPV1 and TRPA1 in trigeminal ganglia neurones (Meng et al. 2009, Meng et al. 2016). Tetbot A and B are botulinum neurotoxin chimaeras that putatively target IB4-negative DRG neurones. *In vivo* analysis of the effects of tetbot A have shown reduction in mechanical hypersensitivity induced by CFA (Ferrari et al. 2013). Current clamp recordings from pre-treated DRG neurones with tetbot A and B have found no changes in excitability induced by IS. These are similar findings to those of BoNT/A. BoNT/A has been found to reduce mechanosensitivity and not to alter DRG excitability (Paterson et al. 2014). It is then possible that both tetbot A and BoNT/A alter the trafficking of a mechanotransduction channel responsible for slowly adapting currents.

Yet, major technical issues were encountered during these acquisitions. The use of OG detergent to dissolve tetbot A severely decreased the success of patch clamp recordings and seems to independently increase DRG excitability. In fact, OG incubation also induced higher CGRP release from DRG neurones when compared to control (Appendix 3). Hence, it is possible that excitability effects of tetbot A are therefore clouded in this vehicle effect. Furthermore, the effects of this IS inflammation model are not fully understood (Chapter 3). It is possible that the combined effects of IS do not involve vesicular fusion of ion channels. Recordings from DRG neurones from mice treated with tetbot A and tetbot B would bypass this problem and is possibly the necessary step towards understanding both reduction of mechanotransduction and perhaps other ion channels using tetbot A and B.

6 - General discussion

In this thesis, I established an *in vitro* inflammation model which included an inflammatory soup (IS). This IS induced hyperexcitability in IB4-negative DRG neurones and an increase in TTX-R Na^+ currents. One of the challenges of the interpretation of these results is the variety of mediators added and their effects on DRG neurones. As most inflammatory mediators interact with GPCRs, some studies have taken a broader approach in understanding nociceptor sensitisation during inflammation. Selective nociceptor $G\alpha_q$, $G\alpha_{11}$, and $G\alpha_{q/11}$ knockout mice were used to understand the role of $G\alpha_q$ signalling on sensitisation. $G\alpha_{q/11}$ knock out mice showed reduced sensitivity to inflammation *in vivo* induced by CFA, formalin, bradykinin and capsaicin (Tappe-Theodor et al. 2012). Interestingly, they also found that in untreated knock out DRG neurones the $G_{q/11}$ modulates the TTX-R Na^+ currents. TTX-R currents were significantly increased at holding membrane potential between -20 and -10 mV whereas TTX-S currents were significantly increased between -30 and -10 mV. Thus, demonstrating a tonic role for GPCRs in DRG neurones and supporting previous research demonstrating the role of PKA and PKC in TTX-R current density (Gold et al. 1998).

The physiological significance of these experiments is limited. The field of pain is remarkably complex due to the variety of pathologies and hallmarks. Given the broad range of inflammatory mediators added and the diversity of possible secretors of those, it is possible that the combination of these inflammatory mediators and the time window of these observations reveal a very specific set of excitability changes. Undoubtedly, any conclusions made are limited to these experimental parameters, but an *in vitro* model provides a powerful tool that can aid the understanding of the complex signalling such as those of pain and trafficking of VGSCs.

In addition to increased excitability, the IS altered the expression levels of Nav1.7 and Nav1.9 at the plasma membrane. The plasma membrane of

neurones is a dynamic and heterogeneous 'surface' that determines the electrical capabilities of the neurones. Ion channels undergo highly dynamic changes such as lateral diffusion, endocytosis, clustering with other channels or receptors, and fuse in vesicles via exocytosis (Heine et al. 2016). One possible explanation for this observation is the change in subcellular location. It has been previously reported that changes in VGSCs density could have a significant impact of DRG excitability (Matzner and Devor 1992) and pain models have reported localised changes (Devor et al. 1993) or increase in expression of VGSCs (section 1.4.8). Hence, it suggests a role in dynamic assembly of VGSCs to tune responses. One striking example of a local interaction has been reported in cardiac myocytes (Dixon et al. 2015). Local interaction of Cav1.2 calcium channels via C-termini determines the size of calcium responses and it is essential for the excitation-contraction coupling of the cardiac myocytes. This amplified calcium current persists longer than the initial current that elicited it and may reflect "molecular memory". Thus, it establishes lasting changes in excitability. These advances in single particle trafficking are then an appealing method to understand VGSCs relocation in pain pathologies. For example, the tuning of action potential firing in DRG neurones in disease and questions of how the channels are inserted into the membrane could be elucidated.

This study demonstrates for the first time the VAMP isoforms expressed in DRG neurones: VAMP1-5, VAMP7 and VAMP8. Considering what has been reported in the CNS, different VAMPs are reported in different neurotransmitter release pathways (Pratt et al. 2011, Ramirez and Kavalali 2011), it is likely that DRG neurones use different VAMP isoforms for vesicular pools that are triggered by different mediators. For instance, VAMP2 mediated exocytosis form the majority of the evoked neurotransmitter release in central synapses (Sudhof and Rothman 2009). Yet, VAMP2 knock out neurones still show spontaneous neurotransmitter release (Schoch et al. 2001). Other VAMPs were found in central synapses at lower levels such as VAMP4 and VAMP7 (Takamori et al. 2006). Reelin, a glycoprotein, was found to elicit the fusion of VAMP7-containing vesicles and thus enhancing neurotransmission (Bal et al.

2013). On the other hand, VAMP4 has been described in a distinct vesicular pool side by side with VAMP2, suggesting that they both are trafficked independently to the synapse and mediate neurotransmission but form independent SNARE complexes (Raingo et al. 2012), proposing that synapses diversify their release properties by using different SNARE proteins. In the context of this thesis, VAMP1, 2 and 7 were observed in the neurites, suggesting a role in neurotransmission or neurite outgrowth (Gupton and Gertler 2010). In addition, VAMP7 was only found in DRG neurones which could indicate a neuron-specific role. Hence, exploring the functional roles of the VAMPs identified in this thesis can provide a molecular insight to the distinct responses nociceptors demonstrate to different pain conditions.

In this thesis, Nav1.7 was not found to co-localise with VAMPs. This is likely a false negative as most of the Nav1.7 was found at the plasma membrane and not being trafficked. Unfortunately, due to time constraints, I did not complete the same set of experiments in the presence of the IS, a likely stimulant for vesicles containing Nav1.7 to fuse with the plasma membrane. Another approach could be the use of PKA or PKC activators as these have been shown to modulate Na^+ current density in DRG neurones (Liu et al. 2010, Lu et al. 2010, Gold et al. 1998). In addition, once an established model for the fusion of vesicles containing Nav1.7 (or other α-subunits) with the plasma membrane, botulinum neurotoxins or chimaeras could be added to identify SNARE proteins interacting with this membrane fusion.

In light of these putative differences in vesicular pools within DRG neurones, botulinum neurotoxins were developed to both target a specific DRG population subset, IB4-negative, and to cleave a specific SNARE. At this stage, tetbot A seems to effectively reduce CGRP secretion, confirming similar results with BoNT/A in trigeminal ganglia (Meng et al. 2007). Likewise, it does not alter the excitability which is in agreement with previous results with BoNT/A (Paterson et al. 2014) or IS-induced hyperexcitability. Key experiments to follow these findings would be measuring the Na^+ current in the presence of either tetbot A or tetbot B pre-incubation and then an inflammatory

insult. Due to the technical issues found during this set of experiments was not acquired. One solution could be via the injection of the chimaeras to the mouse hind paw (as described in Ferrari et al. 2013) before culturing and adding IS, and voltage-clamp recording.

Appendix 1 – Nav1.7, Nav1.8 and Nav1.9 in cortical neurones

Cortical neurones have been described to not express Nav1.7, Nav1.8 and Nav1.9 (Lai and Jan 2006). To evaluate the specificity of the antibodies used in this thesis, cortical neuronal cultures were probed with antibodies against these α-subunits. No immunofluorescence was detected (Figure A1.1).

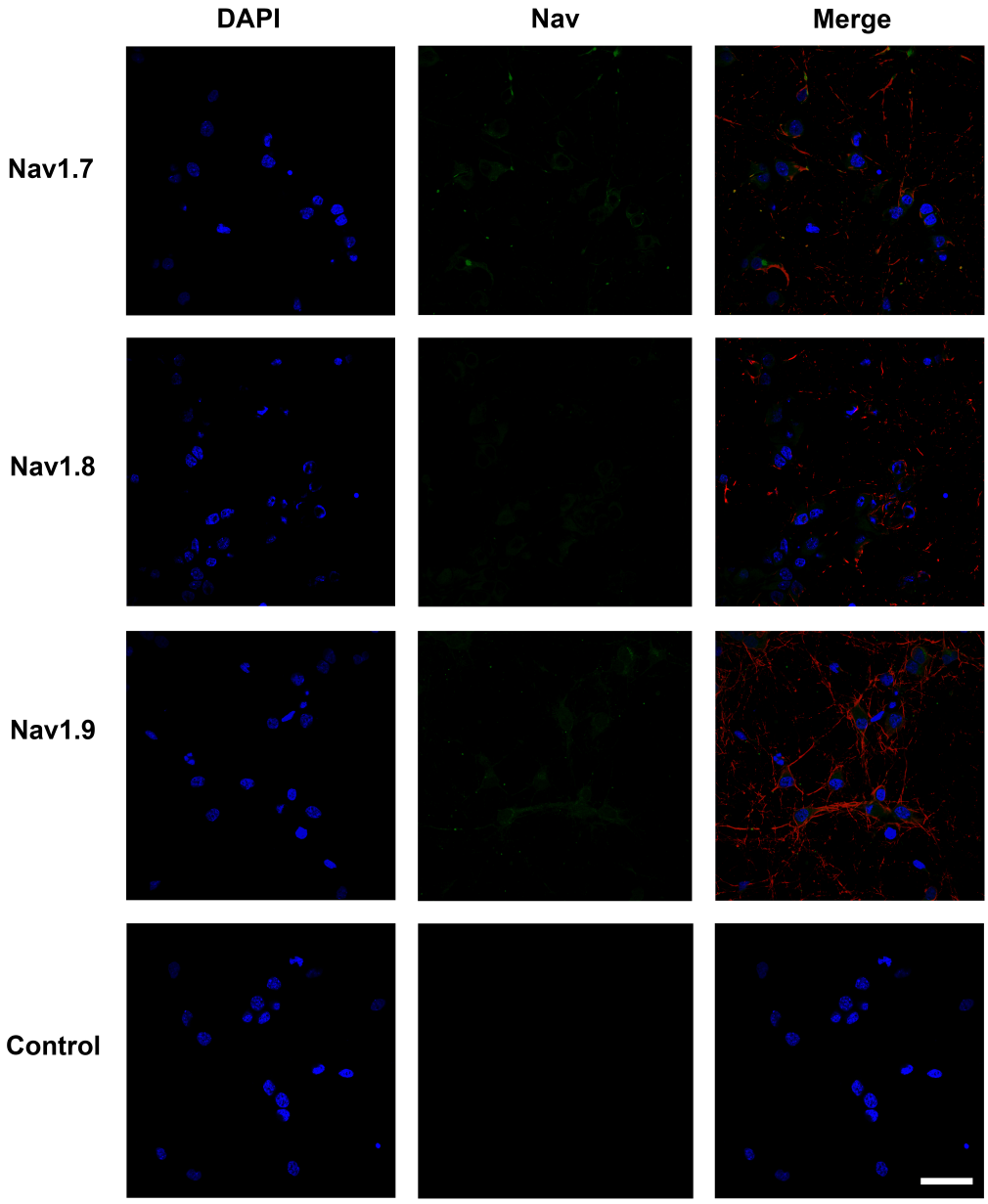

Figure A1.1 Nav1.7, Nav1.8 and Nav1.9 in embryonic cortical neurones in culture. Cortical neurones were isolated from E17.5 rats (dissection and isolation by Dr Claudia Bauer). In red, β-III tubulin; In green, VGSCs α-subunits; In blue, nuclei. Control here is defined as a no primary antibody control. Scale bar shows 30μm.

Appendix 2 - Cleavage of VAMP2 by Tetbot B and 2x Tetbot

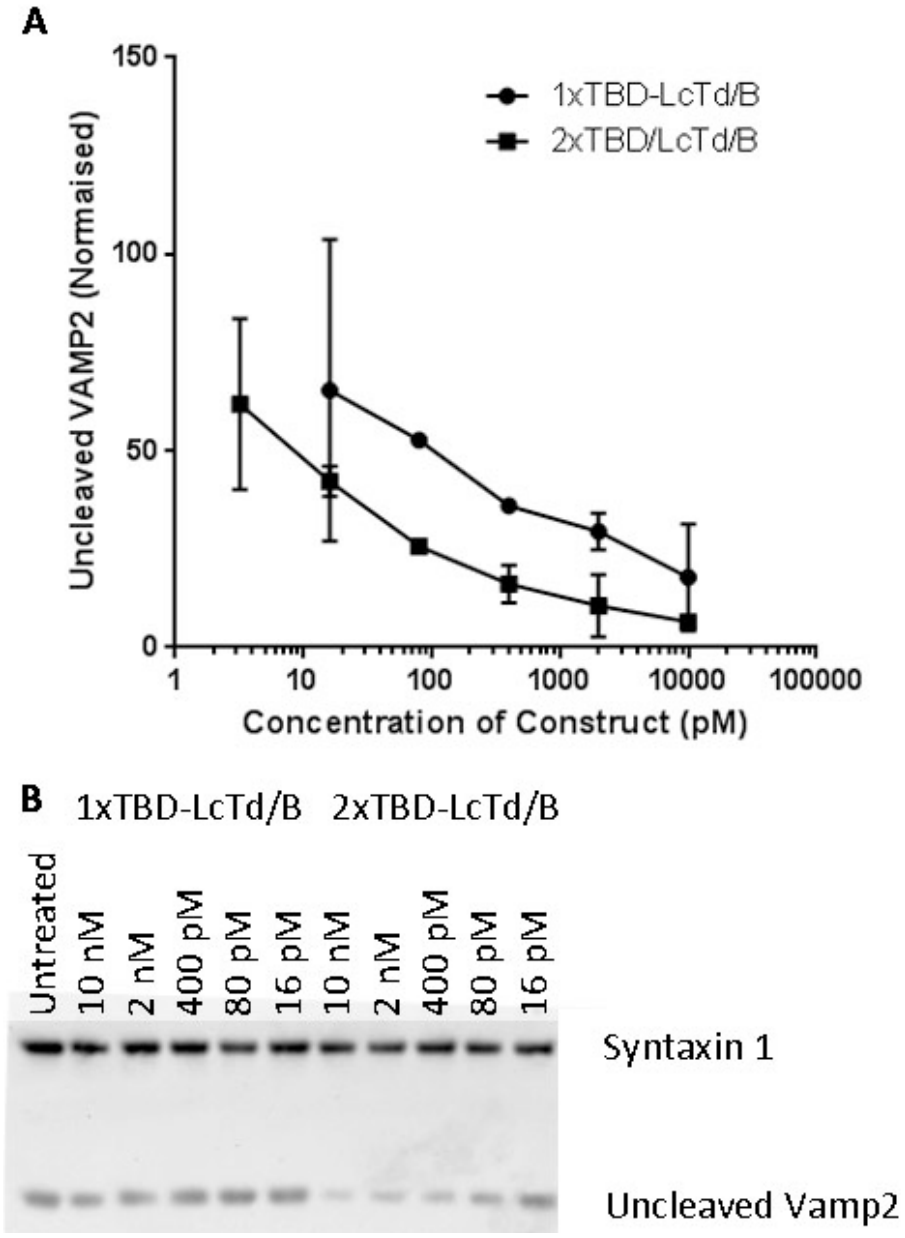

Figure A2.1 Cleavage of VAMP2 by Tetbot B and 2x Tetbot.
Cultures of rat cortical neurones were treated with a range of concentrations for tetbot B (the construct used in this thesis, named 1xTBD-lcTd/B) and 2xTBD/LcTd/B for 65 h. Lysates of these cultures were used to identify the percentage of uncleaved VAMP2 and syntaxin 1 as loading control. The concentration of tetbot B used in this thesis was 10 nM. All experiments and analysis executed by Dr Charlotte Leese.

Appendix 3 - CGRP release from DRG cultures treated with OG and RBDT

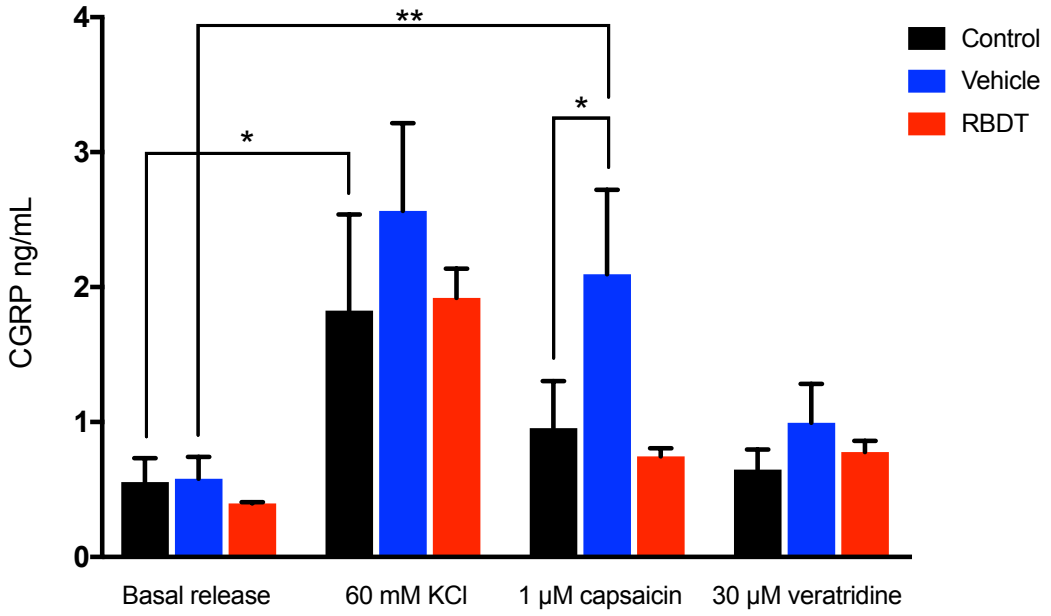

Figure A3.1 CGRP release from DRG cultures treated with OG and RBDT.
Isolated DRG neurones were incubated with 1 µM capsaicin or 60 mM KCl in external recording solution for 30 min. The supernatant was used to detect CGRP levels using a commercial ELISA kit by Phoenix, USA. DRG neurones in control conditions, pre-incubated with vehicle (n-octylglucoside), and the receptor binding domain only of tetbot (RBDT). One-way ANOVA with uncorrected Fisher's LSD (N=3 each data column). Error bars show SEM.

Appendix 4 – Botulinum neurotoxins and chimaeras cleavage sites

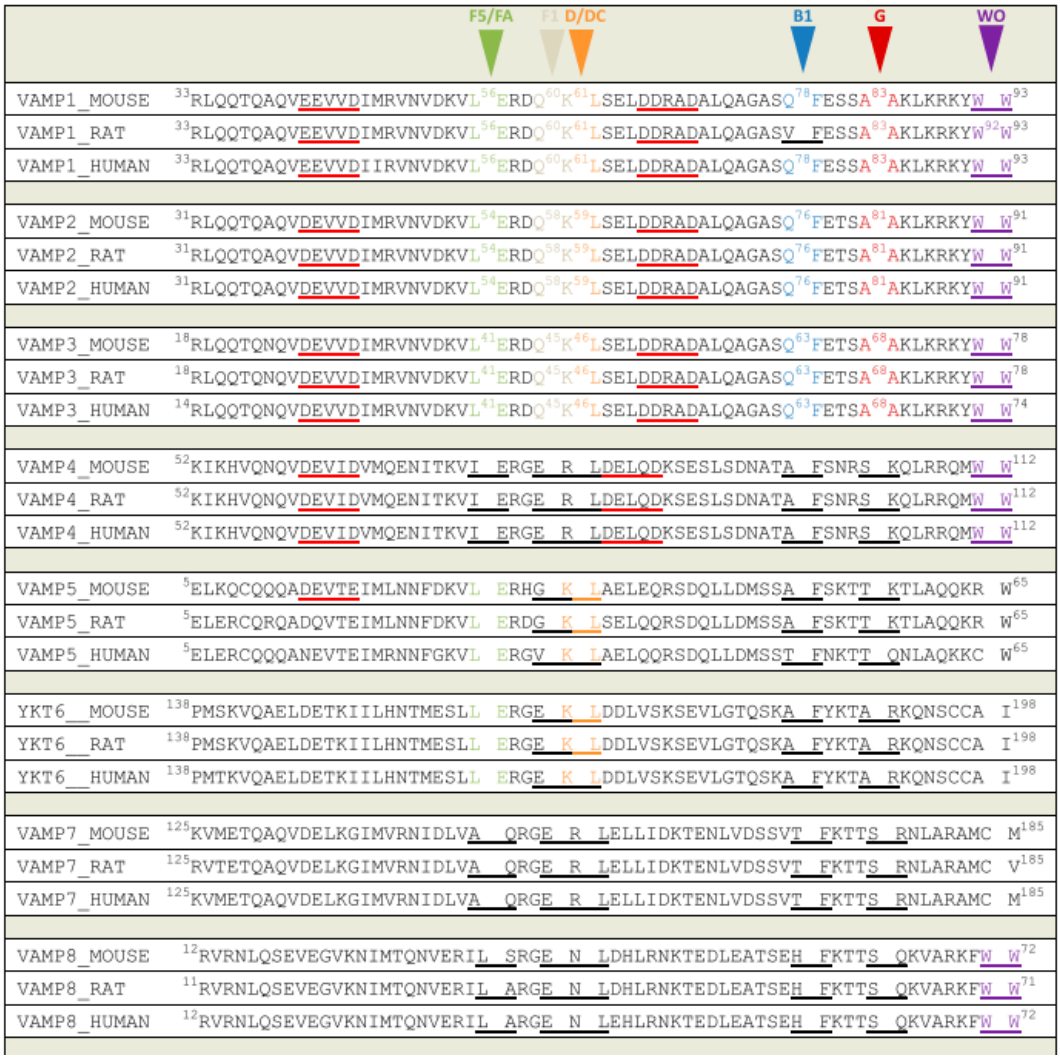

Figure A4.1 VAMP cleavage sites.
Botulinum B is represented in blue (B1). A black underscore demonstrates resistance to the toxin.

Figure A4.2 SNAP25 cleavage sites.
Botulinum neurotoxins is depicted in yellow/green (A). A black underscore demonstrates resistance to the toxin and a coloured means unconfirmed.

References

Abrahamsen, B., J. Zhao, C. O. Asante, C. M. Cendan, S. Marsh, J. P. Martinez-Barbera, M. A. Nassar, A. H. Dickenson & J. N. Wood (2008) The cell and molecular basis of mechanical, cold, and inflammatory pain. *Science,* 321**,** 702-705.

Abrams, S. B. & M. Hallett (2013) Clinical utility of different botulinum neurotoxin preparations. *Toxicon,* 67**,** 81-86.

Advani, R. J., B. Yang, R. Prekeris, K. C. Lee, J. Klumperman & R. H. Scheller (1999) VAMP-7 mediates vesicular transport from endosomes to lysosomes. *Journal of Cell Biology,* 146**,** 765-775.

Ahmad, S., L. Dahllund, A. B. Eriksson, D. Hellgren, U. Karlsson, P. E. Lund, I. A. Meijer, L. Meury, T. Mills, A. Moody, A. Morinville, J. Morten, D. O'Donnell, C. Raynoschek, H. Salter, G. A. Rouleau & J. J. Krupp (2007) A stop codon mutation in SCN9A causes lack of pain sensation. *Human Molecular Genetics,* 16**,** 2114-2121.

Akopian, A. N., V. Souslova, S. England, K. Okuse, N. Ogata, J. Ure, A. Smith, B. J. Kerr, S. B. McMahon, S. Boyce, R. Hill, L. C. Stanfa, A. H. Dickenson & J. N. Wood (1999) The tetrodotoxin-resistant sodium channel SNS has a specialized function in pain pathways. *Nature Neuroscience,* 2**,** 541-548.

Amaya, F., K. Oh-Hashi, Y. Naruse, N. Iijima, M. Ueda, G. Shimosato, M. Tominaga, Y. Tanaka & M. Tanaka (2003) Local inflammation increases vanilloid receptor 1 expression within distinct subgroups of DRG neurons. *Brain Research,* 963**,** 190-196.

Amaya, F., H. B. Wang, M. Costigan, A. J. Allchorne, J. P. Hatcher, J. Egerton, T. Stean, V. Morisset, D. Grose, M. J. Gunthorpe, I. P. Chessell, S. Tate, P. J. Green & C. J. Woolf (2006) The voltage-gated sodium channel Na(v)1.9 is an effector of peripheral inflammatory pain hypersensitivity. *Journal of Neuroscience,* 26**,** 12852-12860.

Amaya-Castellanos, E., J. B. Pineda-Farias, G. Castaneda-Corral, G. C. Vidal-Cantu, J. Murbartian, H. I. Rocha-Gonzalez & V. Granados-Soto (2011) Blockade of 5-HT(7) receptors reduces tactile allodynia in the rat. *Pharmacology Biochemistry and Behavior,* 99**,** 591-597.

Amir, R. & M. Devor (1996) Chemically mediated cross-excitation in rat dorsal root ganglia. *Journal of Neuroscience,* 16**,** 4733-4741.

--- (1997) Spike-evoked suppression and burst patterning in dorsal root ganglion neurons of the rat. *Journal of Physiology-London,* 501**,** 183-196.

Antonin, W., C. Holroyd, D. Fasshauer, S. Pabst, G. F. von Mollard & R. Jahn (2000a) A SNARE complex mediating fusion of late endosomes defines conserved properties of SNARE structure and function. *Embo Journal,* 19**,** 6453-6464.

Antonin, W., C. Holroyd, R. Tikkanen, S. Honing & R. Jahn (2000b) The R-SNARE endobrevin/VAMP-8 mediates homotypic fusion of early endosomes and late endosomes. *Molecular Biology of the Cell,* 11**,** 3289-3298.

Baccaglini, P. I. & P. G. Hogan (1983) SOME RAT SENSORY NEURONS IN CULTURE EXPRESS CHARACTERISTICS OF DIFFERENTIATED PAIN SENSORY CELLS.

Proceedings of the National Academy of Sciences of the United States of America-Biological Sciences, 80**,** 594-598.

Baker, M. D., S. Y. Chandra, Y. N. Ding, S. G. Waxman & J. N. Wood (2003) GTP-induced tetrodotoxin-resistant Na(+) current regulates excitability in mouse and rat small diameter sensory neurones. *Journal of Physiology-London,* 548**,** 373-382.

Bal, M., J. Leitz, A. L. Reese, D. M. O. Ramirez, M. Durakoglugil, J. Herz, L. M. Monteggia & E. T. Kavalali (2013) Reelin Mobilizes a VAMP7-Dependent Synaptic Vesicle Pool and Selectively Augments Spontaneous Neurotransmission. *Neuron,* 80**,** 934-946.

Ballou, L. R., R. M. Botting, S. Goorha, J. Y. Zhang & J. R. Vane (2000) Nociception in cyclooxygenase isozyme-deficient mice. *Proceedings of the National Academy of Sciences of the United States of America,* 97**,** 10272-10276.

Barbosa, C., Z. Y. Tan, R. Z. Wang, W. R. Xie, J. A. Strong, R. R. Patel, M. R. Vasko, J. M. Zhang & T. R. Cummins (2015) Nav beta 4 regulates fast resurgent sodium currents and excitability in sensory neurons. *Molecular Pain,* 11.

Barondes, S. H. (1988) BIFUNCTIONAL PROPERTIES OF LECTINS - LECTINS REDEFINED. *Trends in Biochemical Sciences,* 13**,** 480-482.

Baumert, M., P. R. Maycox, F. Navone, P. Decamilli & R. Jahn (1989) SYNAPTOBREVIN - AN INTEGRAL MEMBRANE-PROTEIN OF 18000 DALTONS PRESENT IN SMALL SYNAPTIC VESICLES OF RAT-BRAIN. *Embo Journal,* 8**,** 379-384.

Bean, B. P. (2007) The action potential in mammalian central neurons. *Nature Reviews Neuroscience,* 8**,** 451-465.

Beckh, S., M. Noda, H. Lubbert & S. Numa (1989) DIFFERENTIAL REGULATION OF 3 SODIUM-CHANNEL MESSENGER-RNAS IN THE RAT CENTRAL NERVOUS-SYSTEM DURING DEVELOPMENT. *Embo Journal,* 8**,** 3611-3616.

Benn, S. C., M. Costigan, S. Tate, M. Fitzgerald & C. J. Woolf (2001) Developmental expression of the TTX-resistant voltage-gated sodium channels Na(v)1.8 (SNS) and Na(v)1.9 (SNS2) in primary sensory neurons. *Journal of Neuroscience,* 21**,** 6077-6085.

Bennett, D. L. H., G. J. Michael, N. Ramachandran, J. B. Munson, S. Averill, Q. Yan, S. B. McMahon & J. V. Priestley (1998) A distinct subgroup of small DRG cells express GDNF receptor components and GDNF is protective for these neurons after nerve injury. *Journal of Neuroscience,* 18**,** 3059-3072.

Black, J. A., T. R. Cummins, C. Plumpton, Y. H. Chen, W. Hormuzdiar, J. J. Clare & S. G. Waxman (1999) Upregulation of a silent sodium channel after peripheral, but not central, nerve injury in DRG neurons. *Journal of Neurophysiology,* 82**,** 2776-2785.

Black, J. A., N. Frezel, S. D. Dib-Hajj & S. G. Waxman (2012) Expression of Nav1.7 in DRG neurons extends from peripheral terminals in the skin to central preterminal branches and terminals in the dorsal horn. *Molecular Pain,* 8.

Black, J. A., S. J. Liu, M. Tanaka, T. R. Cummins & S. G. Waxman (2004) Changes in the expression of tetrodotoxin-sensitive sodium channels within dorsal root ganglia neurons in inflammatory pain. *Pain,* 108**,** 237-247.

Blum, F. C., W. H. Tepp, E. A. Johnson & J. T. Barbieri (2014) Multiple Domains of Tetanus Toxin Direct Entry into Primary Neurons. *Traffic,* 15**,** 1057-1065.

Bock, J. B., H. T. Matern, A. A. Peden & R. H. Scheller (2001) A genomic perspective on membrane compartment organization. *Nature,* 409**,** 839-841.

Bonifacino, J. S. & B. S. Glick (2004) The mechanisms of vesicle budding and fusion. *Cell,* 116**,** 153-166.

Borisovska, M., Y. Zhao, Y. Tsytsyura, N. Glyvuk, S. Takamori, U. Matti, J. Rettig, T. Sudhof & D. Bruns (2005) v-SNAREs control exocytosis of vesicles from priming to fusion. *Embo Journal,* 24**,** 2114-2126.

Brackenbury, W. J. & M. B. A. Djamgoz (2007) Nerve growth factor enhances voltage-gated Na+ channel activity and transwell migration in Mat-LyLu rat prostate cancer cell line. *Journal of Cellular Physiology,* 210**,** 602-608.

Branco, T., A. Tozer, C. J. Magnus, K. Sugino, S. Tanaka, A. K. Lee, J. N. Wood & S. M. Sternson (2016) Near-Perfect Synaptic Integration by Na(v)1.7 in Hypothalamic Neurons Regulates Body Weight. *Cell,* 165**,** 1749-1761.

Braun, V., V. Fraisier, G. Raposo, I. Hurbain, J. B. Sibarita, P. Chavrier, T. Galli & F. Niedergang (2004) TI-VAMP/VAMP7 is required for optimal phagocytosis of opsonised particles in macrophages. *Embo Journal,* 23**,** 4166-4176.

Brown, R. E., D. R. Stevens & H. L. Haas (2001) The physiology of brain histamine. *Progress in Neurobiology,* 63**,** 637-672.

Burgess, G. M., I. Mullaney, M. McNeill, P. M. Dunn & H. P. Rang (1989) 2ND MESSENGERS INVOLVED IN THE MECHANISM OF ACTION OF BRADYKININ IN SENSORY NEURONS IN CULTURE. *Journal of Neuroscience,* 9**,** 3314-3325.

Burgoyne, R. D. & A. Morgan (2003) Secretory granule exocytosis. *Physiological Reviews,* 83**,** 581-632.

Burnstock, G. (2009) Purinergic mechanosensory transduction and visceral pain. *Molecular Pain,* 5.

Buschmann, T., A. Martin-Villalba, J. D. Kocsis, S. G. Waxman, M. Zimmermann & T. Herdegen (1998) Expression of Jun, Fos and ATF-2 proteins in axotomized explanted and cultured adult rat dorsal root ganglia. *Neuroscience,* 84**,** 163-176.

Cardenas, C. G., L. P. Del Mar, A. V. Vysokanov, P. B. Arnold, L. M. Cardenas, D. J. Surmeier & R. S. Scroggs (1999) Serotonergic modulation of hyperpolarization-activated current in acutely isolated rat dorsal root ganglion neurons. *Journal of Physiology-London,* 518**,** 507-523.

Cardenas, L. M., C. G. Cardenas & R. S. Scroggs (2001) 5HT increases excitability of nociceptor-like rat dorsal root Na+ channels. *Journal of Neurophysiology,* 86**,** 241-248.

Carratu, M. R. & D. Mitolochieppa (1989) INTERACTION BETWEEN BRADYKININ AND VOLTAGE-SENSITIVE SODIUM-CHANNELS IN MYELINATED NERVE-FIBERS. *Experientia,* 45**,** 346-349.

Cesare, P., L. V. Dekker, A. Sardini, P. J. Parker & P. A. McNaughton (1999) Specific involvement of PKC-epsilon in sensitization of the neuronal response to painful heat. *Neuron,* 23**,** 617-624.

Chaineau, M., L. Danglot & T. Galli (2009) Multiple roles of the vesicular-SNARE TI-VAMP in post-Golgi and endosomal trafficking. *Febs Letters,* 583**,** 3817-3826.

Chakraborty, S., V. Elvezio, M. Kaczocha, M. Rebecchi & M. Puopolo (2017) Presynaptic inhibition of transient receptor potential vanilloid type 1

(TRPV1) receptors by noradrenaline in nociceptive neurons. *Journal of Physiology-London,* 595**,** 2639-2660.

Chen, R. & S. H. Chung (2014) Mechanism of tetrodotoxin block and resistance in sodium channels. *Biochemical and Biophysical Research Communications,* 446**,** 370-374.

Cheng, H. J., K. T. Ma, L. Li, L. Zhao, Y. Wang & J. Q. Si (2014) Differential expression of alpha-adrenoceptor subtypes in rat dorsal root ganglion after chronic constriction injury. *Journal of Huazhong University of Science and Technology-Medical Sciences,* 34**,** 322-329.

Chiaruttini, G., G. M. Piperno, M. Jouve, F. De Nardi, P. Larghi, A. A. Peden, G. Baj, S. Muller, S. Valitutti, T. Galli & F. Benvenuti (2016) The SNARE VAMP7 Regulates Exocytic Trafficking of Interleukin-12 in Dendritic Cells. *Cell Reports,* 14**,** 2624-2636.

Chiu, I. M., L. B. Barrett, E. Williams, D. E. Strochlic, S. Lee, A. D. Weyer, S. Lou, G. Bryman, D. P. Roberson, N. Ghasemlou, C. Piccoli, E. Ahat, V. Wang, E. J. Cobos, C. L. Stucky, Q. F. Ma, S. D. Liberles & C. J. Woolf (2014) Transcriptional profiling at whole population and single cell levels reveals somatosensory neuron molecular diversity. *Elife,* 3.

Choi, J.-S., S. D. Dib-Hajj & S. G. Waxman (2007) Differential slow inactivation and use-dependent inhibition of Na(v)1.8 channels contribute to distinct firing properties in IB4+ and IB4- DRG neurons. *Journal of Neurophysiology,* 97**,** 1258-1265.

Coggeshall, R. E., S. Tate & S. M. Carlton (2004) Differential expression of tetrodotoxin-resistant sodium channels Na(V)1.8 and Na(V)1.9 in normal and inflamed rats. *Neuroscience Letters,* 355**,** 45-48.

Coimbra, A., Sodrebor.Bp & M. M. Magalhaes (1974) SUBSTANTIA GELATINOSA ROLANDI OF RAT - FINE-STRUCTURE, CYTOCHEMISTRY (ACID-PHOSPHATASE) AND CHANGES AFTER DORSAL ROOT SECTION. *Journal of Neurocytology,* 3**,** 199-217.

Collingridge, G. L., J. T. R. Isaac & Y. T. Wang (2004) Receptor trafficking and synaptic plasticity. *Nature Reviews Neuroscience,* 5**,** 952-962.

Collins, C. E., D. C. Airey, N. A. Young, D. B. Leitch & J. H. Kaas (2010) Neuron densities vary across and within cortical areas in primates. *Proceedings of the National Academy of Sciences of the United States of America,* 107**,** 15927-15932.

Cook, S. P. & E. W. McCleskey (2002) Cell damage excites nociceptors through release of cytosolic ATP. *Pain,* 95**,** 41-47.

Coste, B., N. Osorio, F. Padilla, M. Crest & P. Delmas (2004) Gating and modulation of presumptive Na(V)1.9 channels in enteric and spinal sensory neurons. *Molecular and Cellular Neuroscience,* 26**,** 123-134.

Costigan, M., J. Scholz & C. J. Woolf (2009) Neuropathic Pain: A Maladaptive Response of the Nervous System to Damage. *Annual Review of Neuroscience,* 32**,** 1-32.

Cox, J. J., F. Reimann, A. K. Nicholas, G. Thornton, E. Roberts, K. Springell, G. Karbani, H. Jafri, J. Mannan, Y. Raashid, L. Al-Gazali, H. Hamamy, E. M. Valente, S. Gorman, R. Williams, D. P. McHale, J. N. Wood, F. M. Gribble & C.

G. Woods (2006) An SCN9A channelopathy causes congenital inability to experience pain. *Nature,* 444**,** 894-898.

Cummins, T. R., S. D. Dib-Hajj, J. A. Black, A. N. Akopian, J. N. Wood & S. G. Waxman (1999) A novel persistent tetrodotoxin-resistant sodium current in SNS-null and wild-type small primary sensory neurons. *Journal of Neuroscience,* 19.

Cummins, T. R., S. D. Dib-Hajj, R. I. Herzog & S. G. Waxman (2005) Na(v)1.6 channels generate resurgent sodium currents in spinal sensory neurons. *Febs Letters,* 579**,** 2166-2170.

Cummins, T. R., J. R. Howe & S. G. Waxman (1998) Slow closed-state inactivation: A novel mechanism underlying ramp currents in cells expressing the hNE/PN1 sodium channel. *Journal of Neuroscience,* 18**,** 9607-9619.

Cummins, T. R., A. M. Rush, M. Estacion, S. D. Dib-Hajj & S. G. Waxman (2009) Voltage-clamp and current-clamp recordings from mammalian DRG neurons. *Nature Protocols,* 4**,** 1103-1112.

Cummins, T. R., P. L. Sheets & S. G. Waxman (2007) The roles of sodium channels in nociception: Implications for mechanisms of pain. *Pain,* 131**,** 243-257.

Cummins, T. R. & S. G. Waxman (1997) Downregulation of tetrodotoxin-resistant sodium currents and upregulation of a rapidly repriming tetrodotoxin-sensitive sodium current in small spinal sensory neurons after nerve injury. *Journal of Neuroscience,* 17**,** 3503-3514.

Cunha, T. M., W. A. Verri, S. Y. Fukada, A. T. G. Guerrero, T. Santodomingo-Garzon, S. Poole, C. A. Parada, S. H. Ferreira & F. Q. Cunha (2007) TNF-alpha and IL-1 beta mediate inflammatory hypernociception in mice triggered by B, but not B-2 kinin receptor. *European Journal of Pharmacology,* 573**,** 221-229.

Cusdin, F. S., J. J. Clare & A. P. Jackson (2008) Trafficking and cellular distribution of voltage-gated sodium channels. *Traffic,* 9**,** 17-26.

Dani, J. W., D. M. Armstrong & L. I. Benowitz (1991) MAPPING THE DEVELOPMENT OF THE RAT-BRAIN BY GAP-43 IMMUNOCYTOCHEMISTRY. *Neuroscience,* 40**,** 277-287.

Davis, K. D., R. A. Meyer & J. N. Campbell (1993) CHEMOSENSITIVITY AND SENSITIZATION OF NOCICEPTIVE AFFERENTS THAT INNERVATE THE HAIRY SKIN OF MONKEY. *Journal of Neurophysiology,* 69**,** 1071-1081.

Davletov, B., M. Bajohrs & T. Binz (2005) Beyond BOTOX: advantages and limitations of individual botulinum neurotoxins. *Trends in Neurosciences,* 28**,** 446-452.

Deitcher, D. L., A. Ueda, B. A. Stewart, R. W. Burgess, Y. Kidokoro & T. L. Schwarz (1998) Distinct requirements for evoked and spontaneous release of neurotransmitter are revealed by mutations in the Drosophila gene neuronal-synaptobrevin. *Journal of Neuroscience,* 18**,** 2028-2039.

Devesa, I., C. Ferrandiz-Huertas, S. Mathivanan, C. Wolf, R. Lujan, J. P. Changeux & A. Ferrer-Montiel (2014) alpha CGRP is essential for algesic exocytotic mobilization of TRPV1 channels in peptidergic nociceptors. *Proceedings of the National Academy of Sciences of the United States of America,* 111**,** 18345-18350.

Devor, M., R. Govrinlippmann & K. Angelides (1993) NA+ CHANNEL IMMUNOLOCALIZATION IN PERIPHERAL MAMMALIAN AXONS AND CHANGES FOLLOWING NERVE INJURY AND NEUROMA FORMATION. *Journal of Neuroscience,* 13**,** 1976-1992.

Devor, M., W. Janig & M. Michaelis (1994) MODULATION OF ACTIVITY IN DORSAL-ROOT GANGLION NEURONS BY SYMPATHETIC ACTIVATION IN NERVE-INJURED RATS. *Journal of Neurophysiology,* 71**,** 38-47.

Devor, M., C. H. Keller, T. J. Deerinck, S. R. Levinson & M. H. Ellisman (1989) NA+ CHANNEL ACCUMULATION ON AXOLEMMA OF AFFERENT ENDINGS IN NERVE END NEUROMAS IN APTERONOTUS. *Neuroscience Letters,* 102**,** 149-154.

Devor, M. & P. D. Wall (1990) CROSS-EXCITATION IN DORSAL-ROOT GANGLIA OF NERVE-INJURED AND INTACT RATS. *Journal of Neurophysiology,* 64**,** 1733-1746.

Devor, M., P. D. Wall & N. Catalan (1992) SYSTEMIC LIDOCAINE SILENCES ECTOPIC NEUROMA AND DRG DISCHARGE WITHOUT BLOCKING NERVE-CONDUCTION. *Pain,* 48**,** 261-268.

Dib-Hajj, S., J. A. Black, T. R. Cummins & S. G. Waxman (2002) NaN/Na(v)1.9: a sodium channel with unique properties. *Trends in Neurosciences,* 25**,** 253-259.

Dib-Hajj, S. D., L. Tyrrell, J. A. Black & S. G. Waxman (1998) NaN, a novel voltage-gated Na channel, is expressed preferentially in peripheral sensory neurons and down-regulated after axotomy. *Proceedings of the National Academy of Sciences of the United States of America,* 95**,** 8963-8968.

DibHajj, S., J. A. Black, P. Felts & S. G. Waxman (1996) Down-regulation of transcripts for Na channel alpha-SNS in spinal sensory neurons following axotomy. *Proceedings of the National Academy of Sciences of the United States of America,* 93**,** 14950-14954.

Dixon, R. E., C. M. Moreno, C. Yuan, X. Opitz-Araya, M. D. Binder, M. F. Navedo & L. F. Santana (2015) Graded Ca2+/calmodulin-dependent coupling of voltage-gated Ca(v)1.2 channels. *Elife,* 4.

Djouhri, L., D. Dawbarn, A. Robertson, R. Newton & S. N. Lawson (2001) Time course and nerve growth factor dependence of inflammation-induced alterations in electrophysiological membrane properties in nociceptive primary afferent neurons. *Journal of Neuroscience,* 21**,** 8722-8733.

Dolly, J. O. & M. A. O'Connell (2012) Neurotherapeutics to inhibit exocytosis from sensory neurons for the control of chronic pain. *Current Opinion in Pharmacology,* 12**,** 100-108.

Dong, H., Y. H. Fan, Y. Y. Wang, W. T. Wang & S. J. Hu (2008) Lidocaine suppresses subthreshold oscillations by inhibiting persistent Na+ current in injured dorsal root ganglion neurons. *Physiological Research,* 57**,** 639-645.

Du, X. N., H. Hao, S. Gigout, D. Y. Huang, Y. H. Yang, L. Li, C. X. Wang, D. Sundt, D. B. Jaffe, H. L. Zhang & N. Gamper (2014) Control of somatic membrane potential in nociceptive neurons and its implications for peripheral nociceptive transmission. *Pain,* 155**,** 2306-2322.

Eijkelkamp, N., J. E. Linley, M. D. Baker, M. S. Minett, R. Cregg, R. Werdehausen, F. Rugiero & J. N. Wood (2012) Neurological perspectives on voltage-gated sodium channels. *Brain,* 135**,** 2585-2612.

Eleopra, R., C. Montecucco, G. Devigili, C. Lettieri, S. Rinaldo, L. Verriello, M. Pirazzini, P. Caccin & O. Rossetto (2013) Botulinum neurotoxin serotype D is

poorly effective in humans: An in vivo electrophysiological study. *Clinical Neurophysiology,* 124**,** 999-1004.

Elliott, A. A. & J. R. Elliott (1993) CHARACTERIZATION OF TTX-SENSITIVE AND TTX-RESISTANT SODIUM CURRENTS IN SMALL-CELLS FROM ADULT-RAT DORSAL-ROOT GANGLIA. *Journal of Physiology-London,* 463**,** 39-56.

Emery, E. C., A. M. Habib, J. J. Cox, A. K. Nicholas, F. M. Gribble, C. G. Woods & F. Reimann (2015) Novel SCN9A Mutations Underlying Extreme Pain Phenotypes: Unexpected Electrophysiological and Clinical Phenotype Correlations. *Journal of Neuroscience,* 35**,** 7674-7681.

Emery, E. C., A. P. Luiz, S. Sikandar, R. Magnusdottir, X. Z. Dong & J. N. Wood (2016a) In vivo characterization of distinct modality-specific subsets of somatosensory neurons using GCaMP. *Science Advances,* 2.

Emery, E. C., A. P. Luiz & J. N. Wood (2016b) Na(v)1.7 and other voltage-gated sodium channels as drug targets for pain relief. *Expert Opinion on Therapeutic Targets,* 20**,** 975-983.

England, J. D., F. Gamboni, M. A. Ferguson & S. R. Levinson (1994) SODIUM-CHANNELS ACCUMULATE AT THE TIPS OF INJURED AXONS. *Muscle & Nerve,* 17**,** 593-598.

England, S., S. Bevan & R. J. Docherty (1996) PGE(2) modulates the tetrodotoxin-resistant sodium current in neonatal rat dorsal root ganglion neurones via the cyclic AMP-protein kinase A cascade. *Journal of Physiology-London,* 495**,** 429-440.

Evans, A. R., M. R. Vasko & G. D. Nicol (1999) The cAMP transduction cascade mediates the PGE(2)-induced inhibition of potassium currents in rat sensory neurones. *Journal of Physiology-London,* 516**,** 163-178.

Fasshauer, D., R. B. Sutton, A. T. Brunger & R. Jahn (1998) Conserved structural features of the synaptic fusion complex: SNARE proteins reclassified as Q- and R-SNAREs. *Proceedings of the National Academy of Sciences of the United States of America,* 95**,** 15781-15786.

Fayaz, A., P. Croft, R. M. Langford, L. J. Donaldson & G. T. Jones (2016) Prevalence of chronic pain in the UK: a systematic review and meta-analysis of population studies. *Bmj Open,* 6.

Feldmann, A., C. Winterstein, R. White, J. Trotter & E. M. Kramer-Albers (2009) Comprehensive Analysis of Expression, Subcellular Localization, and Cognate Pairing of SNARE Proteins in Oligodendrocytes. *Journal of Neuroscience Research,* 87**,** 1760-1772.

Ferlito, M., W. B. Fulton, M. A. Zauher, E. Marban, C. Steenbergen & C. J. Lowenstein (2010) VAMP-1, VAMP-2, and syntaxin-4 regulate ANP release from cardiac myocytes. *Journal of Molecular and Cellular Cardiology,* 49**,** 791-800.

Ferrari, E., C. Gu, D. Niranjan, L. Restani, C. Rasetti-Escargueil, I. Obara, S. M. Geranton, J. Arsenault, T. A. Goetze, C. B. Harper, T. H. Nguyen, E. Maywood, J. O'Brien, G. Schiavo, D. W. Wheeler, F. A. Meunier, M. Hastings, J. M. Edwardson, D. Sesardic, M. Caleo, S. P. Hunt & B. Davletov (2013) Synthetic Self-Assembling Clostridial Chimera for Modulation of Sensory Functions. *Bioconjugate Chemistry,* 24**,** 1750-1759.

Fertleman, C. R., M. D. Baker, K. A. Parker, S. Moffatt, F. V. Elmslie, B. Abrahamsen, J. Ostman, N. Klugbauer, J. N. Wood, R. M. Gardiner & M. Rees (2006) SCN9A mutations in paroxysmal extreme pain disorder: Allelic variants underlie distinct channel defects and phenotypes. *Neuron,* 52**,** 767-774.

Fjell, J., T. R. Cummins, B. M. Davis, K. M. Albers, K. Fried, S. G. Waxman & J. A. Black (1999a) Sodium channel expression in NGF-overexpressing transgenic mice. *Journal of Neuroscience Research,* 57**,** 39-47.

Fjell, J., T. R. Cummins, S. Dib-Hajj, K. Fried, J. A. Black & S. G. Waxman (1999b) Differential role of GDNF and NGF in the maintenance of two TTX-resistant sodium channels in adult DRG neurons. *Molecular Brain Research,* 67**,** 267-282.

Foran, P. G., N. Mohammed, G. O. Lisk, S. Nagwaney, G. W. Lawrence, E. Johnson, L. Smith, K. R. Aoki & J. O. Dolly (2003) Evaluation of the therapeutic usefulness of botulinum neurotoxin B, C1, E, and F compared with the long lasting type A - Basis for distinct durations of inhibition of exocytosis in central neurons. *Journal of Biological Chemistry,* 278**,** 1363-1371.

French, C. R., P. Sah, K. J. Buckett & P. W. Gage (1990) A VOLTAGE-DEPENDENT PERSISTENT SODIUM CURRENT IN MAMMALIAN HIPPOCAMPAL-NEURONS. *Journal of General Physiology,* 95**,** 1139-1157.

Fukuoka, T., K. Kobayashi, H. Yamanaka, K. Obata, Y. Dai & K. Noguchi (2008) Comparative study of the distribution of the alpha-subunits of voltage-gated sodium channels in normal and axotomized rat dorsal root ganglion neurons. *Journal of Comparative Neurology,* 510**,** 188-206.

Fulton, B. P. (1987) POSTNATAL CHANGES IN CONDUCTION-VELOCITY AND SOMA ACTION-POTENTIAL PARAMETERS OF RAT DORSAL-ROOT GANGLION NEURONS. *Neuroscience Letters,* 73**,** 125-130.

Gallego, R. & C. Eyzaguirre (1978) MEMBRANE AND ACTION POTENTIAL CHARACTERISTICS OF A-NODOSE AND C-NODOSE GANGLION-CELLS STUDIED IN WHOLE GANGLIA AND IN TISSUE-SLICES. *Journal of Neurophysiology,* 41**,** 1217-1232.

Galli, T., A. Zahraoui, V. V. Vaidyanathan, G. Raposo, J. M. Tian, M. Karin, H. Niemann & D. Louvard (1998) A novel tetanus neurotoxin-insensitive vesicle-associated membrane protein in SNARE complexes of the apical plasma membrane of epithelial cells. *Molecular Biology of the Cell,* 9**,** 1437-1448.

Garry, M. G. & K. M. Hargreaves (1992) ENHANCED RELEASE OF IMMUNOREACTIVE CGRP AND SUBSTANCE-P FROM SPINAL DORSAL HORN SLICES OCCURS DURING CARRAGEENAN INFLAMMATION. *Brain Research,* 582**,** 139-142.

Gold, M. S., J. D. Levine & A. M. Correa (1998) Modulation of TTX-R/(Na) by PKC and PKA and their role in PGE(2)-induced sensitization of rat sensory neurons in vitro. *Journal of Neuroscience,* 18**,** 10345-10355.

Gold, M. S., D. B. Reichling, M. J. Shuster & J. D. Levine (1996) Hyperalgesic agents increase a tetrodotoxin-resistant Na+ current in nociceptors. *Proceedings of the National Academy of Sciences of the United States of America,* 93**,** 1108-1112.

Goldberg, Y. P., J. MacFarlane, M. L. MacDonald, J. Thompson, M. P. Dube, M. Mattice, R. Fraser, C. Young, S. Hossain, T. Pape, B. Payne, C. Radomski, G. Donaldson, E. Ives, J. Cox, H. B. Younghusband, R. Green, A. Duff, E.

Boltshauser, G. A. Grinspan, J. H. Dimon, B. G. Sibley, G. Andria, E. Toscano, J. Kerdraon, D. Bowsher, S. N. Pimstone, M. E. Samuels, R. Sherrington & M. R. Hayden (2007) Loss-of-function mutations in the Na(v)1.7 gene underlie congenital indifference to pain in multiple human populations. *Clinical Genetics,* 71**,** 311-319.

Goldstein, M. E., S. B. House & H. Gainer (1991) NF-L AND PERIPHERIN IMMUNOREACTIVITIES DEFINE DISTINCT CLASSES OF RAT SENSORY GANGLION-CELLS. *Journal of Neuroscience Research,* 30**,** 92-104.

Gorelova, N. & P. B. Reiner (1996) Histamine depolarizes cholinergic septal neurons. *Journal of Neurophysiology,* 75**,** 707-714.

Gould, H. J., J. D. England, R. D. Soignier, P. Nolan, L. D. Minor, Z. P. Liu, S. R. Levinson & D. Paul (2004) Ibuprofen blocks changes in Na-v 1.7 and 1.8 sodium channels associated with complete Freund's adjuvant-induced inflammation in rat. *Journal of Pain,* 5**,** 270-280.

Greene, L. A. (1989) A NEW NEURONAL INTERMEDIATE FILAMENT PROTEIN. *Trends in Neurosciences,* 12**,** 228-230.

Grieco, T. M., J. D. Malhotra, C. Chen, L. L. Isom & I. M. Raman (2005) Open-channel block by the cytoplasmic tail of sodium channel beta 4 as a mechanism for resurgent sodium current. *Neuron,* 45**,** 233-244.

Gu, Y. & R. L. Huganir (2016) Identification of the SNARE complex mediating the exocytosis of NMDA receptors. *Proceedings of the National Academy of Sciences of the United States of America,* 113**,** 12280-12285.

Gupton, S. L. & F. B. Gertler (2010) Integrin Signaling Switches the Cytoskeletal and Exocytic Machinery that Drives Neuritogenesis. *Developmental Cell,* 18**,** 725-736.

Gurtu, S. & P. A. Smith (1988) ELECTROPHYSIOLOGICAL CHARACTERISTICS OF HAMSTER DORSAL-ROOT GANGLION-CELLS AND THEIR RESPONSE TO AXOTOMY. *Journal of Neurophysiology,* 59**,** 408-423.

Hains, B. C., C. Y. Saab, J. P. Klein, M. J. Craner & S. G. Waxman (2004) Altered sodium channel expression in second-order spinal sensory neurons contributes to pain after peripheral nerve injury. *Journal of Neuroscience,* 24**,** 4832-4839.

Hamilton, S. G., J. Warburton, A. Bhattacharjee, J. Ward & S. B. McMahon (2000) ATP in human skin elicits a dose-related pain response which is potentiated under conditions of hyperalgesia. *Brain,* 123**,** 1238-1246.

Harding, L. M., D. J. Beadle & I. Bermudez (1999) Voltage-dependent calcium channel subtypes controlling somatic substance P release in the peripheral nervous system. *Progress in Neuro-Psychopharmacology & Biological Psychiatry,* 23**,** 1103-1112.

Harper, A. A. & S. N. Lawson (1985a) CONDUCTION-VELOCITY IS RELATED TO MORPHOLOGICAL CELL TYPE IN RAT DORSAL-ROOT GANGLION NEURONS. *Journal of Physiology-London,* 359**,** 31-&.

--- (1985b) ELECTRICAL-PROPERTIES OF RAT DORSAL-ROOT GANGLION NEURONS WITH DIFFERENT PERIPHERAL-NERVE CONDUCTION VELOCITIES. *Journal of Physiology-London,* 359**,** 47-63.

Hasan, N., D. Corbin & C. Hu (2010) Fusogenic Pairings of Vesicle-Associated Membrane Proteins (VAMPs) and Plasma Membrane t-SNAREs-VAMP5 as the Exception. *Plos One,* 5.

Heine, M., A. Ciuraszkiewicz, A. Voigt, J. Heck & A. Bikbaev (2016) Surface dynamics of voltage-gated ion channels. *Channels,* 10**,** 267-281.

Ho, C. & M. E. O'Leary (2011) Single-cell analysis of sodium channel expression in dorsal root ganglion neurons. *Molecular and Cellular Neuroscience,* 46**,** 159-166.

Hodgkin, A. L. & A. F. Huxley (1952) A QUANTITATIVE DESCRIPTION OF MEMBRANE CURRENT AND ITS APPLICATION TO CONDUCTION AND EXCITATION IN NERVE. *Journal of Physiology-London,* 117**,** 500-544.

Hong, W. J. (2005) SNARES and traffic. *Biochimica Et Biophysica Acta-Molecular Cell Research,* 1744**,** 120-144.

Hong, W. J. & S. Lev (2014) Tethering the assembly of SNARE complexes. *Trends in Cell Biology,* 24**,** 35-43.

Hua, S. Y., D. A. Raciborska, W. S. Trimble & M. P. Charlton (1998) Different VAMP/synaptobrevin complexes for spontaneous and evoked transmitter release at the crayfish neuromuscular junction. *Journal of Neurophysiology,* 80**,** 3233-3246.

Huang, D. Y., C. Liang, F. Zhang, H. C. Men, X. N. Du, N. Gamper & H. L. Zhang (2016) Inflammatory mediator bradykinin increases population of sensory neurons expressing functional T-type Ca2+ channels. *Biochemical and Biophysical Research Communications,* 473**,** 396-402.

Isensee, J., L. Krahe, K. Moeller, V. Pereira, J. E. Sexton, X. H. Sun, E. Emery, J. N. Wood & T. Hucho (2017) Synergistic regulation of serotonin and opioid signaling contribute to pain insensitivity in Na(v)1.7 knockout mice. *Science Signaling,* 10.

Jackson, J. L., A. Kuriyama & Y. Hayashino (2012) Botulinum Toxin A for Prophylactic Treatment of Migraine and Tension Headaches in Adults A Meta-analysis. *Jama-Journal of the American Medical Association,* 307**,** 1736-1745.

Jahn, R. & R. H. Scheller (2006) SNAREs - engines for membrane fusion. *Nature Reviews Molecular Cell Biology,* 7**,** 631-643.

Jancso, N., Jancsoga.A & J. Szolcsanyi (1967) DIRECT EVIDENCE FOR NEUROGENIC INFLAMMATION AND ITS PREVENTION BY DENERVATION AND BY PRETREATMENT WITH CAPSAICIN. *British Journal of Pharmacology and Chemotherapy,* 31**,** 138-+.

Jeftinija, S. (1994) BRADYKININ EXCITES TETRODOTOXIN-RESISTANT PRIMARY AFFERENT-FIBERS. *Brain Research,* 665**,** 69-76.

Ji, R.-R. & G. Strichartz (2004) Cell signaling and the genesis of neuropathic pain. *Science's STKE : signal transduction knowledge environment,* 2004**,** reE14-reE14.

Ji, R. R., Z. Z. Xu & Y. J. Gao (2014) Emerging targets in neuroinflammation-driven chronic pain. *Nature Reviews Drug Discovery,* 13**,** 533-548.

Jung, J., Y. H. Shin, H. Konishi, S. J. Lee & H. Kiyama (2013) Possible ATP release through lysosomal exocytosis from primary sensory neurons. *Biochemical and Biophysical Research Communications,* 430**,** 488-493.

Jurado, S., D. Goswami, Y. Zhang, A. J. Minano Molina, T. C. Suedhof & R. C. Malenka (2013) LTP Requires a Unique Postsynaptic SNARE Fusion Machinery. *Neuron,* 77**,** 542-558.

Kandel, E. R., J. H. Schwartz, T. M. Jessel, S. A. Siegelbaum & A. J. Hudspeth. 2013. *Principles of neural science*. McGraw Hill, 156 - 158.

Kaplan, D. R. & F. D. Miller (2000) Neurotrophin signal transduction in the nervous system. *Current Opinion in Neurobiology,* 10**,** 381-391.

Karanth, S. S., D. R. Springall, D. M. Kuhn, M. M. Levene & J. M. Polak (1991) AN IMMUNOCYTOCHEMICAL STUDY OF CUTANEOUS INNERVATION AND THE DISTRIBUTION OF NEUROPEPTIDES AND PROTEIN GENE-PRODUCT 9.5 IN MAN AND COMMONLY EMPLOYED LABORATORY-ANIMALS. *American Journal of Anatomy,* 191**,** 369-383.

Karvar, S., X. B. Yao, J. M. Crothers, Y. C. Liu & J. G. Forte (2002) Localization and function of soluble N-ethylmaleimide-sensitive factor attachment protein-25 and vesicle-associated membrane protein-2 in functioning gastric parietal cells. *Journal of Biological Chemistry,* 277**,** 50030-50035.

Katanosaka, K., R. K. Banik, R. Giron, T. Higashi, M. Tominaga & K. Mizumura (2008) Contribution of TRPV1 to the bradykinin-evoked nociceptive behavior and excitation of cutaneous sensory neurons. *Neuroscience Research,* 62**,** 168-175.

Kazarinova-Noyes, K., J. D. Malhotra, D. P. McEwen, L. N. Mattei, E. O. Berglund, B. Ranscht, S. R. Levinson, M. Schachner, P. Shrager, L. L. Isom & Z. C. Xiao (2001) Contactin associates with Na+ channels and increases their functional expression. *Journal of Neuroscience,* 21**,** 7517-7525.

Kerr, B. J., V. Souslova, S. B. McMahon & J. N. Wood (2001) A role for the TTX-resistant sodium channel Nav 1.8 in NGF-induced hyperalgesia, but not neuropathic pain. *Neuroreport,* 12**,** 3077-3080.

Khan, A. A., S. N. Raja, D. C. Manning, J. N. Campbell & R. A. Meyer (1992) THE EFFECTS OF BRADYKININ AND SEQUENCE-RELATED ANALOGS ON THE RESPONSE PROPERTIES OF CUTANEOUS NOCICEPTORS IN MONKEYS. *Somatosensory and Motor Research,* 9**,** 97-106.

Khasar, S. G., M. S. Gold & J. D. Levine (1998) A tetrodotoxin-resistant sodium current mediates inflammatory pain in the rat. *Neuroscience Letters,* 256**,** 17-20.

Kilo, S., C. HardingRose, K. M. Hargreaves & C. M. Flores (1997) Peripheral CGRP release as a marker for neurogenic inflammation: a model system for the study of neuropeptide secretion in rat paw skin. *Pain,* 73**,** 201-207.

Kim, C. H., Y. Oh, J. M. Chung & K. Chung (2002) Changes in three subtypes of tetrodotoxin sensitive sodium channel expression in the axotomized dorsal root ganglion in the rat. *Neuroscience Letters,* 323**,** 125-128.

Kitamura, N., A. Konno, T. Kuwahara & Y. Komagiri (2005) Nerve growth factor-induced hyperexcitability of rat sensory neuron in culture. *Biomedical Research-Tokyo,* 26**,** 123-130.

Klugbauer, N., L. Lacinova, V. Flockerzi & F. Hofmann (1995) STRUCTURE AND FUNCTIONAL EXPRESSION OF A NEW MEMBER OF THE TETRODOTOXIN-SENSITIVE VOLTAGE-ACTIVATED SODIUM-CHANNEL FAMILY FROM HUMAN NEUROENDOCRINE CELLS. *Embo Journal,* 14**,** 1084-1090.

Kobayashi, J., M. Ohta & Y. Terada (1993) C-FIBER GENERATES A SLOW NA+ SPIKE IN THE FROG SCIATIC-NERVE. *Neuroscience Letters,* 162**,** 93-96.

Lai, H. C. & L. Y. Jan (2006) The distribution and targeting of neuronal voltage-gated ion channels. *Nature Reviews Neuroscience,* 7**,** 548-562.

Lai, J., F. Porreca, J. C. Hunter & M. S. Gold (2004) Voltage-gated sodium channels and hyperalgesia. *Annual Review of Pharmacology and Toxicology,* 44**,** 371-397.

Lawson, S. N. & P. J. Waddell (1991) SOMA NEUROFILAMENT IMMUNOREACTIVITY IS RELATED TO CELL-SIZE AND FIBER CONDUCTION-VELOCITY IN RAT PRIMARY SENSORY NEURONS. *Journal of Physiology-London,* 435**,** 41-63.

Leffler, A., T. R. Cummins, S. D. Dib-Hajj, W. N. Hormuzdiar, J. A. Black & S. G. Waxman (2002) GDNF and NGF reverse changes in repriming of TTX-sensitive Na+ currents following axotomy of dorsal root ganglion neurons. *Journal of Neurophysiology,* 88**,** 650-658.

Li, C. Y., R. W. Peoples, T. H. Lanthorn, Z. W. Li & F. F. Weight (1999) Distinct ATP-activated currents in different types of neurons dissociated from rat dorsal root ganglion. *Neuroscience Letters,* 263**,** 57-60.

Lin, C. R., F. Amaya, L. Barrett, H. B. Wang, J. Takada, T. A. Samad & C. J. Woolf (2006) Prostaglandin E-2 receptor EP4 contributes to inflammatory pain hypersensitivity. *Journal of Pharmacology and Experimental Therapeutics,* 319**,** 1096-1103.

Lindia, J. A., M. G. Kohler, W. J. Martin & C. Abbadie (2005) Relationship between sodium channel Nav1.3 expression and neuropathic pain behavior in rats. *Pain,* 117**,** 145-153.

Liu, C., Q. Li, Y. Y. Su & L. Bao (2010) Prostaglandin E-2 Promotes Na(v)1.8 Trafficking via Its Intracellular RRR Motif Through the Protein Kinase A Pathway. *Traffic,* 11**,** 405-417.

Liu, C. N., R. Amir & M. Devor (1999) Effect of age and nerve injury on cross-excitation among sensory neurons in rat dorsal root ganglia. *Neuroscience Letters,* 259**,** 95-98.

Liu, Y., Y. Sugiura & W. C. Lin (2011) The role of Synaptobrevin1/VAMP1 in Ca2+-triggered neurotransmitter release at the mouse neuromuscular junction. *Journal of Physiology-London,* 589**,** 1603-1618.

Lombet, A., P. Laduron, C. Mourre, Y. Jacomet & M. Lazdunski (1985) AXONAL-TRANSPORT OF THE VOLTAGE-DEPENDENT NA+ CHANNEL PROTEIN IDENTIFIED BY ITS TETRODOTOXIN BINDING-SITE IN RAT SCIATIC-NERVES. *Brain Research,* 345**,** 153-158.

Lu, S.-G., X.-L. Zhang, Z. D. Luo & M. S. Gold (2010) Persistent inflammation alters the density and distribution of voltage-activated calcium channels in subpopulations of rat cutaneous DRG neurons. *Pain,* 151**,** 633-643.

Maingret, F., B. Coste, F. Padilla, N. Clerc, M. Crest, S. M. Korogod & P. Delmas (2008) Inflammatory mediators increase Nav1.9 current and excitability in Nociceptors through a coincident detection mechanism. *Journal of General Physiology,* 131**,** 211-225.

Malin, S. A., B. M. Davis, H. R. Koerber, I. J. Reynolds, K. M. Albers & D. C. Molliver (2008) Thermal nociception and TRPV1 function are attenuated in mice lacking the nucleotide receptor P2Y(2). *Pain,* 138**,** 484-496.

Malin, S. A., B. M. Davis & D. C. Molliver (2007) Production of dissociated sensory neuron cultures and considerations for their use in studying neuronal function and plasticity. *Nature Protocols,* 2**,** 152-160.

Malin, S. A. & D. C. Molliver (2010) Gi- and Gq-coupled ADP (P2Y) receptors act in opposition to modulate nociceptive signaling and inflammatory pain behavior. *Molecular Pain,* 6.

Mallard, F., B. L. Tang, T. Galli, D. Tenza, A. Saint-Pol, X. Yue, C. Antony, W. J. Hong, B. Goud & L. Johannes (2002) Early/recycling endosomes-to-TGN transport involves two SNARE complexes and a Rab6 isoform. *Journal of Cell Biology,* 156**,** 653-664.

Mangione, A. S., I. Obara, M. Maiaru, S. M. Geranton, C. Tassorelli, E. Ferrari, C. Leese, B. Davletov & S. P. Hunt (2016) Nonparalytic botulinum molecules for the control of pain. *Pain,* 157**,** 1045-55.

Martens, S. & H. T. McMahon (2008) Mechanisms of membrane fusion: disparate players and common principles. *Nature Reviews Molecular Cell Biology,* 9**,** 543-556.

Martin, L. B., A. Shewan, C. A. Millar, G. W. Gould & D. E. James (1998) Vesicle-associated membrane protein 2 plays a specific role in the insulin-dependent trafficking of the facilitative glucose transporter GLUT4 in 3T3-L1 adipocytes. *Journal of Biological Chemistry,* 273**,** 1444-1452.

Martinez-Arca, S., P. Alberts, A. Zahraoui, D. Louvard & T. Galli (2000) Role of tetanus neurotoxin insensitive vesicle-associated membrane protein (TI-VAMP) in vesicular transport mediating neurite outgrowth. *Journal of Cell Biology,* 149**,** 889-899.

Martling, C. R., A. Saria, J. A. Fischer, T. Hokfelt & J. M. Lundberg (1988) CALCITONIN GENE-RELATED PEPTIDE AND THE LUNG - NEURONAL COEXISTENCE WITH SUBSTANCE-P, RELEASE BY CAPSAICIN AND VASODILATORY EFFECT. *Regulatory Peptides,* 20**,** 125-139.

Maruo, K., H. Yamamoto, S. Yamamoto, T. Nagata, H. Fujikawa, T. Kanno, T. Yaguchi, S. Maruo, S. Yoshiya & T. Nishizaki (2006) Modulation of P2X receptors via adrenergic pathways in rat dorsal root ganglion neurons after sciatic nerve injury. *Pain,* 120**,** 106-112.

Matak, I. & Z. Lackovic (2014) Botulinum toxin A, brain and pain. *Progress in Neurobiology,* 119**,** 39-59.

Mathivanan, S., I. Devesa, J. P. Changeux & A. Ferrer-Montiel (2016) Bradykinin Induces TRPV1 Exocytotic Recruitment in Peptidergic Nociceptors. *Frontiers in Pharmacology,* 7.

Matsutomi, T., C. Nakamoto, T. Zheng, J. Kakimura & N. Ogata (2006) Multiple types of Na+ currents mediate action potential electrogenesis in small neurons of mouse dorsal root ganglia. *Pflugers Archiv-European Journal of Physiology,* 453**,** 83-96.

Matzner, O. & M. Devor (1992) NA+ CONDUCTANCE AND THE THRESHOLD FOR REPETITIVE NEURONAL FIRING. *Brain Research,* 597**,** 92-98.

--- (1994) HYPEREXCITABILITY AT SITES OF NERVE INJURY DEPENDS ON VOLTAGE-SENSITIVE NA+ CHANNELS. *Journal of Neurophysiology,* 72**,** 349-359.

McDonnell, A., B. Schulman, Z. Ali, S. D. Dib-Hajj, F. Brock, S. Cobain, T. Mainka, J. Vollert, S. Tarabar & S. G. Waxman (2016) Inherited erythromelalgia due to

mutations in SCN9A: natural history, clinical phenotype and somatosensory profile. *Brain,* 139**,** 1052-1065.

McLachlan, E. M., W. Janig, M. Devor & M. Michaelis (1993) PERIPHERAL-NERVE INJURY TRIGGERS NORADRENERGIC SPROUTING WITHIN DORSAL-ROOT GANGLIA. *Nature,* 363**,** 543-546.

McMahon, H. T., Y. A. Ushkaryov, L. Edelmann, E. Link, T. Binz, H. Niemann, R. Jahn & T. C. Sudhof (1993) CELLUBREVIN IS A UBIQUITOUS TETANUS-TOXIN SUBSTRATE HOMOLOGOUS TO A PUTATIVE SYNAPTIC VESICLE FUSION PROTEIN. *Nature,* 364**,** 346-349.

Meisler, M. H., J. A. Kearney, L. K. Sprunger, B. T. MacDonald, D. A. Buchner & A. Escayg (2002) Mutations of voltage-gated sodium channels in movement disorders and epilepsy. *Sodium Channels and Neuronal Hyperexcitability,* 241**,** 72-86.

Melzack, R. & P. D. Wall (1965) PAIN MECHANISMS - A NEW THEORY. *Science,* 150**,** 971-&.

Mendez, M., K. W. Gross, S. T. Glenn, J. L. Garvin & O. A. Carretero (2011) Vesicle-associated Membrane Protein-2 (VAMP2) Mediates cAMP-stimulated Renin Release in Mouse Juxtaglomerular Cells. *Journal of Biological Chemistry,* 286**,** 28608-28618.

Meng, J., J. Wang, G. Lawrence & J. O. Dolly (2007) Synaptobrevin I mediates exocytosis of CGRP from sensory neurons and inhibition by botulinum toxins reflects their anti-nociceptive potential. *Journal of Cell Science,* 120**,** 2864-2874.

Meng, J., J. Wang, M. Steinhoff & J. O. Dolly (2016) TNF alpha induces co-trafficking of TRPV1/TRPA1 in VAMP1-containing vesicles to the plasmalemma via Munc18-1/syntaxin1/SNAP-25 mediated fusion. *Scientific Reports,* 6**,** 21226-21226.

Meng, J. H., S. V. Ovsepian, J. F. Wang, M. Pickering, A. Sasse, K. R. Aoki, G. W. Lawrence & J. O. Dolly (2009) Activation of TRPV1 Mediates Calcitonin Gene-Related Peptide Release, Which Excites Trigeminal Sensory Neurons and Is Attenuated by a Retargeted Botulinum Toxin with Anti-Nociceptive Potential. *Journal of Neuroscience,* 29**,** 4981-4992.

Messner, D. J. & W. A. Catterall (1985) THE SODIUM-CHANNEL FROM RAT-BRAIN - SEPARATION AND CHARACTERIZATION OF SUBUNITS. *Journal of Biological Chemistry,* 260**,** 597-604.

Meyer, R. A. & J. N. Campbell (1981) MYELINATED NOCICEPTIVE AFFERENTS ACCOUNT FOR THE HYPERALGESIA THAT FOLLOWS A BURN TO THE HAND. *Science,* 213**,** 1527-1529.

--- (1988) A NOVEL ELECTROPHYSIOLOGICAL TECHNIQUE FOR LOCATING CUTANEOUS NOCICEPTIVE AND CHEMOSPECIFIC RECEPTORS. *Brain Research,* 441**,** 81-86.

Meyer, R. A., K. D. Davis, R. H. Cohen, R. D. Treede & J. N. Campbell (1991) MECHANICALLY INSENSITIVE AFFERENTS (MIAS) IN CUTANEOUS NERVES OF MONKEY. *Brain Research,* 561**,** 252-261.

Minett, M. S., V. Pereira, S. Sikandar, A. Matsuyama, S. Lolignier, A. H. Kanellopoulos, F. Mancini, G. D. Iannetti, Y. D. Bogdanov, S. Santana-Varela, Q. Millet, G. Baskozos, R. MacAllister, J. J. Cox, J. Zhao & J. N. Wood (2015)

Endogenous opioids contribute to insensitivity to pain in humans and mice lacking sodium channel Na(v)1.7. *Nature Communications,* 6.

Mizumura, K., M. Minagawa, H. Koda & T. Kumazawa (1995) INFLUENCE OF HISTAMINE ON THE BRADYKININ RESPONSE OF CANINE TESTICULAR POLYMODAL RECEPTORS IN-VITRO. *Inflammation Research,* 44**,** 376-378.

Moalem, G., P. Grafe & D. J. Tracey (2005) Chemical mediators enhance the excitability of unmyelinated sensory axons in normal and injured peripheral nerve of the rat. *Neuroscience,* 134**,** 1399-1411.

Moczydlowski, E. G. (2013) The molecular mystique of tetrodotoxin. *Toxicon,* 63**,** 165-183.

Molliver, D. C., D. E. Wright, M. L. Leitner, A. S. Parsadanian, K. Doster, D. Wen, Q. Yan & W. D. Snider (1997) IB4-binding DRG neurons switch from NGF to GDNF dependence in early postnatal life. *Neuron,* 19**,** 849-861.

Momin, A. & P. A. McNaughton (2009) Regulation of firing frequency in nociceptive neurons by pro-inflammatory mediators. *Experimental Brain Research,* 196**,** 45-52.

Montecucco, C., G. Schiavo & O. Rossetto (1996) The mechanism of action of tetanus and botulinum neurotoxins. *Toxicology - from Cells to Man,* 18**,** 342-354.

Moriyama, T., T. Higashi, K. Togashi, T. Iida, E. Segi, Y. Sugimoto, T. Tominaga, S. Narumiya & M. Tominaga (2005) Sensitization of TRPV1 by EP1 and IP reveals peripheral nociceptive mechanism of prostaglandins. *Molecular Pain,* 1.

Nagy, J. I. & S. P. Hunt (1982) FLUORIDE-RESISTANT ACID PHOSPHATASE-CONTAINING NEURONS IN DORSAL ROOT-GANGLIA ARE SEPARATE FROM THOSE CONTAINING SUBSTANCE-P OR SOMATOSTATIN. *Neuroscience,* 7**,** 89-97.

Namadurai, S., N. R. Yereddi, F. S. Cusdin, C. L. H. Huang, D. Y. Chirgadze & A. P. Jackson (2015) A new look at sodium channel beta subunits. *Open Biology,* 5.

Nassar, M. A., M. D. Baker, A. Levato, R. Ingram, G. Mallucci, S. B. McMahon & J. N. Wood (2006) Nerve injury induces robust allodynia and ectopic discharges in Na(v)1.3 null mutant mice. *Molecular Pain,* 2.

Nassar, M. A., L. C. Stirling, G. Forlani, M. D. Baker, E. A. Matthews, A. H. Dickenson & J. N. Wood (2004) Nociceptor-specific gene deletion reveals a major role for Na(v)1.7 (PN1) in acute and inflammatory pain. *Proceedings of the National Academy of Sciences of the United States of America,* 101**,** 12706-12711.

Ng, K. Y., B. H. S. Yeung, Y. H. Wong & H. Wise (2013) Isolated dorsal root ganglion neurones inhibit receptor-dependent adenylyl cyclase activity in associated glial cells. *British Journal of Pharmacology,* 168**,** 746-760.

Nicholson, R., J. Small, A. K. Dixon, D. Spanswick & K. Lee (2003) Serotonin receptor rnRNA expression in rat dorsal root ganglion neurons. *Neuroscience Letters,* 337**,** 119-122.

Nicol, G. D., M. R. Vasko & A. R. Evans (1997) Prostaglandins suppress an outward potassium current in embryonic rat sensory neurons. *Journal of Neurophysiology,* 77**,** 167-176.

Nicolson, T. A., A. F. Foster, S. Bevan & C. D. Richards (2007) Prostaglandin E(2) sensitizes primary sensory neurons to histamine. *Neuroscience,* 150**,** 22-30.

Nystuen, A. M., J. K. Schwendinger, A. J. Sachs, A. W. Yang & N. B. Haider (2007) A null mutation in VAMP1/synaptobrevin is associated with neurological defects and prewean mortality in the lethal-wasting mouse mutant. *Neurogenetics,* 8**,** 1-10.

Okuse, K., S. R. Chaplan, S. B. McMahon, Z. D. Luo, N. A. Calcutt, B. P. Scott, A. N. Akopian & J. N. Wood (1997) Regulation of expression of the sensory neuron-specific sodium channel SNS in inflammatory and neuropathic pain. *Molecular and Cellular Neuroscience,* 10**,** 196-207.

Okuse, K., M. Malik-Hall, M. D. Baker, W. Y. L. Poon, H. Y. Kong, M. V. Chao & J. N. Wood (2002) Annexin II light chain regulates sensory neuron-specific sodium channel expression. *Nature,* 417**,** 653-656.

Omri, G. & H. Meiri (1990) CHARACTERIZATION OF SODIUM CURRENTS IN MAMMALIAN SENSORY NEURONS CULTURED IN SERUM-FREE DEFINED MEDIUM WITH AND WITHOUT NERVE GROWTH-FACTOR. *Journal of Membrane Biology,* 115**,** 13-29.

Ostman, J. A. R., M. A. Nassar, J. N. Wood & M. D. Baker (2008) GTP up-regulated persistent Na(+) current and enhanced nociceptor excitability require Na(V)1.9. *Journal of Physiology-London,* 586**,** 1077-1087.

Oyelese, A. A., M. A. Rizzo, S. G. Waxman & J. D. Kocsis (1997) Differential effects of NGF and BDNF on axotomy-induced changes in GABA(A)-receptor-mediated conductance and sodium currents in cutaneous afferent neurons. *Journal of Neurophysiology,* 78**,** 31-42.

Paillart, C., J. L. Boudier, J. A. Boudier, H. Rochat, F. Couraud & B. Dargent (1996) Activity-induced internalization and rapid degradation of sodium channels in cultured fetal neurons. *Journal of Cell Biology,* 134**,** 499-509.

Park, K. A., J. C. Fehrenbacher, E. L. Thompson, D. B. Duarte, C. M. Hingtgen & M. R. Vasko (2010) SIGNALING PATHWAYS THAT MEDIATE NERVE GROWTH FACTOR-INDUCED INCREASE IN EXPRESSION AND RELEASE OF CALCITONIN GENE-RELATED PEPTIDE FROM SENSORY NEURONS. *Neuroscience,* 171**,** 910-923.

Park, S. Y., J. Y. Choi, R. U. Kim, Y. S. Lee, H. J. Cho & D. S. Kim (2003) Downregulation of voltage-gated potassium channel alpha gene expression by axotomy and neurotrophins in rat dorsal root ganglia. *Molecules and Cells,* 16**,** 256-259.

Paterson, K., S. Lolignier, J. N. Wood, S. B. McMahon & D. L. H. Bennett (2014) Botulinum Toxin-A Treatment Reduces Human Mechanical Pain Sensitivity and Mechanotransduction. *Annals of Neurology,* 75**,** 591-596.

Peden, A. A., G. Y. Park & R. H. Scheller (2001) The di-leucine motif of vesicle-associated membrane protein 4 is required for its localization and AP-1 binding. *Journal of Biological Chemistry,* 276**,** 49183-49187.

Pratt, K. G., P. Zhu, H. Watari, D. G. Cook & J. M. Sullivan (2011) A Novel Role for gamma-Secretase: Selective Regulation of Spontaneous Neurotransmitter Release from Hippocampal Neurons. *Journal of Neuroscience,* 31**,** 899-906.

Premkumar, L. S. & G. P. Ahern (2000) Induction of vanilloid receptor channel activity by protein kinase C. *Nature,* 408**,** 985-990.

Priest, B. T., B. A. Murphy, J. A. Lindia, C. Diaz, C. Abbadie, A. M. Ritter, P. Liberator, L. M. Iyer, S. F. Kash, M. G. Kohler, G. J. Kaczorowski, D. E. MacIntyre & W. J. Martin (2005) Contribution of the tetrodotoxin-resistant voltage-gated sodium channel Na(v)1.9 to sensory transmission and nociceptive behavior. *Proceedings of the National Academy of Sciences of the United States of America,* 102**,** 9382-9387.

Procino, G., C. Barbieri, G. Tamma, L. De Benedictis, J. E. Pessin, M. Svelto & G. Valenti (2008) AQP2 exocytosis in the renal collecting duct - involvement of SNARE isoforms and the regulatory role of Munc18b. *Journal of Cell Science,* 121**,** 2097-2106.

Pryor, P. R., B. M. Mullock, N. A. Bright, M. R. Lindsay, S. R. Gray, S. C. W. Richardson, A. Stewart, D. E. James, R. C. Piper & J. P. Luzio (2004) Combinatorial SNARE complexes with VAMP7 or VAMP8 define different late endocytic fusion events. *Embo Reports,* 5**,** 590-595.

Quasthoff, S., J. Grosskreutz, J. M. Schroder, U. Schneider & P. Grafe (1995) CALCIUM POTENTIALS AND TETRODOTOXIN-RESISTANT SODIUM POTENTIALS IN UNMYELINATED-C FIBERS OF BIOPSIED HUMAN SURAL NERVE. *Neuroscience,* 69**,** 955-965.

Raingo, J., M. Khvotchev, P. Liu, F. Darios, Y. C. Li, D. M. O. Ramirez, M. Adachi, P. Lemieux, K. Toth, B. Davletov & E. T. Kavalali (2012) VAMP4 directs synaptic vesicles to a pool that selectively maintains asynchronous neurotransmission. *Nature Neuroscience,* 15**,** 738-745.

Raman, I. M. & B. P. Bean (1997) Resurgent sodium current and action potential formation in dissociated cerebellar Purkinje neurons. *Journal of Neuroscience,* 17**,** 4517-4526.

Ramirez, D. M. O. & E. T. Kavalali (2011) Differential regulation of spontaneous and evoked neurotransmitter release at central synapses. *Current Opinion in Neurobiology,* 21**,** 275-282.

Rang, H. P. & J. M. Ritchie (1988) DEPOLARIZATION OF NONMYELINATED FIBERS OF THE RAT VAGUS NERVE PRODUCED BY ACTIVATION OF PROTEIN KINASE-C. *Journal of Neuroscience,* 8**,** 2606-2617.

Rao, S. K., C. Huynh, V. Proux-Gillardeaux, T. Galli & N. W. Andrews (2004) Identification of SNAREs involved in synaptotagmin VII-regulated lysosomal exocytosis. *Journal of Biological Chemistry,* 279**,** 20471-20479.

Raptis, A., B. Torrejon-Escribsno, I. G. de Aranda & J. Blasi (2005) Distribution of synaptobrevin/VAMP 1 and 2 in rat brain. *Journal of Chemical Neuroanatomy,* 30**,** 201-211.

Regazzi, R., C. B. Wollheim, J. Lang, J. M. Theler, O. Rossetto, C. Montecucco, K. Sadoul, U. Weller, M. Palmer & B. Thorens (1995) VAMP-2 AND CELLUBREVIN ARE EXPRESSED IN PANCREATIC BETA-CELLS AND ARE ESSENTIAL FOR CA2+ - BUT NOT FOR GTP-GAMMA-S-INDUCED INSULIN-SECRETION. *Embo Journal,* 14**,** 2723-2730.

Renganathan, M., T. R. Cummins & S. G. Waxman (2001) Contribution of Na(v)1.8 sodium channels to action potential electrogenesis in DRG neurons. *Journal of Neurophysiology,* 86**,** 629-640.

Restani, L., F. Giribaldi, M. Manich, K. Bercsenyi, G. Menendez, O. Rossetto, M. Caleo & G. Schiavo (2012a) Botulinum Neurotoxins A and E Undergo Retrograde Axonal Transport in Primary Motor Neurons. *Plos Pathogens,* 8.

Restani, L., E. Novelli, D. Bottari, P. Leone, I. Barone, L. Galli-Resta, E. Strettoi & M. Caleo (2012b) Botulinum Neurotoxin A Impairs Neurotransmission Following Retrograde Transynaptic Transport. *Traffic,* 13**,** 1083-1089.

Revelo, N. H., D. Kamin, S. Truckenbrodt, A. B. Wong, K. Reuter-Jessen, E. Reisinger, T. Moser & S. O. Rizzoli (2014) A new probe for super-resolution imaging of membranes elucidates trafficking pathways. *Journal of Cell Biology,* 205**,** 591-606.

Ritter, A. M. & L. M. Mendell (1992) SOMAL MEMBRANE-PROPERTIES OF PHYSIOLOGICALLY IDENTIFIED SENSORY NEURONS IN THE RAT - EFFECTS OF NERVE GROWTH-FACTOR. *Journal of Neurophysiology,* 68**,** 2033-2041.

Rose, A. J., J. Jeppesen, B. Kiens & E. A. Richter (2009) Effects of contraction on localization of GLUT4 and v-SNARE isoforms in rat skeletal muscle. *American Journal of Physiology-Regulatory Integrative and Comparative Physiology,* 297**,** R1228-R1237.

Rossetto, O., L. Gorza, G. Schiavo, N. Schiavo, R. H. Scheller & C. Montecucco (1996) VAMP synaptobrevin isoforms 1 and 2 are widely and differentially expressed in nonneuronal tissues. *Journal of Cell Biology,* 132**,** 167-179.

Rouwette, T., J. Sondermann, L. Avenali, D. Gomez-Varela & M. Schmidt (2016a) Standardized Profiling of The Membrane-Enriched Proteome of Mouse Dorsal Root Ganglia (DRG) Provides Novel Insights Into Chronic Pain. *Molecular & Cellular Proteomics,* 15**,** 2152-2168.

--- (2016b) Standardized Profiling of The Membrane-Enriched Proteome of Mouse Dorsal Root Ganglia (DRG) Provides Novel Insights Into Chronic Pain. *Molecular & Cellular Proteomics,* 15**,** 2152-2168.

Rush, A. M., T. R. Cummins & S. G. Waxman (2007) Multiple sodium channels and their roles in electrogenesis within dorsal root ganglion neurons. *Journal of Physiology-London,* 579**,** 1-14.

Rush, A. M. & S. G. Waxman (2004) PGE(2) increases the tetrodotoxin-resistant Na(v)1.9 sodium current in mouse DRG neurons via G-proteins. *Brain Research,* 1023**,** 264-271.

Salzer, I., E. Gantumur, A. Yousuf & S. Boehm (2016) Control of sensory neuron excitability by serotonin involves 5HT2C receptors and Ca2+-activated chloride channels. *Neuropharmacology,* 110**,** 277-286.

Sangameswaran, L., L. M. Fish, B. D. Koch, D. K. Rabert, S. G. Delgado, M. Ilnicka, L. B. Jakeman, S. Novakovic, K. Wong, P. Sze, E. Tzoumaka, G. R. Stewart, R. C. Herman, H. Chan, R. M. Eglen & J. C. Hunter (1997) A novel tetrodotoxin-sensitive, voltage-gated sodium channel expressed in rat and human dorsal root ganglia. *Journal of Biological Chemistry,* 272**,** 14805-14809.

Sara, Y., T. Virmani, F. Deak, X. R. Liu & E. T. Kavalali (2005) An isolated pool of vesicles recycles at rest and drives spontaneous neurotransmission. *Neuron,* 45**,** 563-573.

Schafer, I. B., G. G. Hesketh, N. A. Bright, S. R. Gray, P. R. Pryor, P. R. Evans, J. P. Luzio & D. J. Owen (2012) The binding of Varp to VAMP7 traps VAMP7 in a

closed, fusogenically inactive conformation. *Nature Structural & Molecular Biology,* 19**,** 1300-+.

Schiavo, G., F. Benfenati, B. Poulain, O. Rossetto, P. P. Delaureto, B. R. Dasgupta & C. Montecucco (1992) TETANUS AND BOTULINUM-B NEUROTOXINS BLOCK NEUROTRANSMITTER RELEASE BY PROTEOLYTIC CLEAVAGE OF SYNAPTOBREVIN. *Nature,* 359**,** 832-835.

Schmidt, J. W. & W. A. Catterall (1986) BIOSYNTHESIS AND PROCESSING OF THE ALPHA-SUBUNIT OF THE VOLTAGE-SENSITIVE SODIUM-CHANNEL IN RAT-BRAIN NEURONS. *Cell,* 46**,** 437-445.

Schoch, S., F. Deak, A. Konigstorfer, M. Mozhayeva, Y. Sara, T. C. Sudhof & E. T. Kavalali (2001) SNARE function analyzed in synaptobrevin/VAMP knockout mice. *Science,* 294**,** 1117-1122.

Scott, B. S. & B. A. V. Edwards (1980) ELECTRIC MEMBRANE-PROPERTIES OF ADULT-MOUSE DRG NEURONS AND THE EFFECT OF CULTURE DURATION. *Journal of Neurobiology,* 11**,** 291-301.

Sherrington, C. S. (1903) Qualitative difference of spinal reflex corresponding with qualitative difference of cutaneous stimulus. *Journal of Physiology-London,* 30**,** 39-46.

Shimojo, M., J. Courchet, S. Pieraut, N. Torabi-Rander, R. Sando, F. Polleux & A. Maximov (2015) SNAREs Controlling Vesicular Release of BDNF and Development of Callosal Axons. *Cell Reports,* 11**,** 1054-1066.

Shinder, V., R. Amir & M. Devor (1998) Cross-excitation in dorsal root ganglia does not depend on close cell-to-cell apposition. *Neuroreport,* 9**,** 3997-4000.

Silverman, J. D. & L. Kruger (1988a) ACID-PHOSPHATASE AS A SELECTIVE MARKER FOR A CLASS OF SMALL SENSORY GANGLION-CELLS IN SEVERAL MAMMALS - SPINAL-CORD DISTRIBUTION, HISTOCHEMICAL PROPERTIES, AND RELATION TO FLUORIDE-RESISTANT ACID-PHOSPHATASE (FRAP) OF RODENTS. *Somatosensory Research,* 5**,** 219-246.

--- (1988b) LECTIN AND NEUROPEPTIDE LABELING OF SEPARATE POPULATIONS OF DORSAL-ROOT GANGLION NEURONS AND ASSOCIATED NOCICEPTOR THIN AXONS IN RAT TESTIS AND CORNEA WHOLE-MOUNT PREPARATIONS. *Somatosensory Research,* 5**,** 259-267.

--- (1990) SELECTIVE NEURONAL GLYCOCONJUGATE EXPRESSION IN SENSORY AND AUTONOMIC GANGLIA - RELATION OF LECTIN REACTIVITY TO PEPTIDE AND ENZYME MARKERS. *Journal of Neurocytology,* 19**,** 789-801.

Singh, B. B., T. P. Lockwich, B. C. Bandyopadhyay, X. B. Liu, S. Bollimuntha, S. C. Brazer, C. Combs, S. Das, A. G. M. Leenders, Z. H. Sheng, M. A. Knepper, S. V. Ambudkar & I. S. Ambudkar (2004) VAMP2-dependent exocytosis regulates plasma membrane insertion of TRPC3 channels and contributes to agonist-stimulated Ca2+ influx. *Molecular Cell,* 15**,** 635-646.

Slugg, R. M., R. A. Meyer & J. N. Campbell (2000) Response of cutaneous A- and C-fiber nociceptors in the monkey to controlled-force stimuli. *Journal of Neurophysiology,* 83**,** 2179-2191.

Snider, W. D. & S. B. McMahon (1998) Tackling pain at the source: New ideas about nociceptors. *Neuron,* 20**,** 629-632.

Sorensen, J. B., G. Nagy, F. Varoqueaux, R. B. Nehring, N. Brose, M. C. Wilson & E. Neher (2003) Differential control of the releasable vesicle pools by SNAP-25 splice variants and SNAP-23. *Cell,* 114**,** 75-86.

Steranka, L. R., D. C. Manning, C. J. Dehaas, J. W. Ferkany, S. A. Borosky, J. R. Connor, R. J. Vavrek, J. M. Stewart & S. H. Snyder (1988) BRADYKININ AS A PAIN MEDIATOR - RECEPTORS ARE LOCALIZED TO SENSORY NEURONS, AND ANTAGONISTS HAVE ANALGESIC ACTIONS. *Proceedings of the National Academy of Sciences of the United States of America,* 85**,** 3245-3249.

Strickland, I. T., J. C. Martindale, P. L. Woodhams, A. J. Reeve, I. P. Chessell & D. S. McQueen (2008) Changes in the expression of Na(V)1.7, Na(V)1.8 and Na(V)1.9 in a distinct population of dorsal root ganglia innervating the rat knee joint in a model of chronic inflammatory joint pain. *European Journal of Pain,* 12**,** 564-572.

Stucky, C. L. & G. R. Lewin (1999) Isolectin B-4-positive and -negative nociceptors are functionally distinct. *Journal of Neuroscience,* 19**,** 6497-6505.

Sudhof, T. C. & J. E. Rothman (2009) Membrane Fusion: Grappling with SNARE and SM Proteins. *Science,* 323**,** 474-477.

Suedhof, T. C. (2013) Neurotransmitter Release: The Last Millisecond in the Life of a Synaptic Vesicle. *Neuron,* 80**,** 675-690.

Sufka, K. J., F. M. Schomburg & J. Giordano (1992) RECEPTOR MEDIATION OF 5-HT-INDUCED INFLAMMATION AND NOCICEPTION IN RATS. *Pharmacology Biochemistry and Behavior,* 41**,** 53-56.

Sutton, R. B., D. Fasshauer, R. Jahn & A. T. Brunger (1998) Crystal structure of a SNARE complex involved in synaptic exocytosis at 2.4 angstrom resolution. *Nature,* 395**,** 347-353.

Szallasi, A. & P. M. Blumberg (1999) Vanilloid (capsaicin) receptors and mechanisms. *Pharmacological Reviews,* 51**,** 159-211.

Takamori, S., M. Holt, K. Stenius, E. A. Lemke, M. Gronborg, D. Riedel, H. Urlaub, S. Schenck, B. Brugger, P. Ringler, S. A. Muller, B. Rammner, F. Grater, J. S. Hub, B. L. De Groot, G. Mieskes, Y. Moriyama, J. Klingauf, H. Grubmuller, J. Heuser, F. Wieland & R. Jahn (2006) Molecular anatomy of a trafficking organelle. *Cell,* 127**,** 831-846.

Takeda, M., M. Ikeda, T. Tanimoto, J. Lipski & S. Matsumoto (2002) Changes of the excitability of rat trigeminal root ganglion neurons evoked by alpha(2)-adrenoreceptors. *Neuroscience,* 115**,** 731-741.

Tanaka, M., T. R. Cummins, K. Ishikawa, S. D. Dib-Hajj, J. A. Black & S. G. Waxman (1998) SNS Na+ channel expression increases in dorsal root ganglion neurons in the carrageenan inflammatory pain model. *Neuroreport,* 9**,** 967-972.

Tappe-Theodor, A., C. E. Constantin, I. Tegeder, S. G. Lechner, M. Langeslag, P. Lepcynzsky, R. I. Wirotanseng, M. Kurejova, N. Agarwal, G. Nagy, A. Todd, N. Wettschureck, S. Offermanns, M. Kress, G. R. Lewin & R. Kuner (2012) G alpha(q/11) signaling tonically modulates nociceptor function and contributes to activity-dependent sensitization. *Pain,* 153**,** 184-196.

Tate, S., S. Benn, C. Hick, D. Trezise, V. John, R. J. Mannion, M. Costigan, C. Plumpton, D. Grose, Z. Gladwell, G. Kendall, K. Dale, C. Bountra & C. J. Woolf

(1998) Two sodium channels contribute to the TTX-R sodium current in primary sensory neurons. *Nature Neuroscience,* 1**,** 653-655.

Thakur, M., M. Crow, N. Richards, G. I. J. Davey, E. Levine, J. H. Kelleher, C. C. Agley, F. Denk, S. D. R. Harridge & S. B. McMahon (2014) Defining the nociceptor transcriptome. *Frontiers in Molecular Neuroscience,* 7.

Treede, R. D., R. A. Meyer, S. N. Raja & J. N. Campbell (1992) PERIPHERAL AND CENTRAL MECHANISMS OF CUTANEOUS HYPERALGESIA. *Progress in Neurobiology,* 38**,** 397-421.

--- (1995) EVIDENCE FOR 2 DIFFERENT HEAT TRANSDUCTION MECHANISMS IN NOCICEPTIVE PRIMARY AFFERENTS INNERVATING MONKEY SKIN. *Journal of Physiology-London,* 483**,** 747-758.

Trimble, W. S., D. M. Cowan & R. H. Scheller (1988) VAMP-1 - A SYNAPTIC VESICLE-ASSOCIATED INTEGRAL MEMBRANE-PROTEIN. *Proceedings of the National Academy of Sciences of the United States of America,* 85**,** 4538-4542.

Tripathi, P. K., C. G. Cardenas, C. A. Cardenas & R. S. Scroggs (2011) UP-REGULATION OF TETRODOTOXIN-SENSITIVE SODIUM CURRENTS BY PROSTAGLANDIN E-2 IN TYPE-4 RAT DORSAL ROOT GANGLION CELLS. *Neuroscience,* 185**,** 14-26.

Usoskin, D., A. Furlan, S. Islam, H. Abdo, P. Lonnerberg, D. Lou, J. Hjerling-Leffler, J. Haeggstrom, O. Kharchenko, P. V. Kharchenko, S. Linnarsson & P. Ernfors (2015) Unbiased classification of sensory neuron types by large-scale single-cell RNA sequencing. *Nat Neurosci,* 18**,** 145-53.

Utzschneider, D., J. Kocsis & M. Devor (1992) Mutual excitation among dorsal-root ganglion neurons in the rat. *Neuroscience Letters,* 146**,** 53-56.

Valenti, C., S. Giuliani, C. Cialdai, M. Tramontana & C. A. Maggi (2010) Anti-inflammatory synergy of MEN16132, a kinin B-2 receptor antagonist, and dexamethasone in carrageenan-induced knee joint arthritis in rats. *British Journal of Pharmacology,* 161**,** 1616-1627.

Vellani, V., S. Mapplebeck, A. Moriondo, J. B. Davis & P. A. McNaughton (2001) Protein kinase C activation potentiates gating of the vanilloid receptor VR1 by capsaicin, protons, heat and anandamide. *Journal of Physiology-London,* 534**,** 813-825.

Vellani, V., O. Zachrisson & P. A. McNaughton (2004) Functional bradykinin B1 receptors are expressed in nociceptive neurones and are upregulated by the neurotrophin GDNF. *Journal of Physiology-London,* 560**,** 391-401.

Villarreal, C. F., D. Sachs, F. D. Cunha, C. A. Parada & S. H. Ferreira (2005) The role of Na(V)1.8 sodium channel in the maintenance of chronic inflammatory hypernociception. *Neuroscience Letters,* 386**,** 72-77.

Villiere, V. & E. M. McLachlan (1996) Electrophysiological properties of neurons in intact rat dorsal root ganglia classified by conduction velocity and action potential duration. *Journal of Neurophysiology,* 76**,** 1924-1941.

Volkow, N. D. & F. S. Collins (2017) The Role of Science in Addressing the Opioid Crisis. *New England Journal of Medicine,* 377**,** 391-394.

Wallace, T. L. & E. M. Johnson (1989) CYTOSINE-ARABINOSIDE KILLS POSTMITOTIC NEURONS - EVIDENCE THAT DEOXYCYTIDINE MAY HAVE A ROLE IN NEURONAL SURVIVAL THAT IS INDEPENDENT OF DNA-SYNTHESIS. *Journal of Neuroscience,* 9**,** 115-124.

Wang, C. C., C. P. Ng, L. Lu, V. Atlashkin, W. Zhang, L. F. Seet & W. J. Hong (2004) A role of VAMP8/endobrevin in regulated exocytosis of pancreatic acinar cells. *Developmental Cell,* 7**,** 359-371.

Wang, P. C., M. D. Howard, H. H. Zhang, N. R. Chintagari, A. Bell, N. L. Jin, A. Mishra & L. Liu (2012) Characterization of VAMP-2 in the lung: implication in lung surfactant secretion. *Cell Biology International,* 36**,** 785-791.

Waxman, S. G., T. R. Cummins, S. Dib-Hajj, J. Fjell & J. A. Black (1999) Sodium channels, excitability of primary sensory neurons, and the molecular basis of pain. *Muscle & Nerve,* 22**,** 1177-1187.

Waxman, S. G., J. D. Kocsis & J. A. Black (1994) TYPE-III SODIUM-CHANNEL MESSENGER-RNA IS EXPRESSED IN EMBRYONIC BUT NOT ADULT SPINAL SENSORY NEURONS, AND IS REEXPRESSED FOLLOWING AXOTOMY. *Journal of Neurophysiology,* 72**,** 466-470.

Waxman, S. G. & J. M. Ritchie (1985) ORGANIZATION OF ION CHANNELS IN THE MYELINATED NERVE-FIBER. *Science,* 228**,** 1502-1507.

Wong, S. H., T. Zhang, Y. Xu, V. N. Subramaniam, G. Griffiths & W. J. Hong (1998) Endobrevin, a novel synaptobrevin/VAMP-like protein preferentially associated with the early endosome. *Molecular Biology of the Cell,* 9**,** 1549-1563.

Woolf, C. J., B. Safiehgarabedian, Q. P. Ma, P. Crilly & J. Winter (1994) NERVE GROWTH-FACTOR CONTRIBUTES TO THE GENERATION OF INFLAMMATORY SENSORY HYPERSENSITIVITY. *Neuroscience,* 62**,** 327-331.

Xie, J. G., Y. H. Lee, C. Wang, J. M. Chung & K. Chung (2001) Differential expression of alpha1-adrenoceptor subtype mRNAs in the dorsal root ganglion after spinal nerve ligation. *Molecular Brain Research,* 93**,** 164-172.

Xie, Y. K., J. M. Zhang, M. Petersen & R. H. Lamotte (1995) FUNCTIONAL-CHANGES IN DORSAL-ROOT GANGLION-CELLS AFTER CHRONIC NERVE CONSTRICTION IN THE RAT. *Journal of Neurophysiology,* 73**,** 1811-1820.

Yamasaki, S., A. Baumeister, J. Blasi, E. Link, F. Cornille, B. Roques, E. M. Fykse, T. C. Sudhof, R. Jahn, H. Niemann & T. Binz (1994) CLEAVAGE OF MEMBERS OF THE SYNAPTOBREVIN/VAMP FAMILY BY TYPE-D AND TYPE-F BOTULINAL NEUROTOXINS AND TETANUS TOXIN. *Journal of Biological Chemistry,* 269**,** 12764-12772.

Yanagita, T., H. Kobayashi, R. Yamamoto, H. Kataoka, H. Yokoo, S. Shiraishi, S. Minami, M. Koono & A. Wada (2000) Protein kinase C-alpha and -epsilon down-regulate cell surface sodium channels via differential mechanisms in adrenal chromaffin cells. *Journal of Neurochemistry,* 74**,** 1674-1684.

Yanagita, T., A. Wada, R. Yamamoto, H. Kobayashi, T. Yuhi, M. Urabe & H. Niina (1996) Protein kinase C-mediated down-regulation of voltage-dependent sodium channels in adrenal chromaffin cells. *Journal of Neurochemistry,* 66**,** 1249-1253.

Yang, B., L. Gonzalez, R. Prekeris, M. Steegmaier, R. J. Advani & R. H. Scheller (1999) SNARE interactions are not selective - Implications for membrane fusion specificity. *Journal of Biological Chemistry,* 274**,** 5649-5653.

Yeomans, D. C., S. R. Levinson, M. C. Peters, A. G. Koszowski, A. Z. Tzabazis, W. F. Gilly & S. P. Wilson (2005) Decrease in inflammatory hyperalgesia by herpes

vector-mediated knockdown of Na(v)1.7 sodium channels in primary afferents. *Human Gene Therapy,* 16**,** 271-277.

Yoshida, S., Y. Matsuda & A. Samejima (1978) TETRODOTOXIN-RESISTANT SODIUM AND CALCIUM COMPONENTS OF ACTION POTENTIALS IN DORSAL ROOT GANGLION-CELLS OF ADULT MOUSE. *Journal of Neurophysiology,* 41**,** 1096-1106.

Yousuf, A., F. Klinger, K. Schicker & S. Boehm (2011) Nucleotides control the excitability of sensory neurons via two P2Y receptors and a bifurcated signaling cascade. *Pain,* 152**,** 1899-1908.

Yu, J., Q. Fang, G. D. Lou, W. T. Shou, J. X. Yue, Y. Y. Tang, W. W. Hou, T. L. Xu, H. Ohtsu, S. H. Zhang & Z. Chen (2013) Histamine Modulation of Acute Nociception Involves Regulation of Na(v)1.8 in Primary Afferent Neurons in Mice. *Cns Neuroscience & Therapeutics,* 19**,** 649-658.

Yu, L., F. Yang, H. Luo, F.-Y. Liu, J.-S. Han, G.-G. Xing & Y. Wan (2008) The role of TRPV1 in different subtypes of dorsal root ganglion neurons in rat chronic inflammatory nociception induced by complete Freund's adjuvant. *Molecular Pain,* 4.

Zamponi, G. W., J. Striessnig, A. Koschak & A. C. Dolphin (2015) The Physiology, Pathology, and Pharmacology of Voltage-Gated Calcium Channels and Their Future Therapeutic Potential. *Pharmacological Reviews,* 67**,** 821-870.

Zarei, M. M., B. Toro & E. W. McCleskey (2004) Purinergic synapses formed between rat sensory neurons in primary culture. *Neuroscience,* 126**,** 195-201.

Zeng, Q., V. N. Subramaniam, S. H. Wong, B. L. Tang, R. G. Parton, S. Rea, D. E. James & W. J. Hong (1998) A novel synaptobrevin/VAMP homologous protein (VAMP5) is increased during in vitro myogenesis and present in the plasma membrane. *Molecular Biology of the Cell,* 9**,** 2423-2437.

Zeng, Q., T. T. H. Tran, H. X. Tan & W. J. Hong (2003) The cytoplasmic domain of Vamp4 and Vamp5 is responsible for their correct subcellular targeting - The N-terminal extension of Vamp4 contains a dominant autonomous targeting signal for the trans-Golgi network. *Journal of Biological Chemistry,* 278**,** 23046-23054.

Zhang, X., Y. Chen, C. Wang & L. Y. M. Huang (2007) Neuronal somatic ATP release triggers neuron-satellite glial cell communication in dorsal root ganglia. *Proceedings of the National Academy of Sciences of the United States of America,* 104**,** 9864-9869.

Zhang, Y. H., M. R. Vasko & G. D. Nicol (2002) Ceramide, a putative second messenger for nerve growth factor, modulates the TTX-resistant Na+ current and delayed rectifier K+ current in rat sensory neurons. *Journal of Physiology-London,* 544**,** 385-402.

Zhao, J., M.-C. Lee, A. Momin, C.-M. Cendan, S. T. Shepherd, M. D. Baker, C. Asante, L. Bee, A. Bethry, J. R. Perkins, M. A. Nassar, B. Abrahamsen, A. Dickenson, B. S. Cobb, M. Merkenschlager & J. N. Wood (2010) Small RNAs Control Sodium Channel Expression, Nociceptor Excitability, and Pain Thresholds. *Journal of Neuroscience,* 30**,** 10860-10871.

Zheng, T., J. Kakimura, T. Matsutomi, C. Nakamoto & N. Ogata (2007) Prostaglandin E-2 has no effect on two components of tetrodotoxin-resistant Na+ current

in mouse dorsal root ganglion. *Journal of Pharmacological Sciences,* 103**,** 93-102.